November 2017

THE ROLE OF CHAIN CONFIGURATION IN GOVERNING THE RATIONAL DESIGN OF POLYMERS FOR ADHESION

Onyenkachi Wamuo

THE ROLE OF CHAIN CONFIGURATION IN GOVERNING THE RATIONAL DESIGN OF POLYMERS FOR ADHESION

A Dissertation Presented

by

ONYENKACHI C. WAMUO

Submitted to the Graduate School of the
University of Massachusetts Amherst in partial fulfillment
of the requirements for the degree of

DOCTOR OF PHILOSOPHY

September 2017

Polymer Science and Engineering

THE ROLE OF CHAIN CONFIGURATION IN GOVERNING THE RATIONAL DESIGN OF POLYMERS FOR ADHESION

A Dissertation Presented

by

ONYENKACHI C. WAMUO

Approved as to style and content by:

_____

Shaw Ling Hsu, Chair

_____

Samuel P. Gido, Member

_____

E. Bryan Coughlin, Member

_____

Henning Winter, Member

_____

E. Bryan Coughlin, Member, Department Head

Polymer Science and Engineering

ACKNOWLEDGEMENT

I will first and foremost like to offer my profound gratitude to my thesis advisor, Professor Shaw Ling Hsu. Thank you for taking me under your wings as a member of your research group, I feel very privileged. I would particularly like to emphasize the admiration I have for your organization, passion, dedication and diligence to research I have seen you demonstrate over the years. Your scientific insight and guidance has made me a better scientist and has made this whole process come to fruition. At the initial period of joining the Hsu group, you always emphasized on being explorative in research and trying different things in the laboratory in fact one of your numerous quotes: this is the best time of your life, seemed impossible to see then but now looking back, I could not agree any more. You were right! as always.

I will also like to extend my sincere appreciation to Prof. E. Bryan Coughlin, Prof. Sam Gido and Prof. Henning H. Winter who all agreed to serve in my committee without any hassles, your suggestions and the conversations we had especially during the process of fulfilling my doctoral requirements were vitally important in transforming my research thinking and also appreciating the depth of knowledge that you all displayed during our discussions.

My research was highly collaborative and had an industry-centered focus. I will like to extend my gratitude to my collaborators and funding source: Henkel Corporation. The experience that I gained from our interactions invaluable and instructive. I would like to specifically express my thanks to Chuck Paul and Andrew Slark for giving me the opportunity to work in projects which I felt were relevant and interesting. The technical

staff and the administrative staff in PSE were all awesome. They were all ready to offer assistance whenever I needed. I would like to specifically send my thanks to Lisa Groth who made sure that I did not need to worry about the paperwork, registrations, paychecks, insurance and everything else. She really made things easy for me.

During my time in the Hsu Research Group, I was extremely fortunate to interact or work with extremely talented scientists. My extreme gratitude goes to Dr Sahas Rathi and Omkar Vyavahare for helping me overcome those anxious moments of the cumulative examination preparation and their assistance in getting me settled and started in the laboratory. I also worked really closely with some visiting scholars from China who helped me during the course of my research: Ying Wu, Ying Jin, Zou, Caixai, Zhai, Tsai and Song to mention a few were really helpful. I enjoyed our interactions and look forward to future collaborations. Jignesh, Subrajeet, Lina, Henry, Alex, Jackson offered tremendous emotional and scientific support all along. I will also not forget almost going routinely to the five dining commons with Jignesh, Subrajeet and also occasionally Prof. Hsu and the fun conversations we had through it all. My interest in research was heightened by my bosom friends: Chinomso Nwosu and Onyekachi Oparaji. Both of you have been instrumental in my life as a whole and are part of the reasons why I came to the US in furtherance of my education. Thank you for you emotional support and always having an infectious but positive perspective towards life. I made quite a lot of friends here in my time at Amherst, too many friends to mention but I thank you all for your contribution to my life.

My family is the bedrock of my life. Your understanding, love, instructions, and assistance at every stage of my life has followed me all through my life. Distance never

has and will never be a barrier for me to reciprocate the love and care that you shower me to an even greater magnitude My dad and I are strong soccer lovers and would always analyze the results of soccer matches occasionally on the weekends, my mom expressed her care by asking about my mental and physical well-being as well as when I was getting hitched all those interactions helped me keep a balanced life here. My siblings (Emmanuel, Chisom, and Ugochi) have always been supportive of all my endeavors. During my time in UMass, I, unfortunately, did not get to attend my sisters' weddings, but I will surely make up for that soonest.

ABSTRACT

THE ROLE OF CHAIN CONFIGURATION IN GOVERNING THE RATIONAL DESIGN OF POLYMERS FOR ADHESION

SEPTEMBER 2017

ONYENKACHI C. WAMUO, B.Eng., FEDERAL UNIVERSITY OF TECHNOLOGY, OWERRI (FUTO), NIGERIA
M.S., UNIVERSITY OF MASSACHUSETTS AMHERST

Ph.D., UNIVERSITY OF MASSACHUSETTS AMHERST

Directed by: Professor Shaw Ling Hsu

The chain configurational control of polymers used in adhesion can be utilized as a means of tuning the cohesive properties of hot melt adhesives (HMAs). The cohesive properties control the solidification, strength, setting speed. Propylene-Ethylene copolymers (PP-co-PE) and thermoplastic polyurethanes (TPUs) were studied. In the first project, the effects of sequence distribution of the two types of the (PP-PE) copolymers, with propylene being the dominant component, on the associated crystallization behavior were analyzed. The average sequence lengths of the crystallizable propylene sequences in these copolymers are different, although the ethylene content was virtually identical. In one circumstance, the chain configuration was completely random with crystallizable propylene sequences following Bernouillian statistics. In the other case, we have used a bimodal distribution of crystallizable sequences. The crystallization kinetics, the crystallization temperature, and the degree of crystallinity were significantly higher for the latter sample as compared to the former. When crystallizing from the melt, the longest crystallizable propylene sequences crystallized first at any supercooling, thus controlling the segmental mobility of other segments in the distribution. This is especially evident in copolymers with the bimodal segmental distribution. The distribution of crystallizable

polypropylene sequences also controls the size distribution and thermal stability of the crystallites formed. The elucidation of the crystallization behavior of these copolymers is crucial in defining the application driven setting speeds of hot melt adhesives, the principal application of interest in our laboratory.

Due to its polarity and thermoplastic nature of its structure, TPUs can be used advantageously for binding a variety of substrates. The challenge with current polyurethanes based on conventional 1,4-butanediols is the long time dependency taken for their morphology and properties to set. These slow dynamics is unfavorable in HMAs where fast setting speeds are necessary and responsible for their widespread use in packaging applications. We hypothesize that the increased mobility and flexibility of the traditional 1,4-butanediol system enables slow morphology development in the traditional TPUs. We have therefore changed the mobility of the chain extenders by using a 1,2-propanediol chain extender which incorporates a methyl pendant group into the TPU structure. The presence of the pendant groups in this system incorporates rigidity to the chain extender and makes the HS made from it lack the mobility to move away from the SS matrix. We have shown this to be vital in creating stable domains whose properties do not change over time. Using DSC as well as LFNMR we established mobility differences between the symmetric and asymmetric chain extenders. Temporal DSC and FTIR were used to show the stable and time-independent morphologies associated with the 1,2-propanediol chain extender. In this study, we have achieved chain configurational control by changing the architecture of the chain extender. This concept of chain configurational control using chain extenders is highly useful in controlling the setting speed for HMAs.

TABLE OF CONTENTS

Page

LIST OF TABLES

Table Page

LIST OF FIGURES

Figure Page

CHAPTER 1
INTRODUCTION

1.1 General Overview

Adhesives are materials that are used for joining a variety of substrates. The use of adhesives is relevant to many scientific and technological areas. Scientifically, a variety of adhesion theories has been proposed to account for the mechanism in which substrates are bonded[1]. Technologically, adhesives have been used heavily in replacing traditional joining techniques such as bolting, riveting, screw joining among others[2]. The use of adhesives in technology helps save weight, improve stress distribution and provide adequate aesthetics. There are various classes of adhesives, and in this study, the focus will be on hot melt adhesives (HMAs).

Hot melt adhesives are solvent free thermoplastic solid materials which are thermally activated using a heated gun or spray, applied in the molten form to the substrate to be bonded and solidify upon cooling [3]. Besides the fact that they are environmentally friendly and non-toxic due to their solid nature and absence of solvents, their major utility is derived from their usage in fast production processes since set simply by cooling rather than by evaporation of solvents which is a slow process. We intend even further increase the setting speed to make these adhesive types further attractive in the HMA industry. Therefore we shall control the setting speed, a critical process which is heavily dependent on the cohesive property.

This thesis is focused directly on the use of the concept of chain configurational control of polymers in tuning the cohesive properties of polymers used in hot melt adhesives

(HMAs). An optimum balance between the cohesive and adhesive properties is required for a good adhesive material tailored to a specific application area.[4] Properties such as wettability, open time, green strength and setting speed amongst others are essential properties of adhesive systems that need to be optimized depending on the application type.[5] The adhesive properties of an adhesive is controlled by factors that influence its wetting behavior and its interaction with the substrate to be bonded.[5] On the other hand, the cohesive properties comprising of the set speed, green strength and mechanical integrity of deal with factors that control the morphology of the polymer used in formulating the HMA. One of such factors is the chain configuration of the polymer.

The chain configuration not only refers to the structural constituents of the polymer chain but also describes the sequence and manner of arrangement of each structural unit along the macromolecular backbone.[6] Properties such as the crystallization and phase separation kinetics which are morphological properties are greatly controlled by the chain configuration of polymers. Understanding how to control chain configuration of polymers can, therefore, be used in tuning the morphology of the polymers and by extension the knowledge can be used in controlling process parameters of polymers used in adhesion. [7-9]

1.2 Overview of Dissertation

The fundamental knowledge of the chain configuration of polymers used as hot melt adhesives and the main roles in controlling the major properties of HMAs as studied in my dissertation will organized in the following chapters outlined below.

An overview of the history of adhesive systems and in particular hot melt adhesives will be reviewed in chapter 1. The chapter also explores fundamentals that enable morphological control in crystallizable propylene copolymers and the physics governing the phase behavior in the TPU systems. Chapter 2 deals with the effect of chain configurational structure of propylene-ethylene copolymers in determining the crystallization behavior as well as the thermodynamic properties of two different kinds of chain configurational types: random vs. a bimodal distribution of crystallizable sequence. Evaluation of the chain configuration behavior using ^{13}C NMR, thermal fractionation techniques such as the SSA and the assessment of the regularity bands and the subsequent application to ascertain the configurational effects on the crystallizability and crystallization behavior.

In chapter 3, the structural requirements needed for the application of TPUs as HMAs will be highlighted. The role played by chain extender, typically employed in most formulations, in altering the morphology and segmental dynamics of polyurethanes will be elucidated. The aim of this study is to understand the role that the symmetry of chain extenders plays in controlling morphology. Therefore, two symmetry types will be explored: the traditional symmetric chain extenders as well as the non-traditional chain-extenders. The chain extenders are synthesized with amorphous polyols and 4,4-methylene diphenyl diisocyanate (MDI). Time dependent DSC, FTIR amongst other techniques are used in understanding the thermal properties and the morphology development of these differently chain-extended polyurethanes to simulate in-use conditions.

Chapter 4 presents a continuation of work done in chapter 3; semicrystalline components are added to the amorphous polyester polyols to enhance the modulus of the original material. The effect of the symmetry of the chain extender in influencing the crystallization behavior of the semicrystalline component was also elaborated on. The mobility/flexibility of chain extender seems to play a huge role on the kinetics of crystallization. LFNMR studies will be used to characterize the segmental dynamics/mobility of the variously chain-extended systems. The influence of temperature and time will be studied via in situ FTIR and DSC characterization. A general conclusion of the entire study is discussed in Chapter 5, and possible future work on the prospective research area discussed.

1.3 Historical perspectives on the use of adhesives

The engineering application of adhesives has been linked to the history of man..[10-11] For laminating woods and making of furniture, the Egyptians used animal and casein glue and evidence of some of these art works and still in existence. The first commercial plant for the manufacture of glue was found in Holland in the 1600's. [11] In the US, the use of adhesives started in the early 19th century. The Table 1.1 below summarizes the early history of the use of adhesives in the US.

Table 1.1 Historical development of adhesive in the USA[11]

Year	Material
1814	Glue from animal bones (patent)
1872	Domestic manufacture of fish glues (isinglass)
1874	First U.S. fish glue patent
1875	Laminating of thin wood veneers attains commercial importance
1909	Vegetable adhesives from cassava flour (F. G. Perkins)
1912	Phenolic resin to plywood (Baekeland-Thurlow)
1915	Blood albumin in adhesives for wood (Haskelite Co.)
1917	Casein glues for aircraft construction
1920–1930	Developments in cellulose ester adhesives and alkyd resin adhesives
1927	Cyclized rubber in adhesives (Fischer-Goodrich Co.)
1928	Chloroprene adhesives (McDonald–B. B. Chemical Co.)
1928–1930	Soybean adhesives (I. F. Laucks Co.)
1930	Urea–formaldehyde resin adhesives
1930–1935	Specialty pressure-sensitive tapes: rubber base (Drew–Minnesota Mining & Mfg. Co.)
1935	Phenolic resin adhesive films (Resinous Products & Chemical Co.)
1939	Poly(vinyl acetate) adhesives (Carbide & Carbon Chemicals Co.)
1940	Chlorinated rubber adhesives
1941	Melamine–formaldehyde resin adhesives (American Cyanamid Corp.) and Redux by de Bruyne (Aero Research Ltd).
1942	Cycleweld metal adhesives (Saunders-Chrysler Co.)
1943	Resorcinol–formaldehyde adhesives (Penn. Coal Products Co.)
1944	Metal-bond adhesives (Havens, Consolidated Vultee-Aircraft Corp.)
1945	Furane resin adhesives (Delmonte, Plastics Inst.) and Pliobond (Goodyear Tire and Rubber Co.)

The adhesive industry has evolved from prehistoric times where adhesives based on plant/tree sap or latex were used in bonding articles [12-13] to present day requirements where current manufactured adhesives are centered on systems that are lightweight, structurally stable and environmentally friendly with applications including the aerospace, automotive, building and construction, food, and consumer electronics industries among others.[11, 14-16] One class of adhesive that has gained prominence in recent years is hot melt adhesives. The first record of HMAs invention is found in a 1940 US patent .[17] Following the patent, a variety of other HMAs has been discovered. [18]

HMAs are solids at room temperature, applied to the substrate to be bonded in the molten form and solidify on cooling. [3, 19] It is therefore easy to visualize that a critical process parameter will be to understand the physics that govern the solidification processes and to

use that understanding in tuning the properties of the resultant material. HMAs are heavily used in fast production processes, where the process speed is critical, simply because they do not have any carrier vehicles (solvent or water) that needs to be evaporated before a bond of acceptable strength is formed.[3, 19] The most commonly used HMA is based on Ethylene Vinyl acetate (EVA) copolymers, with ethylene as the predominant monomer.[3, 20] EVAs have been widely used due to the wide variety of grades of EVA that can be obtained just by altering the comonomer content thus yield materials which possess the ability to adhere to a variety of substrates. HMAs based on these systems are easy to apply and exhibit robust properties for use at temperatures lower than 80 ºC .[20-21] To extend the performance of hot melt adhesives to elevated temperature applications, higher melting polymers and polymers possessing high green strength at elevated temperatures are used as potential candidates. [9] This dissertation seeks to explore two different categories of polymers which are to be employed in HMA applications.

A constant theme of the project will be centered on how to use the concept of chain configurational control in tuning the properties of polymers for HMAs application. The first project will emphasize chain configurational control of crystallizable polypropylene copolymer systems whereas, in the second project, polymers based on thermoplastic polyurethanes (TPUs) possessing a significant amount of polarity and functional groups which promote adhesion to a variety of substrates will be studied.

1.4 Background on chain configuration of propylene-ethylene copolymers

Polyolefins based on polypropylene and polyethylene accounts for the majority of the commodity plastics consumed today. [22-23] Propylene based materials particularly have tremendous relevance in the commodity plastics industry. [22-23] Beyond their relevance in the manufacture of commodity products, polypropylenes have also found relevance in the hot melt industry due to their excellent processibility and also their elevated temperature stability. A fully isotactic polypropylene (iPP) homopolymer crystallizes readily and has a relatively high melting temperature (~165 °C)[24] and exhibits about ~50% crystallinity depending on annealing condition. [25] In reality, such a high melting point is unnecessary from an engineering perspective. To maintain a low melt viscosity for applying the hot melt adhesive, a rapid crystallization kinetics (setting speed) and adhesive performance, copolymers involving propylene with much lower melting temperatures can be employed. The comonomer most readily used is ethylene. Copolymerization of propylene and ethylene not only reduces the cost but also improves the toughness and flexibility of the final product formed. Figure 1.1 shown below is a schematic representation of a propylene-ethylene copolymer system, the x and y in this structure represents the molar composition of the propylene and ethylene components, with the x being around ~90% in our studies

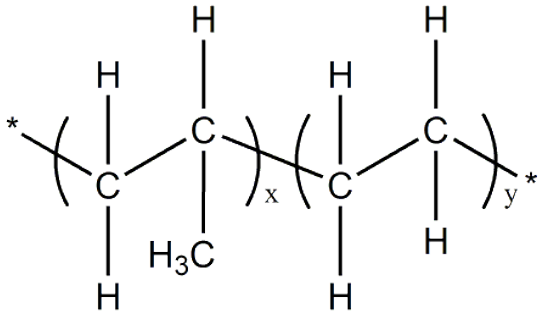

Figure 1.1 Structure of propylene-ethylene copolymer

The properties of polypropylene can also be altered by changing the tacticity, the sequence length distribution and by introducing of comonomers such as ethylene to the backbone. [26] Polypropylenes are prochiral structurally, and for this reason, exhibit structural and stereochemical.[26] The structural isomerism refers to the sequence and the orientation of the monomer as it is into the increasing polymer chain. Three different possibilities are known to exist; head-head, head-tail and tail-tail structures, these structures can create the possibilities of creating regioregular or regiorandom structures. An important requirement for having crystalline structures is the formation of regioregularity (H-T) arrangement. Stereochemical/configurational isomerism, on the other hand, pertains to the spatial disposition and arrangement of the monomeric unit of the polymer units. In polypropylene, it deals with the spatial placement of the methyl group leading to different configurations. If the methyl group in the polymer is all placed on the same side of the chain, they are called isotactic, if they are on alternate sides of the chain, they are referred to as being syndiotactic, and a random arrangement of the methyl group will lead to an atactic structure.

1.4.1 Melt crystallization of polymers

. Polymer crystallization can occur in various forms: It can occur during polymerization, under flow, and in quiescent conditions. [27] This work does not focus on flow induced crystallization or crystallization during polymerization. The crystallization emphasized on here is the quiescent crystallization of polymers. Quiescent crystallization can occur either in the solution state or the molten form. Crystallization from the melt is a practical

approach of studying polymer crystallization since this is commonly encountered during polymer melt processing and thus will be the focus of this study. During polymer crystallization from the melt, crystallization proceeds incompletely, leading to the formation of amorphous and crystalline domains as opposed to fully crystalline equilibrium structures because crystallization in polymers is dominated by kinetic effects as opposed to thermodynamics. Chain folding, prevalent in melt crystallized polymers diminishes the crystallization kinetics and degree of crystallinity in the polymer material.

Crystallization is broadly said to undergo two major events, i.e., nucleation and crystal growth events. [27-28] The nucleation step involves generation of the nuclei from the supercooled melt; this happens as a result of rapid density fluctuations on a molecular scale in a homogeneous phase that is in a state of metastable equilibrium. In order for stable nuclei to form, an energy penalty has to be paid. In other words, an activation barrier has to be surmounted for stable nuclei to be formed. This is shown in Figure 1.2 below.

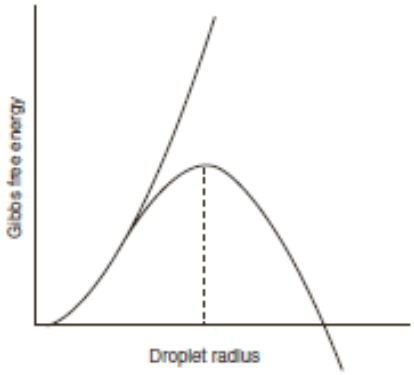

Figure 1.2 Dependence of nuclei size on Gibb's free energy[27]

The nucleation step is further categorized into the primary and secondary nucleation processes. Primary nucleation deals with the initial formation of a crystal in the absence of any other crystal in the system; it is the initial step that ensures the formation of polymer crystals. The primary nucleation can either be homogeneous or heterogeneous. The homogeneous nucleation is not influenced by the presence of seeds but evolves as a result of thermal fluctuations in the system. It should be noted about the impracticality of the homogeneous nucleation system as it is virtually impossible to eliminate impurities such as catalyst residue in the system which can act as a site for nucleation. The heterogeneous nucleation step relies on the presence of surface through seeds or impurities for nuclei to form. With heterogeneous nucleation, a lower supercooling is required to overcome energy constraints for the formation of stable nuclei. Secondary nucleation conversely involves the formation of nuclei in the due to the presence of pre-existing nuclei, mostly impurities which act as a seed to enhance the growth of the crystal, this process is described by the Lauritzen-Hoffman(LH) theory. [29] Secondary nucleation occurs after the primary nucleation process, and it controls the growth rate even after the primary crystals have grown.

Once the energy cost required for the formation is overcome, crystal nuclei can grow in the crystal growth stage to form stable nuclei. It entails the creation of a new surface on the growing primary crystal surface.

1.4.2 Thermodynamics of polymer crystallization

The thermodynamics of polymer crystallization is a simple yet relevant tool for the prediction of crystallization behavior. From classical thermodynamic treatment, we learn

that the total free energy for the formation of a crystal can be expressed mathematically as:

Equation 1.1 $$\Delta G = \sum A_{lat}\sigma + 2A\sigma_e - \Delta FAl$$ [29]

Where A_{lat}, A, and l correspond to the lateral surface area, the folded surface area, and the lamellar thickness, respectively. The first two terms express the surface energy requirements whereas the third term accounts for the change in the bulk free energy. The equation assumes that the surface energy per area and the bulk energy per volume are invariant with crystal size [30]. For enormous crystals, the folded surface area is much greater than the lateral surface area which results in the most common form of the expression:

Equation 1.2 $$\Delta G = 2A\sigma_e - \Delta FAl$$

The bulk free energy change is expressed as

Equation 1.3 $$\Delta F = \Delta H - T\Delta S$$

Where ΔH and ΔS are the enthalpy and entropy changes at temperature T. When ΔG = 0 the minimal lamellar thickness l_{min} for an infinitely large lamellar crystal becomes:

$$l_{min} = \frac{2\sigma_e}{\Delta F}$$

The Gibbs–Thomson [31-32] which is the equation that relates the crystal size to the undercooling is derived from the thermodynamics of polymer crystallization.

Equation 1.4 $$l_c = \frac{2\sigma_e}{\Delta H}\left[\frac{T_m^o}{\Delta T}\right]$$

1.4.3 Copolymer crystallization

Copolymers are derived from the polymerization of chemically distinct monomeric species. This is done to tailor the morphology of the resultant polymer to an application of one's interest. Several copolymer architectures are obtained depending on the manner in which the sequence is distributed along the main chain. Common copolymer architectures include the block, alternating and random sequence of copolymer distribution. The effects on the thermodynamic properties of crystallization on the incorporation of comonomers are well known. Copolymerization reduces the degree of crystallinity, broadens the melting transition as well as depresses the crystalline melting temperature.

There are different views governing the thermodynamics of copolymer crystallization. The Flory and Sanchez-Eby theory being the most prominent ones. [33-34] Flory's view of copolymer crystallization makes the assumption that the B units are excluded from the crystallites formed by the A units. Flory's copolymer crystallization theory goes on to state that the crystallizability of a copolymer is dependent on its sequence length, ξ as well as the temperature at which the crystallization is carried. At higher temperatures, sequences ξ greater than a critical value, ξ^* can crystallize, forming thicker crystals that can melt at higher temperatures. As crystallization temperature reduces, shorter sequences can crystallize and form shorter crystals. The lamella thickness formed is strongly correlated to the driving force for crystallization, the undercooling. Equation 1.15 clearly expresses this. At low undercooling, thick crystallites are formed, and at large undercooling, thinner crystallites are formed.

Equation 1.15 $$l \propto \frac{1}{\Delta T}\ , where\ \Delta T = \ T_m^o - T_c$$

In my thesis, an understanding of these concepts will be essential in trying to control the crystallization kinetics of copolymers. It is well known in most crystallization processes that a few crystals formed initially can significantly reduce segmental mobility thus limiting further crystalline growth. My work will seek to design a bimodal distribution of crystals to control the crystallization behavior in these copolymer systems. By using a system having large blocks of iPP that crystallize at the initial stages, green strength can be induced at the early stages of crystallization. The larger population of long sequences will be compensated by having fewer medium or shorter iPP sequences; these shorter sequences will provide the mobility for thickening and secondary crystallization of the polymer. In other words, instead of having a distribution following purely random distribution, we elect to use a bimodal distribution to achieve the rapid crystallization speed. This study provides additional guidance in designing copolymers to act as special adhesives for use at elevated temperatures

1.5 Background on chain configuration of thermoplastic polyurethane (TPU)

Although HMAs based on polyolefins have good temperature stability due to their high melting temperatures, they are limited in their application as adhesive materials owing to the non-polar nature of their structure. For the polyolefin systems, tackifiers, waxes and other adhesion promoters are incorporated to improve its adhesion. The introduction of this various components may lead to non-homogeneity in the composition and produce detrimental effects on the mechanical integrity of the adhesive material. Polyurethanes, on the other hand, are highly polar and does not need a variety of the components

mentioned above to increase its adhesion properties. Polyurethanes, therefore, present interesting opportunities for use in the HMAs industry. The polar nature of their molecular structure gives them self-adhesive properties and enables them to be bonded to a broad range of substrates. [35-36]

Thermoplastic polyurethanes particularly consists of the covalent reaction between soft and hard segments in the polymer backbone. The soft segment is usually flexible macrodiols with glass transition temperatures below ambient temperature while the hard segments are formed from the reaction between diisocyanates and chain extenders possessing Tg well above the use temperature. Unlike conventional elastomers, TPUs are elastomers which are melt processable owing to the extensive self-association in the hard segment domain enabling them acts as physical crosslinks which can be broken down and reformed during heating and cooling cycles.

Polyurethanes are versatile in their application ranging from their use as foams (flexible and rigid), fibers, coatings, sealants, elastomers amongst other areas. [37-38] Their versatility is attributed to the ease with which their chemistry is tuned by changing stoichiometry, monomer type or temperature amongst other parameters thus resulting in various interesting morphological features that. A simplistic view of the chemistry of polyurethanes, especially segmented PUs involves reacting a macroglycol (polyester, polyether polyols, etc.), chain-extender (water, diamines, diols, etc.) and a diisocyanate resulting in a carbamate functional group. [39-40] Figure 1.3 shows the reaction between an isocyanate functional group and an alcohol to give a carbamate functional group.

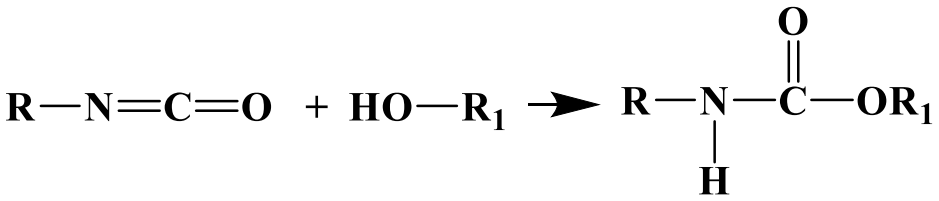

Figure 1.3 Isocyanate reaction with hydroxyl group

The most commercially important diisocyanates used in the synthesis of polyurethanes are the diisocyanates based on 2,4- and 2,6-toluene diisocyanates (TDI); 4,4 -diphenylmethanediisocyanates (MDI) and 1,5-naphthalene diisocyanate (NDI). The MDI and TDI diisocyanates are commonly used in both the adhesives and foam industries[37]. With increasing environmental concerns particularly about the volatility and toxicity of the TDI based systems, a broad range of research work has been devoted to the study of the influence of changing the diisocyanate structure and symmetry on the properties of TPUs.[41-42]

The polyols which are employed in the synthesis of polyurethanes are generally compounded having molecular weights around 500-5000 g/mol. The structure of polyols that is commonly used in industry have been based on polyethers and polyesters. The polyether based polyols generally used in polyurethane manufacture are the ones based on PTMG and PPG, these polyether polyols impart a greater degree of softness, flexibility and hydrolytic stability to the polyurethanes made from them[37]. TPUs made from the polyester based polyols have certain advantages over the polyether based polyols such as superior mechanical properties, oil resistance, and thermal properties. They are therefore generally used in making systems where high structural integrity is needed such as rigid foams, polyurethane struts, and structural adhesives. However, a

common drawback with these polyols is their limited hydrolytic stability. Recent research efforts are dedicated to the enhancement of the hydrolytic stability behavior of polyester polyols. Polyester polyols based on polycarbonates and polycaprolactone are seen as possible alternatives owing to their much higher stability. The polyester polyols we have employed in our studies are proprietary and have an enhanced stability[39].

Chain extenders, which are small bifunctional molecules are important components for the manufacture of polyurethanes as they are not only utilized to increase the molecular weight of the prepolymer but also play a crucial role in controlling the morphological and aggregation behavior of the resultant TPUs. The 1,4-butanediol chain extender is the "standard" chain extender that is predominantly used. The excellent geometric requirements that the traditional 1,4 butanediol chain extender possesses provides available dipoles, enabling the formation of strong hydrogen bonding interactions within the system and thereby leading to the formation of phase separated structures in the TPU polymer.[43]

Asides from the 1,4-BDO chain extenders, very few other chain extenders have been explored in TPU synthesis. Some of these chain extenders have focused on the effect of having odd versus even number of carbons in the chemical structure of linear aliphatic diol chain extenders on the aggregation structure and its hydrogen bonding capacity.[43-44]

Another study has carried out a comparison of the dynamic mechanical property of TPUs obtained using the linear and nonlinear structure of chain-extenders have been carried by Bae et al. [45] In their DMA study they found out that the morphology obtained when nonlinear chain extenders were used phase-mixed morphologies rather than phase-

separation like in the case of the linear 1,4-BDO thus resulting in the absence of a clearly defined rubbery modulus unlike for the linear chain-extenders where a rubbery modulus was present. No morphological data was provided in their studies, but it can be appreciated that changing the structure of chain-extenders can be used as a means to tune morphological behavior leading to a variety of interesting properties which can become useful in the design of HMAs. In all these, it can be observed that there is a vast window of opportunities in the study of morphological control using chain extenders and this will constitute a core focus of this portion of my research.

Morphologically, TPUs are characterized by a segmented block copolymer structure containing hard and soft segments which are covalently bonded together. [39, 46] The morphological properties of polyurethanes are attributed to their propensity to undergo microphase separation. [46] Microphase separation in this system is driven by many factors which can be molecular, structural and physical factors in nature.[42] The microphase separated morphologies of polyurethanes can either be driven by thermodynamic or kinetic factors.

1.5.1 Thermodynamics of phase separation in TPUs

In thermodynamics terms, the presence of phase separation is ascribed to the incompatibility between the hard and the soft domains. Thermodynamically, a prediction of the compatibility between each block can be made using Gibbs free energy of mixing, given by Equation 1.6

Equation 1.6 $$\Delta \boldsymbol{G_{mix}} = \Delta \boldsymbol{H_{mix}} - \boldsymbol{T}\Delta \boldsymbol{S_{mix}}$$

If ΔG_{mix} is negative, then the system will be thermodynamically miscible whereas a positive valuable will connote miscibility. It can be clearly seen that entropic as well as enthalpic factors can influence the miscibility of the system. An expanded equation of the Gibbs free energy of mixing gives the Flory-Huggins equation which is shown below in the equation below

Equation 1.7 $$\Delta \boldsymbol{G_{mix}} = \boldsymbol{RT}(\boldsymbol{n_1 ln\phi_1} + \boldsymbol{n_2 ln\phi_2} + \boldsymbol{n_1\phi_2\chi_{12}})$$

wheren_1, n_2, ϕ_1, ϕ_2, R, T and χ represent the number of moles of components 1 and 2, the volume fraction of components 1 and 2, the universal gas constant, temperature and "chi" parameter, χ also known as the polymer-polymer or polymer-solvent interaction parameter, representing the extent of compatibility between the components involved. In the equation 1.7 above, the first two terms, represent the entropic factors controlling miscibility while the last term, is responsible for enthalpic requirements. χ can also be related to the solubility parameter, δ, making it estimate the phase behavior of the system from knowledge of solubility parameters values. Equation 1.8 shows this relation. A positive value of χ greater than a critical chi, χ_c leads the system to phase separate. Table 1.2 and 1.3 gives the values of the solubility parameters of commonly used hard and soft segments.

Equation 1.8 $$\chi_{12} = \frac{(\delta_1 - \delta_2)^2 V}{RT}$$

Table 1.2 The solubility parameter of HS [41]

Chemical structure	Group name	CED (J/cm^3)	δ (J/cm^3)$^{1/2}$	δ_h (J/cm^3)$^{1/2}$
	Urethane	1385	37.2	25.4
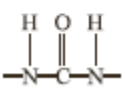	Urea	2079	45.6	34.2

Table 1.3 Solubility parameter of soft segment [41]

Chemical name	Code	Chemical structure of the repeating unit	δ (J/cm^3)$^{1/2}$
Poly(ethylene oxide)	PEO	(CH_2CH_2O)	20.2
Poly(propylene oxide)	PPO	(CH_2CHO) with CH_3	18.9
Poly(tetramethylene oxide)	PTMO	$(CH_2CH_2CH_2CH_2O)$	17.6
Poly(butylene adipate)	PBA	$(O(CH_2)_4OC(CH_2)_4C)$ with O O	17.0

1.5.2 Effect of Hydrogen bonding

The majority of polyurethanes are strongly hydrogen bonded,[47] With hydrogen bonded systems, the expectation is the increased intermolecular interactions will enhance solubility. [47-48] This, however, is not the case for the majority of polyurethanes which exhibit phase-separation even with a negative χ. The phase separation is driven by strong self-association of the hard segments through hydrogen bonding. [49] An association model accounting for the presence of hydrogen bonding has been used proposed.[47-48]

Equation 1.9 $$\Delta G_{mix} = RT(n_1 ln\phi_1 + n_2 ln\phi_2 + n_1\phi_2\chi_{12}) + \Delta G_{HB}$$

The role of hydrogen bonding in driving phase-separation seems to be exaggerated as phase separation has also been shown to occur in polyurethanes devoid of hydrogen bonding. [50-51]This indicates that intermolecular interaction may not be the only factor influencing phase behavior but structural parameters such as the rigidity of the hard segment may have a contribution to the phase behavior.

1.5.3 Kinetic/structural factors that affect phase separation in TPUs

Phase separation is also greatly influenced by kinetic factors. In polyurethanes, these kinetic factors influence how different domains interact leading to the formation of either

discrete phases or the intermixing of various components that make up the system. Some of the kinetic influences which are most relevant to this work are structural and will be controlled by changing the chain architecture of the chain extender. [41-42, 52] Previous studies have shown the existence of kinetic effects driven by system viscosity, hard segment interaction, and flexibility as important factors governing the structure of polyurethanes. They studied this by changing the flexibility of the diisocyanate as well by altering the functional groups of the chain extenders (amine or hydroxyl) which constitutes the hard segment structure and observed the influence of the flexibility, interaction and the system viscosity in controlling phase-behavior.[41, 52] From those studies, it can be deduced that changes, particularly in the symmetry of the diisocyanate structure yielded variations in the degree of ordering, segmental mobility amongst other properties of the polyurethanes.

Effects such as the chain architecture and amount of intermolecular interaction have an effect in controlling the morphology. [41, 52] Surprisingly, the use of TPUs in the area of hot melt adhesion has not been explored to a great extent. Published work has focused on reactive HMAs, which are essentially moisture-curable adhesives that react on exposure to moisture. [36, 53] TPUs devoid of isocyanate functional groups are attractive due to the outstanding green strength, adhesion to a multitude of substrates and excellent environmental friendliness amongst other reasons. The excellent bonding strength in these HMAs is due to the increased intermolecular interaction such as van der Waals forces and hydrogen bonding that can exist between most urethanes and substrates among other factors. [36]

In trying to explore the use of TPUs as HMAs, the chain configuration and amount of intermolecular interaction of the polymer will be tuned by changing the chain extender architecture. Two chain extender classes will be explored; a symmetric chain extender such as the classical 1,4-butanediol amongst others and the atypical asymmetric chain extender such as the 1,2-propanediol system. An essential requirement for HMAs is the presence of rapid setting speed, so the potential for the use of these classes of chain-extenders to attain fast setting speed will also be discussed in the chapters ahead.

1.6 References

1. Packham, D. E., Theories of fundamental adhesion. In *Handbook of Adhesion Technology*, Springer: 2011; pp 9-38.

2. Troughton, M. J., *Handbook of plastics joining: a practical guide*. William Andrew: 2008.

3. Paul, C., Hot-melt adhesives. *MRS bulletin* **2003,** *28* (6), 440-444.

4. Benedek, I., *Developments in pressure-sensitive products*. CRC Press: 2005.

5. Pocius, A. V.; Dillard, D. A., *Adhesion science and engineering: surfaces, chemistry and applications*. Elsevier: 2002.

6. Koenig, J. L., *Chemical microstructure of polymer chains*. Wiley: 1980.

7. Baker, W.; Fuller, C., Intermolecular Forces and Chain Configuration in Linear Polymers—The Effect of N-Methylation on the X-Ray Structures and Properties of Linear Polyamides. *Journal of the American Chemical Society* **1943,** *65* (6), 1120-1130.

8. Li, S. H.; Woo, E. M., Effects of chain configuration on UCST behavior in blends of poly (L-lactic acid) with tactic poly (methyl methacrylate) s. *Journal of Polymer Science Part B: Polymer Physics* **2008,** *46* (21), 2355-2369.

9. Wamuo, O.; Wu, Y.; Hsu, S. L.; Paul, C. W.; Eodice, A.; Huang, K.-Y.; Chen, M.-H.; Chang, Y.-H.; Lin, J.-L., Effects of chain configuration on the crystallization behavior of polypropylene based copolymers. *Polymer* **2017,** *116*, 342-349.

10. Delmonte, J., Technology of adhesives. **1947**.

11. Pizzi, A.; Mittal, K. L., *Handbook of adhesive technology, revised and expanded*. CRC press: 2003.

12. Braude, F., Adhesives. **1943**.

13. Houwink, R.; Bruyne, N. A. d.; Salomon, G., Adhesion and adhesives. **1965**.

14. Diogo, A. C., Polymers in Building and Construction. In *Materials for Construction and Civil Engineering*, Springer: 2015; pp 447-499.

15. Licari, J. J.; Swanson, D. W., *Adhesives technology for electronic applications: materials, processing, reliability*. William Andrew: 2011.

16. Benedek, I., *Pressure-sensitive adhesives and applications*. CRC Press: 2004.

17. Robert, D. H., Hot melt. Google Patents: 1940.

18. Satriana, M., Hot melt adhesives: manufacture aad applications. In *Chemical technological review*, Noyes Data Corporation.; New Jersey: 1974.

19. Li, W.; Bouzidi, L.; Narine, S. S., Current research and development status and prospect of hot-melt adhesives: A review. *Industrial & Engineering Chemistry Research* **2008,** *47* (20), 7524-7532.

20. Kalish, J. P.; Ramalingam, S.; Wamuo, O.; Vyavahare, O.; Wu, Y.; Hsu, S. L.; Paul, C. W.; Eodice, A., Role of n-alkane-based additives in hot melt adhesives. *International Journal of Adhesion and Adhesives* **2014,** *55*, 82-88.

21. Park, Y.-J.; Kim, H.-J., Hot-melt adhesive properties of EVA/aromatic hydrocarbon resin blend. *International journal of adhesion and adhesives* **2003,** *23* (5), 383-392.

22. Maddah, H. A., Polypropylene as a promising plastic: A review. *American Journal of Polymer Science* **2016,** *6* (1), 1-11.

23. Sastri, V. R., Commodity Thermoplastics-6: Polyvinyl Chloride, Polyolefins, and Polystyrene. **2014**.

24. Coates, G. W.; Waymouth, R. M., Oscillating stereocontrol: a strategy for the synthesis of thermoplastic elastomeric polypropylene. *Science* **1995,** *267* (5195), 217.

25. Parenteau, T.; Ausias, G.; Grohens, Y.; Pilvin, P., Structure, mechanical properties and modelling of polypropylene for different degrees of crystallinity. *Polymer* **2012,** *53* (25), 5873-5884.

26. De Rosa, C.; Auriemma, F., *Crystals and crystallinity in polymers: diffraction analysis of ordered and disordered crystals*. John Wiley & Sons: 2013.

27. Mandelkern, L., *Crystallization of polymers*. McGraw-Hill New York: 1964; Vol. 38.

28. Wunderlich, B., *Macromolecular physics*. Elsevier: 2012; Vol. 2.

29. Lauritzen, J. I.; Hoffman, J. D., Theory of formation of polymer crystals with folded chains in dilute solution. *J. Res. Natl. Bur. Stand. A* **1960,** *64* (1), 73102.

30. Zhang, M. C.; Guo, B.-H.; Xu, J., A Review on Polymer Crystallization Theories. *Crystals* **2016,** *7* (1), 4.

31. Thomson, J. J., *Applications of dynamics to physics and chemistry*. Macmillan: 1888.

32. Gibbs, J. W., *The scientific papers of J. Willard Gibbs*. Longmans, Green and Company: 1906; Vol. 1.

33. Sanchez, I.; Eby, R., Thermodynamics and crystallization of random copolymers. *Macromolecules* **1975,** *8* (5), 638-641.

34. Flory, P. J., Theory of crystallization in copolymers. *Transactions of the Faraday Society* **1955,** *51*, 848-857.

35. Engels, H. W.; Pirkl, H. G.; Albers, R.; Albach, R. W.; Krause, J.; Hoffmann, A.; Casselmann, H.; Dormish, J., Polyurethanes: versatile materials and sustainable problem solvers for today's challenges. *Angewandte Chemie International Edition* **2013,** *52* (36), 9422-9441.

36. Tang, Q.; He, J.; Yang, R.; Ai, Q., Study of the synthesis and bonding properties of reactive hot-melt polyurethane adhesive. *Journal of Applied Polymer Science* **2013,** *128* (3), 2152-2161.

37. Szycher, M., *Szycher's handbook of polyurethanes*. CRC press: 2012.

38. Oertel, G.; Abele, L., *Polyurethane handbook: chemistry, raw materials, processing, application, properties*. Hanser Publishers. Distributed in USA by Scientific and Technical Books, Macmillan: 1985.

39. Krol, P., Synthesis methods, chemical structures and phase structures of linear polyurethanes. Properties and applications of linear polyurethanes in polyurethane elastomers, copolymers and ionomers. *Progress in materials science* **2007,** *52* (6), 915-1015.

40. Saunders, J. H.; Frisch, K. C., Polyurethanes: chemistry and technology. **1962**.

41. Li, Y.; Ren, Z.; Zhao, M.; Yang, H.; Chu, B., Multiphase structure of segmented polyurethanes: effects of hard-segment flexibility. *Macromolecules* **1993,** *26* (4), 612-622.

42. Yilgör, I.; Yilgör, E.; Wilkes, G. L., Critical parameters in designing segmented polyurethanes and their effect on morphology and properties: A comprehensive review. *Polymer* **2015,** *58*, A1-A36.

43. Born, L.; Hespe, H.; Crone, J.; Wolf, K., The physical crosslinking of polyurethane elastomers studied by X-ray investigation of model urethanes. *Colloid & Polymer Science* **1982,** *260* (9), 819-828.

44. Blackwell, J.; Nagarajan, M.; Hoitink, T., Structure of polyurethane elastomers. X-ray diffraction and conformational analysis of MDI-propandiol and MDI-ethylene glycol hard segments. *Polymer* **1981,** *22* (11), 1534-1539.

45. Bae, J.; Chung, D.; An, J.; Shin, D., Effect of the structure of chain extenders on the dynamic mechanical behaviour of polyurethane. *Journal of materials science* **1999,** *34* (11), 2523-2527.

46. Koberstein, J. T.; Stein, R. S., Small-angle X-ray scattering studies of microdomain structure in segmented polyurethane elastomers. *Journal of Polymer Science Part B: Polymer Physics* **1983,** *21* (8), 1439-1472.

47. Coleman, M. M.; Painter, P. C.; Graf, J. F., *Specific interactions and the miscibility of polymer blends*. CRC Press: 1995.

48. Painter, P. C.; Park, Y.; Coleman, M. M., Hydrogen bonding in polymer blends. 2. Theory. *Macromolecules* **1988,** *21* (1), 66-72.

49. Lee, H. S.; Hsu, S. L., An analysis of phase separation kinetics of model polyurethanes. *Macromolecules* **1989,** *22* (3), 1100-1105.

50. Ng, H.; Allegrezza, A.; Seymour, R.; Cooper, S. L., Effect of segment size and polydispersity on the properties of polyurethane block polymers. *Polymer* **1973,** *14* (6), 255-261.

51. Harrell Jr, L., Segmented polyurethans. Properties as a funcation of segment size and distribution. *Macromolecules* **1969,** *2* (6), 607-612.

52. Li, Y.; Gao, T.; Chu, B., Synchrotron SAXS studies of the phase-separation kinetics in a segmented polyurethane. *Macromolecules* **1992,** *25* (6), 1737-1742.

53. Jeong, Y. G.; Hashida, T.; Hsu, S. L.; Paul, C. W., Factors influencing curing Behavior in phase-separated structures. *Macromolecules* **2005,** *38* (7), 2889-2896.

CHAPTER 2
EFFECTS OF CHAIN CONFIGURATION ON THE CRYSTALLIZATION BEHAVIOR OF POLYPROPYLENE BASED COPOLYMERS

(Reproduced in part with permission fromWamuo, O., Wu, Y., Hsu, S.L., Paul, C.W., Eodice, A., Huang, K.Y., Chen, M.H., Chang, Y.H. and Lin, J.L., 2017.*Polymer* 116 **(2017),** 342-349)

2.1 Introduction

This chapter deals with controlling the crystallization behavior of propylene-ethylene copolymers so as to control the set speed for hot melt adhesive application. Controlling the crystallization behavior of various copolymers is extremely interesting from a fundamental perspective. In our laboratory, we are interested in the rate of crystallization achievable because it is crucial to the success of high-performance hot melt adhesives (HMAs). Although many polymers can be used in hot melt adhesive formulations, most applications have adopted ethylene copolymers along with appropriate tackifiers, and low molecular weight waxes in specific formulations [1]. These HMAs are easy to apply and exhibit robust properties for use at temperatures lower than 80 ºC. In order to raise the performance of hot melt adhesives at elevated temperatures, higher melting copolymers involving isotactic polypropylene (iPP) can be employed. The polypropylene homopolymer crystallizes readily and has a relatively high melting temperature (~165 °C). In order to maintain a low melt viscosity for applying the hot melt adhesive, a rapid crystallization kinetics (setting speed) and adhesive performance, copolymers involving propylene with somewhat lower melting temperatures should be employed. The comonomer most readily used is ethylene. These ethylene-propylene copolymers with different compositions and physical properties are readily available and at a relatively low cost [2].

Recently a number of systematic crystallization studies of random copolymers involving ethylene and propylene have been carried out [3-4]. However, the crystallization mechanism of random copolymers is far from understood [5-9]. Unlike a homopolymer, the crystallization process of a random copolymer is complex [10-11]. Because of the randomness in chain configuration, the enthalpic contribution favorable for stable nuclei to form is difficult to achieve. As in most crystallization processes, even a small amount of crystals formed initially can significantly reduce segmental mobility thus limiting further crystalline growth [12]. In addition, mismatching of crystallizable chain segment length is highly probable, making crystalline growth an extremely slow event for the ethylene-propylene copolymers employed [13].

In our previous studies, the usual slow crystallization kinetics and the low degree of crystallinity achievable for random ethylene-vinyl acetate (EVA) copolymers were overcome by blending the copolymers with the appropriate size of n-alkanes [9, 14]. Unexpectedly, by matching the size of n-alkanes to the most probable crystallizable methylene segment length in the EVA, the overall degree of crystallinity can be increased beyond the expected sum from the two individual components. We found the combination of EVA that contains 28% (wt.) vinyl acetate groups matched particularly well with model alkanes of 32-36 carbons and can co-crystallize in a rapid fashion. The size of n-alkanes proven to be effective is the most probable crystallizable segment much longer than the average crystallizable length of only 18 methylene units in the EVA. It was clear that the long crystallizable segments were effective in inducing nucleation and large crystallites needed for structural stability.

In this current study, we have investigated two different types of chain configuration to achieve rapid crystallization kinetics and an increase in the degree of crystallinity. It has been established in a number of copolymers, that the blockiness of the individual components or the crystallizable sequence length distribution significantly affects the crystallization behavior in speed and morphological features formed [5-9]. If the insertion of the ethylene comonomer along the chain follows Bernouillian statistics, and since ethylene and propylene sequences do not co-crystallize, the degree of crystallinity of this type of copolymer usually is quite low [15-16]. We hypothesize that ethylene-propylene copolymers with the same composition but with chain configuration distribution that differs from random may prove to be beneficial. In these specific copolymers, instead of having a random distribution of crystallizable iPP sequences, we elect to synthesize a higher population of long iPP sequences. This larger population of long sequences is compensated by having fewer medium or shorter iPP sequences. In other words, instead of having a distribution following purely random statistics, we elect to use a bimodal distribution, with a large population of long and short iPP sequences. We would then be able to achieve a higher nucleation rate arising from the long sequences and employ the mobility of the short sequences to achieve the rapid crystallization necessary for hot melt adhesives.

Ethylene-propylene copolymers of these two types of chain configuration have been obtained by peroxide degradation during the extrusion process. The differences in their crystallization behavior are analyzed in terms of the effective crystallizable sequence length, i. e. the long runs of isotactic polypropylene sequences associated with each type of copolymer. Chain configuration analysis of propylene-ethylene copolymers

or even homopolymers can be challenging and dependent on thermal profiles used in the experiments [17]. Instead of depending only on the traditional thermal analysis, we have employed the successive self-nucleation and annealing (SSA) technique to deconvolute the endothermic melting transitions derived from DSC into various crystalline portions, formed due to the different length of crystallizable iPP sequences in polymers that incorporate some type of structural defects [4, 18]. Finally, the similarity and differences in the crystalline features and thermal stability also have been analyzed. Remarkable differences were found and are reported here.

2.2 Experimental section

2.2.1 Materials

Three propylene-ethylene copolymers were studied. Copolymer 1 was supplied by Henkel. It was degraded using peroxide (3,6,9-triethyl-3,6,9-trimethyl-1,4,7-triperoxonane was (T301)) in an extrusion process. Copolymers 2 and 3 were synthesized at Industrial Technology Research Institute (ITRI) of Taiwan. Following previous studies [19-20], the peroxides used were dicumyl peroxide (DCP) 2,5-di(tert-butylpeoxy)-2,5-dimethyl-3-hexyne (DTBHY) used in combination and T301. These peroxides were purchased from Aldrich Chemical and used without further purification. Copolymer 2 was prepared using (DCP/DTBHY in equal amounts), and Copolymer 3 was prepared using T301. The physical characteristics of the three copolymers are listed in Table 2.1. Ethylene content was determined using ^{13}C NMR in deuterated 1,1,2,2 tetrachloroethane.

Table 2.1 Physical properties of the poly(propylene-ethylene) copolymers

Samples	**Propylene mol %**	**ΔH(J/g)**	**T_m(ºC)**	**T_c(ºC)**	**$X_{C(\%)}$**
Copolymer 1	89	61	127	88	33
Copolymer 2	92	74	135	95	38
Copolymer 3	91	68	134	90	36

2.2.2 Characterization techniques employed

2.2.2.1 Thermal analysis

The crystallinity, melting and crystallization temperature were measured with a TA instrument Q100 DSC equipped with a nitrogen purged refrigerated cooling system. Temperature calibration was carried out using Indium (T_m = 156.6 °C; equilibrium heat of fusion = 28.6 J/g). For the non-isothermal crystallization studies, the samples were heated to 200 ^oC in a nitrogen atmosphere and held for 5 min in order to eliminate previous thermal history. The samples were then cooled to 0 ^oC at a rate of 10 ^oC/min in order to evaluate the crystallization behavior. The samples were then reheated to 200 ^oC to evaluate the crystallinity obtained. A value of 207 J/g was used as the equilibrium heat of fusion (ΔH_m^O) for polypropylene [21] to calculate the degree crystallinity obtained for the various ethylene-propylene copolymers.

The melting peak of these three copolymers usually exhibits a prominent peak and a shoulder (Figure 2.1). This is true even for the iPP homopolymers [22-23]. The measurements were repeated three times for each sample.

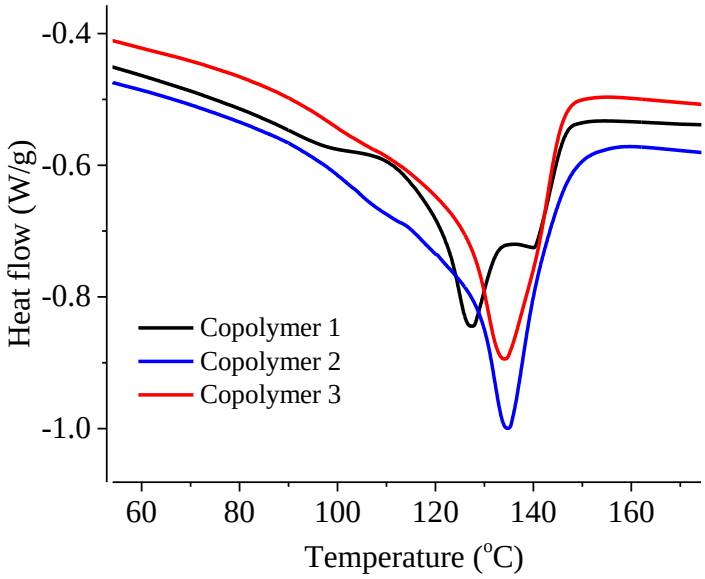

Figure 2.1 Melting peaks of the three copolymers studied

The bimodality in the melting peak detected in the copolymer 1 is a commonly observed phenomenon in PP and PP based copolymers [24-26]. The occurrence of multiple melting endotherms have been attributed to several factors such as the presence of frustrated structures polymorphic transitions, the occurrence of crystal habitat containing varying degrees of perfection and due to the presence of a recrystallization or reorganization of some crystallized fractions during the heating experiments[24-26]. In order to determine if the origin of the multiple melting transitions were from the melting recrystallization and remelting (mrr) phenomena, DSC experiments were done at different cooling rates. The existence of a single peak or the disappearance of the multiple endotherms and slow cooling rates will point to the origin of the multiple endotherms being from the mrr phenomena. The DSC experiments were carried as such: The sample was first heated to 200 ºC and equilibrated for 5 mins to eliminate thermal history inherent in the sample, different cooling rates from fast to slow cooling was

employed to vary the crystal organization in the polymer, the sample was now heated at 20 ºC/min to reveal the nature of the melting endotherm. Figure 2.2 shows the obtained melting endotherms for both copolymers 1 and 2 respectively. The figure below shows the melting endotherms for the two copolymer types. It can be observed and deduced that the multiple melting transitions still persist even at slow cooling rates, contrary to expectations of a single endotherm at slow cooling rate. This leads to other factors other than mrr as a possible cause for the existence of bimodality in the melting behavior. This will be a particularly interesting area of investigation in the future.

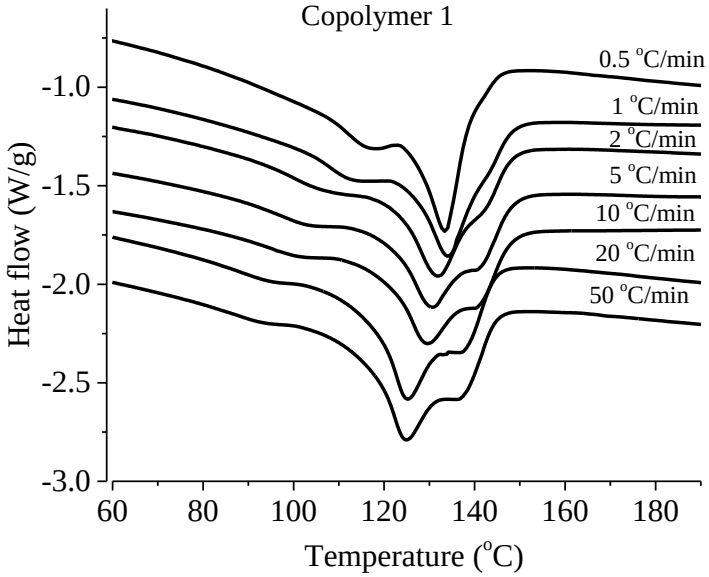

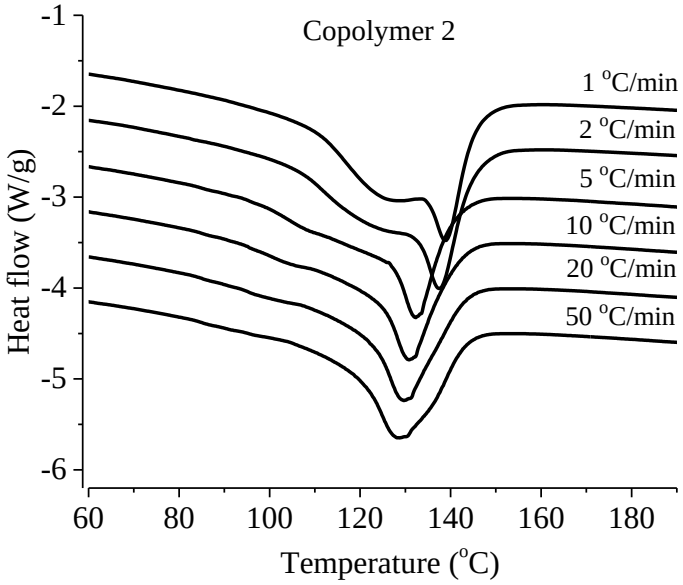

Figure 2.2 The melting transition of copolymers non-isothermally crystallized at different rates

The traditional comparison of the crystallization behavior of the homopolymers or copolymers, all experiments are carried out at a specific supercooling thus requiring the determination of the equilibrium melting point, $T_m{}^o$ for each sample. Because of the broad melting peaks measured, the Hoffman-Weeks algorithm could not be used [27]. Because of the lack of model systems the uncertainties associated with polypropylene measurements are even greater [27]. Therefore, we have carried out isothermal crystallization experiments using the end temperatures as has been suggested recently [4] as well as employing a range of isothermal crystallization temperatures as suggested in recent publications [3, 17].

2.2.2.2 Nuclear Magnetic Resonance (NMR) Spectroscopy

The ^{13}C NMR spectra were recorded at 100 °C using a Bruker DPX400 spectrometer. 10 wt vol% of polymer solutions were prepared in deuterated 1,1,2,2 tetrachloroethane. The assignment of resonances was based on published values [28-29].

2.2.2.3 Wide-angle X-ray scattering (WAXS)

WAXS measurements were performed on a Ganesha 300XL instrument (SAXSLAB ApS, Copenhagen/Denmark) equipped with a GENIX 3D microfocus X-ray source (50 kV/0.6 mA, Cu Kα, $\lambda = 0.1542$ nm) and a three-slit collimation system, a fully evacuated sample chamber and beam path, and a movable 2D Pilatus 300 K was used as the detector. WAXS images were corrected for the intensity of the primary beam, time, and sample thickness.

2.2.2.4 Fourier transform infrared spectroscopy

All infrared data were obtained using attenuated total reflectance (ATR-IR) technique or in the transmission mode. A Perkin Elmer 100 FT-IR spectrometer was utilized in both types of experiments. For all infrared data, 32 scans of 4 cm^{-1} resolution were co-added. Elevated temperature measurements to a maximum value of 160 °C were carried out using a home-built heating cell. The sample temperature was monitored using a thermocouple embedded in the sample.

2.3 Results and Discussions

2.3.1 Configurational analysis of poly(propylene-ethylene) copolymers

In order to obtain a stable structure particularly in the initial stage of crystallization from the melt, one would imagine that it would be important for copolymers to possess long crystallizable sequences that would form crystals at lower supercooling. However, the long crystallizable sequences cannot be a large fraction. If so, the sample formed would have a high degree of crystallinity but losing the elastic property needed to be an adhesive. Therefore, an ideal crystallizable sequence distribution should contain a significant fraction of long chains but also a significant fraction of short chains in order to maintain segmental mobility when a higher supercooling occurs during the cooling process. Therefore the most crucial aspect of this study is to control the crystallizable iPP sequence length distribution. Once formed, the configuration needs to be determined accurately. In this study, we have determined the chain configuration using two different methods, a thermal fractionation method (SSA) and NMR.

2.3.2 Thermal fractionation method

Various thermal fractionation techniques to ascertain sequence distribution have been well established [4, 18, 30-31]. We have given particular emphasis to the Self-nucleation/Annealing technique (SSA) developed previously. [4, 18, 30-31] This technique allows sufficient time and mobility for the different crystallizable chain segments in the distribution to separately crystallize. The maximum crystallization rate of each sample is dependent on

the nucleation density and segmental mobility. The nucleation density decreases with decreasing supercooling ($\Delta T=T_m-T_c$), whereas the segmental mobility increases with decreasing ΔT. By crystallizing from a molten state to lower temperatures successively, it is possible to fractionate the longer crystallizable segments from shorter ones. As the T_c decreases sequentially, crystals of different lamellar thicknesses form, corresponding to the sequence length distribution found in each copolymer. A number of thermal fraction techniques are available to determine the distribution of crystallizable segments in various copolymers. [9, 32-33] Because of its efficiency, we have consistently used SSA. [4, 18, 30-31]

This SSA technique requires the determination of the temperature that exhibits the highest self-nucleation rate and sets that temperature as the initial point and subsequently lowers the temperature step-wise as a function of time. Following the procedure developed previously, for Copolymers 1, 2 and 3, the initial T_s has been measured to be 146, 153 and 148 °C, respectively. [9, 31, 34] This temperature should be low enough to preserve the small crystal fragments that can self-seed the polymer during cooling. Our values are obtained following the procedure described previously [18]. The DSC data for copolymer 3 is shown in Figure 2.4. The Ts for this copolymer as other two samples is described as the minimum temperature when the peak at 148 °C due to annealing is absent [4, 18]. The heating profile used in our experiments are shown in Figure 2.3. The thermal data for copolymer 3, as an example, obtained using such a thermal profile is shown in Figure 2.4.

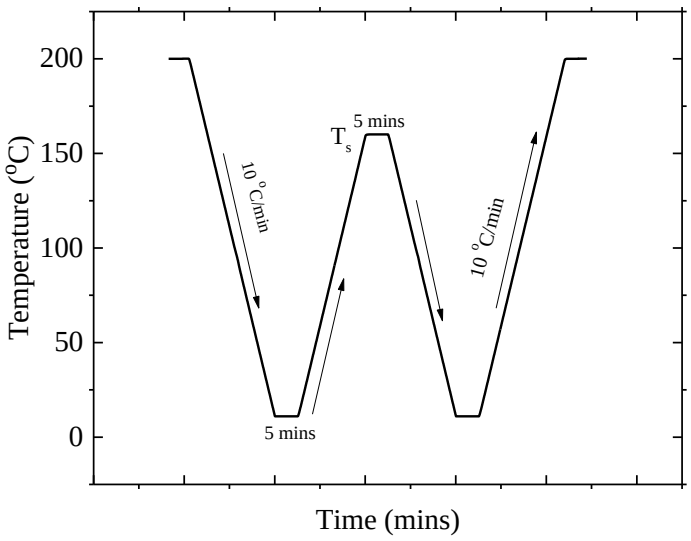

Figure 2.3 Thermal profile used in the determination of Ts for each sample

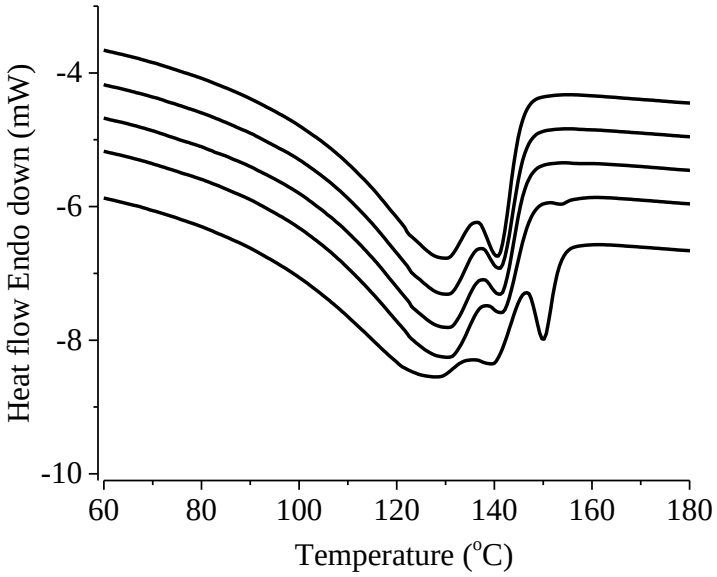

Figure 2.4 The DSC data obtained for Copolymer 3 using the thermal profile as shown in

Figure 2.3 From top to bottom, the data are obtained at an annealing temperature of 150, 148, 147, 144 and 140 °C.

Using measured T_s's, each copolymer was successively nucleated and crystallized at a 5 °C interval as shown schematically in Figure 2.5 12 cycles were used for each sample. Five-minute intervals were used at each temperature. The following melting data obtained for the samples crystallized in this way are shown in Figure 2.6.

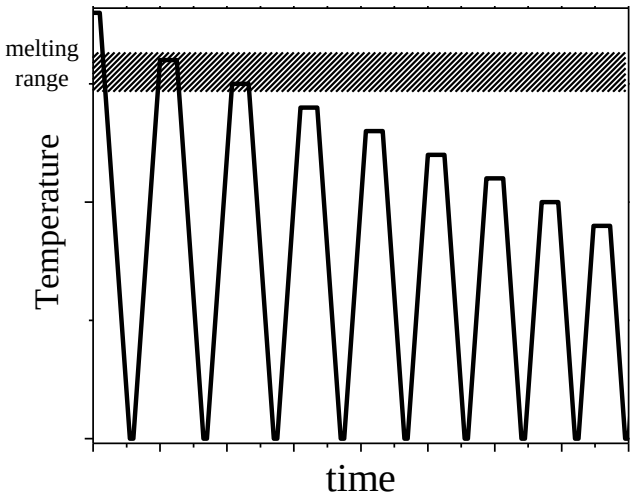

Figure 2.5 Thermal profile used in SSA thermal fractionation procedure

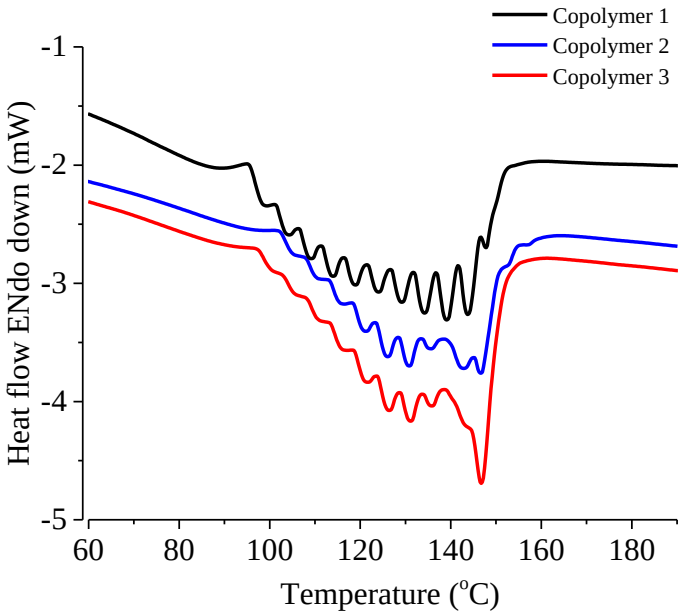

Figure 2.6 Heating curves from thermal fractionation experiment for the three copolymers

The appearance of a series of melting peaks in the heating curves of each copolymer indicates that thermal fractionation has occurred during SSA treatment and each peak corresponds to the melting of a particular lamellar population. The crystals obtained at the lowest supercooling with the thickest lamellae melt at higher temperatures. Conversely, the thinner crystals melt at lower temperatures. The lamellae thickness of the crystals has a wide distribution in these copolymers and directly reflects the broad distribution of the crystallizable iPP chain segment length in each sample. Compared to Copolymers 2 and 3, Copolymer 1 has a significant fraction of short crystallizable propylene sequences and forms smaller and thinner crystals. On average, Copolymers 2 and 3 have more long sequences of crystallizable propylene units with Copolymer 2 possessing the most.

Our interpretation of the DSC data depends on the assumption that all propylene sequences crystallize into the same form. In fact, the characteristic diffractions for crystalline iPP at 14.2, 16.8, 18.6 and 21.9 ^{o} are all observed as shown in Figure 2.7 [35-36]. There are some differences in the diffraction peaks observed for the two types of copolymers. To the best of our knowledge, no systematic studies exist for this type of polypropylene-ethylene copolymer. The small differences observed for the two types of chain configurations used in this study are not surprising. Previous studies of ethylene dominated PE/PP copolymer suggest that differences in spacing may be correlated to the presence of configurational defects [37]. Small shifts in diffraction peaks have also been observed for propylene-ethylene and propylene-butene copolymers [38-39]. In that case, the observed shifts of some of the reflections were also attributed to an expansion of the crystal lattice upon the incorporation of the comonomer defect. No X-ray evidence of polyethylene crystals was found in our study.

In addition, we also did not observe the typical crystal field splitting expected for the polyethylene orthorhombic unit cells in all infrared data [40]. Based on these considerations, all the peaks observed in the thermal data are attributed to the same crystalline form of polypropylene.

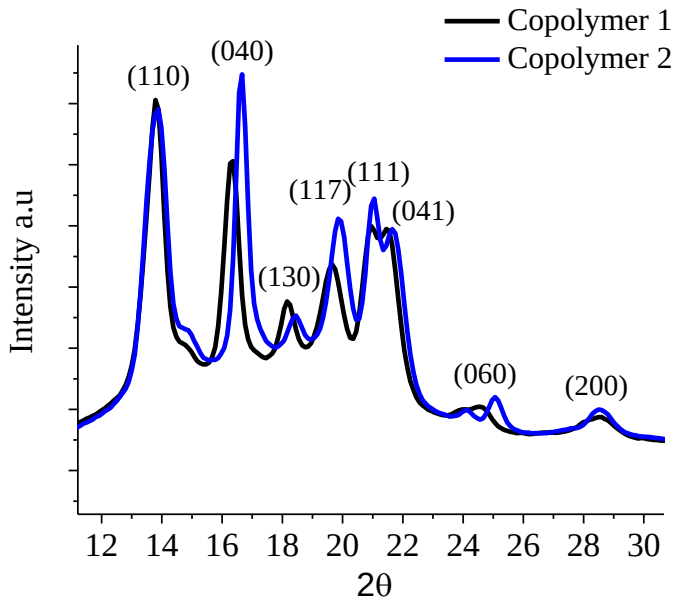

Figure 2.7 Wide angle X-ray Diffraction of copolymer samples crystallized at 105 ^{o} C

2.3.3 NMR analysis of chain configuration

^{13}C-NMR spectroscopy has been shown to be a powerful technique for characterizing the detailed molecular structure of copolymer chains, including the monomer sequence distribution and compositional variations. [41] Following the convention used in previous studies, Table 2.2 shows the integrated intensity for the different carbon atoms in the ^{13}C-NMR spectra of the three different copolymers. [28-29] The chemical composition of each copolymer was calculated from the scheme proposed earlier. [29, 41] The ethylene contents of

the three copolymers were found to be 8 to 9 mol % (Table 1) with the rest being propylene. [42-43]. The dyad and triad sequences are also shown in Table 2.2.

Table 2.2 Integrated intensities for the carbon atoms in propylene–ethylene copolymer in 13C-NMR spectra

Sequence	Copolymer 1	Copolymer 2	Copolymer 3
P	0.89	0.92	0.91
E	0.09	0.08	0.09
PPP	0.70	0.80	0.77
PPE	0.03	0.11	0.11
EPE	0.15	0.01	0.01
PEP	0.08	0.05	0.08
EEP	0.00	0.02	0.01
EEE	0.01	0.01	0.01
PP	0.76	0.86	0.83
PE	0.16	0.12	0.15
EE	0.01	0.01	0.02

The NMR data, because of the limited number of sequences that can be measured, cannot be used to directly establish the stereoregularity of the propolylene sequences. However, the measurable dyad and triad populations are consistent with the thermal fractionation analysis presented above. As expected, the triad propylene sequence lengths exhibit the greatest differences for the 3 copolymers with the highest percentage formed for Copolymer 2. This copolymer also has the largest percentage of long propylene sequences in

the thermal fractionation data shown in Figure 2.6. The sequences of the crystallizable propylene segments in Copolymers 2 and 3 are definitely less random than for Copolymer 1.

Based on the NMR data, the number-average sequences of propylene and ethylene comonomer units are tabulated in Table 2.3, from which it is apparent that in all the copolymers the average ethylene sequence length is very short, reaching to about a value of 1.31 corresponding to isolated E or EE units. This is consistent with the lack of polyethylene crystalline features in either the infrared or the X-ray data.

Table 2.3 Number-average ethylene and propylene sequence lengths in the copolymers

Samples	n_p	n_e
Copolymer 1	10.74	1.13
Copolymer 2	15.08	1.24
Copolymer 3	12.36	1.31

2.3.4 Stereoregularity of each copolymer; their meso-sequence length

In addition to the composition analysis shown above, based on the SSA thermal data, we intend to provide a more quantitative analysis of the SSA data obtained for the three copolymers. Each peak in the SSA data corresponds to the melting temperature of a specific lamellar thickness. Therefore, the relative areas associated with the "peaks," or the relative amount of specific crystallizable iPP sequences, provide a description of the chain configuration. It is then possible to determine the average stereoregularity of the iPP sequences in various polypropylene samples. [32-33]

Using Copolymer 1 as an example, its SSA plot was subdivided into 11 fractions as is shown in Figure 2.8. As used previously, an experimental parameter, Meso-Sequence Length (MSL), can then be obtained to characterize the stereoregularity of the copolymer using the following expression:

Equation 2.1 $$MSL = 3\frac{l}{c}$$

Where, l is the lamellae thickness, and c is the height of a unit cell of a monoclinic crystalline form, which is 0.65 nm [44]. The prefactor of 3 is used since there are 3 monomer units in a 3_1 helix of iPP. We have used the analysis based Thompson-Gibbs equation published previously to calculate the lamellae thickness and the Meso Sequence Length associated with each fraction of the three copolymers (Table 2.4) [32-33]. This table also shows a value known as the average isotactic sequence length, which describes the average of the total isotactic sequence present in the copolymer studied.

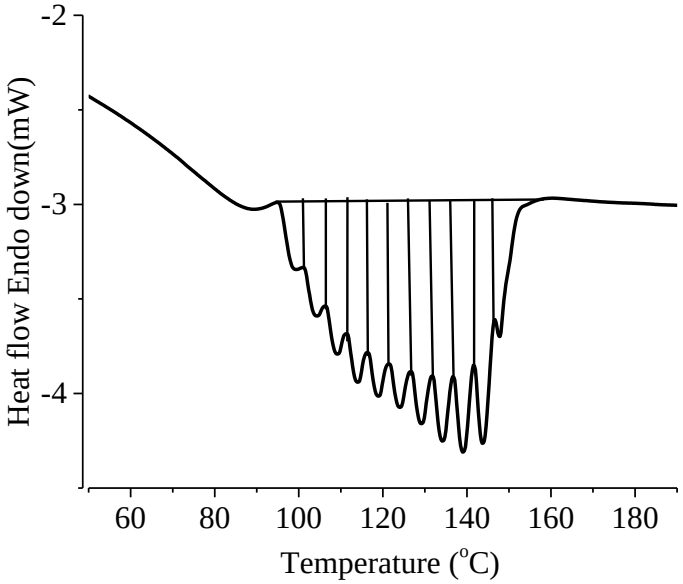

Figure 2.8 Representative SSA plots using Copolymer 1 divided into 11 sections

Table 2.4 Average isotactic sequence length calculated for Copolymer 1

Percent area	Temperature/ °C	MSL	Lamellae thickness (nm)
3.41	98.83	36.31	7.87
5.71	104.42	38.27	8.29
8.02	109.31	40.16	8.70
9.17	113.98	42.16	9.13
10.88	118.88	44.48	9.64
10.67	124.02	47.20	10.20
11.32	129.15	50.27	10.90
11.96	134.29	53.78	11.70
12.15	138.96	57.41	12.40
11.15	143.63	61.58	13.30
5.56	147.86	65.91	14.30

The three copolymers possess the MSLs that would be expected. Copolymers 1, 2 and 3 have MSLs of 50, 53 and 52 respectively. This is consistent with the fact that SSA and NMR have already established that Copolymer 1 has the shortest crystallizable propylene sequences in its distribution as compared to Copolymers 2 and 3.

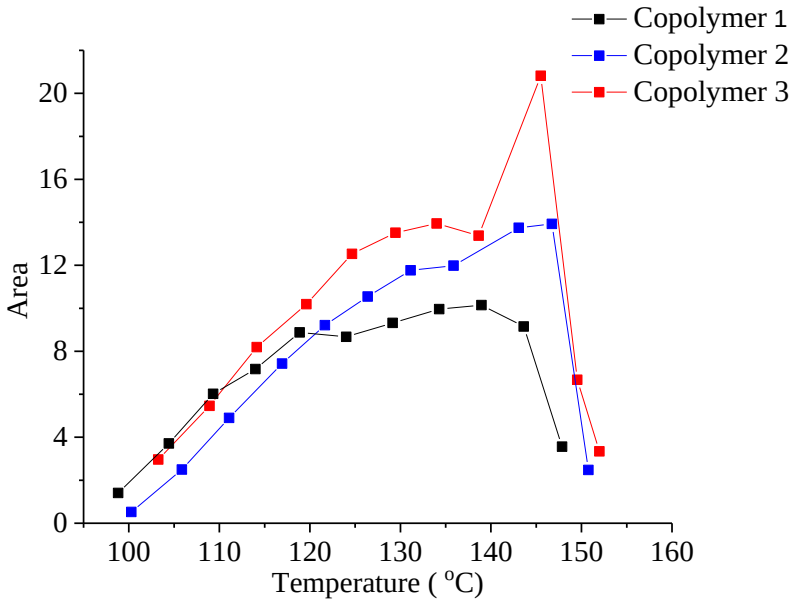

Figure 2.9 Curve showing summary of SSA analysis

Figure 2.9 represents a summary of the crystallization area fraction versus temperature for the three copolymer types. From the curves above the clear distinction between a random and a bimodal distribution is established. As used in this work, bimodal chain configuration refers to the way the sequence length distribution is arranged in the copolymers 2 and 3 respectively. This may be as a result of bimodality in the molecular weight distribution. However, GPC results do not show any traces of bimodality, so the bimodality in these copolymers talks about the manner in which the polymers are

distributed along the polymer chain. Different from the copolymers 1 in which there is a random distribution of the chain configuration, in the bimodal case, we believe that the crystal thickness distribution is arranged in a "random blocky" way in which the polymer crystallites are separated into two distinct crystal thickness populations, and, therefore, a bimodal thickness distribution, this bimodality is revealed to a greater degree in the SSA curves shown in our subsequent studies.

2.3.5 Crystallization behavior of the different types of copolymers

As described above, one of the most important characteristics in the determination of the setting speed of the olefin based hot melt adhesives is the crystallization rate of the crystallizable sequences in the polymers used. As these samples cool from the melt, the exotherm is typically used to represent the onset of the crystallization process. There are substantial differences in T_c's measured for the two types of copolymers. But as shown above, the melting endotherms (Figure 2.1) are similar to a primary melting peak at ~145 °C with a broad distribution on the lower temperature side.

As illustrated previously [9, 14] the crystallization kinetics of each sample can be carried out using an isothermal technique. In the current study, we have used two different techniques reaching the same conclusion, i. e. the copolymer #2 exhibits the most rapid crystallization kinetics as shown in Figure 2.10. As described above, the equilibrium melting temperature cannot be determined definitively [27].

By setting the sample at 50 degrees below the end melting temperature determined as describe above and in previous publications [4], it is then possible to assess

the crystallization kinetics in terms of the degree of crystallinity formed as a function of time. These are shown in Figure 2.11. There are 2 methods that use somewhat different crystallization temperatures [3-4]. Alternatively it is also possible to use a crystallization temperature at ~25 degrees below the lowest measurable melting temperature. Both methods lead to the same conclusion. It is clear that there are significant differences for the three copolymers. Copolymer 1 with the most random configuration clearly exhibits the slowest kinetics. In contrast, Copolymer #2 with the longest propylene sequences crystallized most rapidly. The key point of our study is to explain the relationship between the chain configuration, i. e. the crystallizable segment length distribution of each sample, to the overall crystallization behavior, both the kinetics of crystallization and the degree of crystallinity achieved.

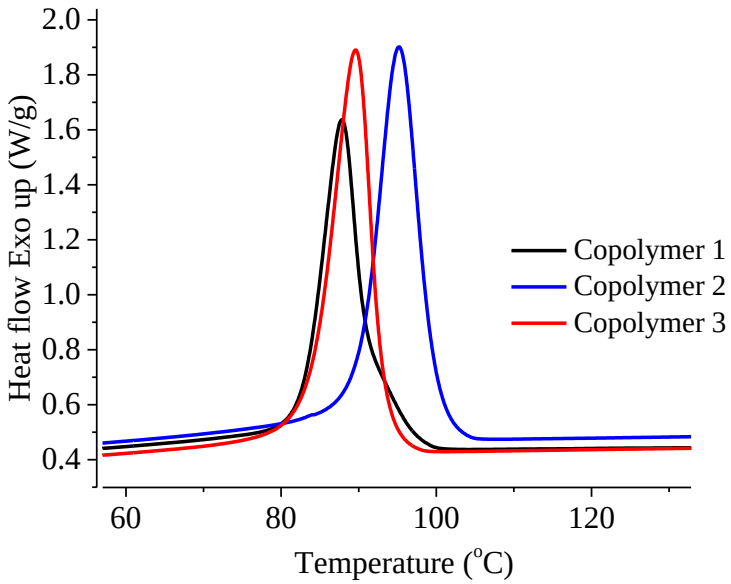

Figure 2.10 Cooling curve showing the crystallization temperatures of the copolymers

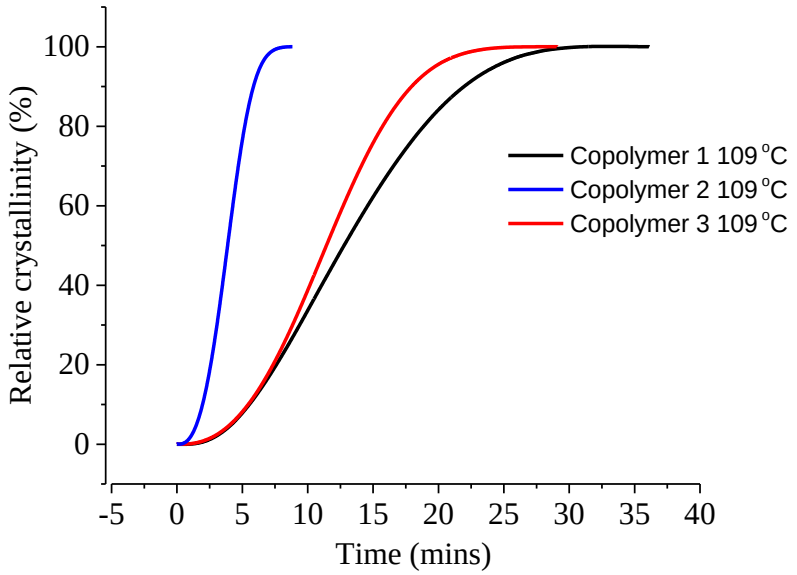

Figure 2.11 Crystallization kinetics observed for each copolymer

The crystallization isotherms obtained for each of the copolymer samples were further analyzed according to the Avrami equation [45] in the following form :

Equation 2.2 $$1 - X_t = \exp(-Kt^n)$$

Where X_t represents the crystallinity, k is the crystallization rate constant due to the nucleation and growth process, and n represents the Avrami exponent which depends on the nature of nucleation and spatial dimensions of crystal growth process. The methods described by Lorenzo has been taken into detailed consideration during the analysis [45]. The crystallization data obtained for a range of crystallization temperatures are reported in Table 2.5. The half time of crystallization $t_{1/2}$ corresponds to the time at which crystallization has reached 50%. A higher $t_{1/2}$ is indicative of slower kinetics while a lower value represents faster crystallization speed. The bimodally distributed copolymers

shower faster kinetics as compared to the copolymer following random chain distribution as is described by their $t_{1/2}$ values.

Table 2.5 Avrami parameters obtained from crystallization isotherms for a range of crystallization temperatures

Samples	**Tc (°C)**	**n**	**k(min^{-n})**	**$t^{½}$**
Copolymer 1	105	2.53	0.0092	5.51
	107	2.51	0.00377	7.98
	109	2.58	0.00121	11.72
Copolymer 2	105	3	0.227	1.451
	107	2.987	0.0567	2.3
	109	2.91	0.01572	3.673
Copolymer 3	105	3.05	0.00618	4.7
	107	2.91	0.00228	7.13
	109	2.64	0.00145	10.351

As shown in Figure 2.10, when crystallizing from the melt, the crystallization temperature (T_c) of the non-isothermal crystallization process shifts to higher temperatures for Copolymers 2 and 3 as compared to Copolymer 1. The longer propylene segments in the former favor the formation of stable nuclei thus accelerating the crystallization significantly, represented by the higher T_c's. One also should not ignore the mobility of each type of chain configuration. From the NMR data obtained, the average flexible ethylene sequence length is longer in Copolymers 2 and 3 as compared to Copolymer 1, thus showing higher mobility. Consequently, with the bimodal configuration, Copolymers 2 and 3 can crystallize faster than Copolymer 1. Moreover, the exotherm of Copolymer 1 widens appreciably with a concurrent decrease in enthalpy, also indicating increasing difficulty to crystallize. All this

evidence suggests Copolymer 1, a more random copolymer, crystallizes more slowly as compared to Copolymers 2 and 3 at same crystallization condition.

2.3.6 Morphology observed for the three copolymers and properties derived

The primary purpose using these propylene-based copolymers in hot melt adhesives is to increase adhesive performance at elevated temperatures. Stability of the crystalline state in the three copolymers was studied by using infrared spectroscopy and DSC. The infrared active crystalline features have been identified using attenuated total reflectance infrared. Figure 2.12 shows the representative infrared spectra of Copolymer 3. There are a number of conformationally sensitive bands in the 700 to 1200 cm^{-1} region [46-47]. All these regularity of bands at 809, 841, 898, 943, 973, 998, 1103 cm^{-1} characteristic of iPP helix are found in the spectra obtained for these 3 copolymers. Specific absorption bands have also been correlated to the "size" of the polypropylene crystalline units [46, 48-50].Bands at 973, 1103, 809, 898, 998, 841, and 943 cm^{-1} have been assigned to crystalline units of 3, 6, 7, 8, 10, 12 and >14 monomer units long, respectively. The relative intensity of several bands, normalized to the conformationally insensitive bands at 1460 cm^{-1}, such as the 898 (n=8), 998 (n=10), 841 (n=12), 1220 (n=14), 943 (n>14)cm^{-1} is shown in Table 2.6. Based on our data it is clear that Copolymers 2 and 3 have larger crystallites than Copolymer #1. This is consistent with previous observations for various iPP samples [32-33].Copolymers 2 and 3 exhibit similar infrared features. But the conformationally sensitive bands are broader in Copolymer 1 as compared to the other two copolymers. This difference in bandwidth suggests a higher degree of structural disorder associated with Copolymer 1. This is consistent with the

considerably larger population of short iPP segments in the crystallizable segment distribution.

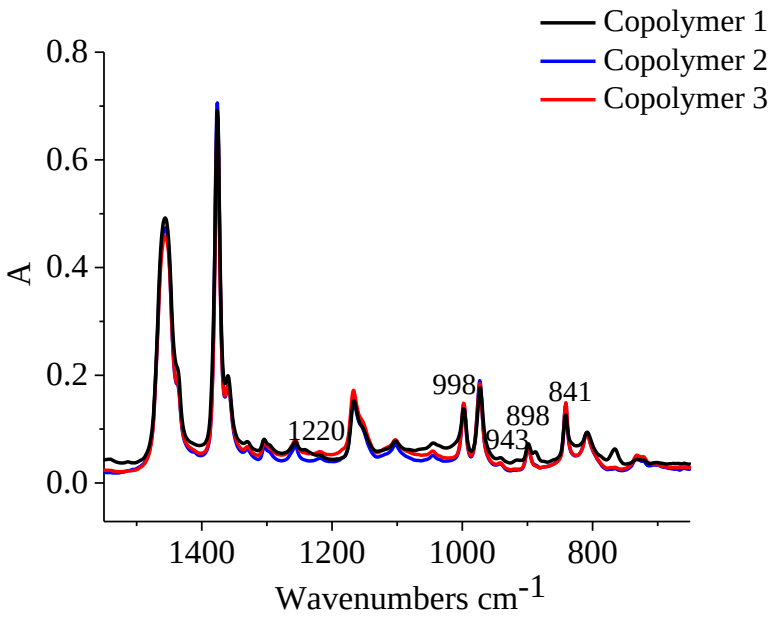

Figure 2.12 ATR-FTIR spectra of the various samples showing the regularity band range of frequencies

Table 2.6 Integrated intensity of regularity band in respective copolymers

	Integrated intensity		
Regularity Band (cm^{-1})	Copolymer 1	Copolymer 2	Copolymer 3
841	0.0045	0.0060	0.0063
898	0.3700	0.3900	0.4100
943	0.0400	0.0500	0.0600
998	0.7200	0.8600	0.8800

1220	0.0001	0.0041	0.0048

2.4 Conclusions

Two different types of chain configurations were studied, one random or following Bernoullian distribution, and the other exhibiting a bimodal distribution in crystallizable propylene sequences. Average sequence length and the distribution of propylene sequences of random PP-PE copolymers was experimentally determined by using ^{13}C-NMR. The actual distribution of crystallizable propylene sequences was obtained using a thermal fractionation technique (SSA).

The effect of sequence distribution of the propylene chains on the crystallization behavior of PP-PE copolymers was significant. The detailed crystallization behavior and the morphology formed have been investigated by using DSC and infrared spectroscopy. Longer sequence length led to an increase in T_c of PP-PE copolymer. The isothermal crystallization study demonstrated that the crystallization rate of PP-PE copolymer was increased with an increase in the sequence length of PP. From this comparison, it was concluded that the length of crystallizable sequences determines the crystallization temperature and the degree of crystallinity. It is possible that the longer ethylene sequence length between propylene segments enhances the mobility of copolymer chains, thus favoring the crystallization kinetics of copolymers containing a bimodal distribution of PP sequences. This study provides additional guidance in designing copolymers to act as special adhesives for use at elevated temperatures.

2.5 References

1. Benedek, I.; Feldstein, M. M., *Technology of pressure-sensitive adhesives and products*. CRC Press: 2008.
2. Bedia, E. L.; Astrini, N.; Sudarisman, A.; Sumera, F.; Kashiro, Y., Characterization of polypropylene and ethylene–propylene copolymer blends for industrial applications. *Journal of applied polymer science* **2000,** *78* (6), 1200-1208.
3. Hosier, I.; Alamo, R.; Esteso, P.; Isasi, J.; Mandelkern, L., Formation of the α and γ polymorphs in random metallocene-propylene copolymers. Effect of concentration and type of comonomer. *Macromolecules* **2003,** *36* (15), 5623-5636.
4. Sangroniz, L.; Cavallo, D.; Santamaria, A.; Müller, A. J.; Alamo, R. G., Thermorheologically Complex Self-Seeded Melts of Propylene–Ethylene Copolymers. *Macromolecules* **2017**.
5. Rahaman, M.; Tsuji, H., Isothermal crystallization and spherulite growth behavior of stereo multiblock poly (lactic acid) s: effects of block length. *Journal of Applied Polymer Science* **2013,** *129* (5), 2502-2517.
6. Michell, R. M.; Müller, A. J.; Deshayes, G.; Dubois, P., Effect of sequence distribution on the isothermal crystallization kinetics and successive self-nucleation and annealing (SSA) behavior of poly (ε-caprolactone-co-ε-caprolactam) copolymers. *European Polymer Journal* **2010,** *46* (6), 1334-1344.
7. Michell, R. M.; Muller, A. J.; Castelletto, V.; Hamley, I.; Deshayes, G.; Dubois, P., Effect of Sequence Distribution on the Morphology, Crystallization, Melting,

and Biodegradation of Poly (ε-caprolactone-co-ε-caprolactam) Copolymers. *Macromolecules* **2009,** *42* (17), 6671-6681.

8. Hosoda, S.; Nozue, Y.; Kawashima, Y.; Suita, K.; Seno, S.; Nagamatsu, T.; Wagener, K. B.; Inci, B.; Zuluaga, F.; Rojas, G., Effect of the Sequence Length Distribution on the Lamellar Crystal Thickness and Thickness Distribution of Polyethylene: Perfectly Equisequential ADMET Polyethylene vs Ethylene/α-Olefin Copolymer. *Macromolecules* **2010,** *44* (2), 313-319.
9. Kalish, J.; S, R.; Wamuo, O.; Vyavahare, O.; Y, W.; SL, H.; Paul, C.; Eodice, A., Role of n-alkane-based Additives in hot melt adhesives. *International Journal of Adhesion and Adhesives* **2014,** *(in press).*
10. Reid, B. O.; Vadlamudi, M.; Mamun, A.; Janani, H.; Gao, H.; Hu, W.; Alamo, R. G., Strong memory effect of crystallization above the equilibrium melting point of random copolymers. *Macromolecules* **2013,** *46* (16), 6485-6497.
11. Crist, B.; Howard, P., Crystallization and melting of model ethylene-butene copolymers. *Macromolecules* **1999,** *32* (9), 3057-3067.
12. Horst, R. H.; Winter, H. H., Stable Critical Gels of a Crystallizing Copolymer of Ethene and 1-Butene. *Macromolecules* **2000,** *33* (1), 130-136.
13. Jeon, K.; Palza, H.; Quijada, R.; Alamo, R. G., Effect of comonomer type on the crystallization kinetics and crystalline structure of random isotactic propylene 1-alkene copolymers. *Polymer* **2009,** *50* (3), 832-844.
14. Kalish, J. P.; Ramalingam, S.; Bao, H. M.; Hall, D.; Wamuo, O.; Hsu, S. L.; Paul, C. W.; Eodice, A.; Low, Y. G., An analysis of the role of wax in hot melt adhesives. *International Journal of Adhesion and Adhesives* **2015,** *60*, 63-68.

15. Zimmermann, H.; Hoechst, A., Structural analysis of random propylene-ethylene copolymers. *Journal of Macromolecular Science, Part B: Physics* **1993,** *32* (2), 141-161.

16. Gahleitner, M.; Jääskeläinen, P.; Ratajski, E.; Paulik, C.; Reussner, J.; Wolfschwenger, J.; Neißl, W., Propylene–ethylene random copolymers: Comonomer effects on crystallinity and application properties. *Journal of Applied Polymer Science* **2005,** *95* (5), 1073-1081.

17. Janevski, A.; Bogoeva-Gaceva, G.; Grozdanov, A., Crystallization and melting behavior of iPP studied by DSC. *Journal of applied polymer science* **1998,** *67*, 395-404.

18. Müller, A. J.; Michell, R. M.; Pérez, R. A.; Lorenzo, A. T., Successive Self-nucleation and Annealing (SSA): Correct design of thermal protocol and applications. *European Polymer Journal* **2015,** *65*, 132-154.

19. Thitithammawong, A.; Nakason, C.; Sahakaro, K.; Noordermeer, J., Effect of different types of peroxides on rheological, mechanical, and morphological properties of thermoplastic vulcanizates based on natural rubber/polypropylene blends. *Polymer Testing* **2007,** *26* (4), 537-546.

20. Badrossamay, M. R.; Sun, G., A study of radical graft copolymerization on polypropylene during extrusion using two peroxide initiators. *Polymer International* **2010,** *59* (2), 155-161.

21. Xu, J.; Srinivas, S.; Marand, H.; Agarwal, P., Equilibrium Melting Temperature and Undercooling Dependence of the Spherulitic Growth Rate of Isotactic Polypropylene. *Macromolecules* **1998,** *31* (23), 8230-8242.

22. Paukkeri, R.; Lehtinen, A., Thermal behaviour of polypropylene fractions: 2. The multiple melting peaks. *Polymer* **1993,** *34* (19), 4083-4088.

23. Petraccone, V.; De Rosa, C.; Guerra, G.; Tuzi, A., On the double peak shape of melting endotherms of isothermally crystallized isotactic polypropylene samples. *Die Makromolekulare Chemie, Rapid Communications* **1984,** *5* (10), 631-634.

24. Samuels, R. J., Quantitative structural characterization of the melting behavior of isotactic polypropylene. *Journal of Polymer Science Part B: Polymer Physics* **1975,** *13* (7), 1417-1446.

25. Kardos, J.; Christiansen, A.; Baer, E., Structure of pressure-crystallized polypropylene. *Journal of Polymer Science Part B: Polymer Physics* **1966,** *4* (5), 777-788.

26. Pae, K., γ–α Solid–solid transition of isotactic polypropylene. *Journal of Polymer Science Part B: Polymer Physics* **1968,** *6* (4), 657-663.

27. Alamo, R. G.; Viers, B. D.; Mandelkern, L., A re-examination of the relation between the melting temperature and the crystallization temperature: linear polyethylene. *Macromolecules* **1995,** *28* (9), 3205-3213.

28. Carman, C.; Harrington, R.; Wilkes, C., Monomer sequence distribution in ethylene-propylene rubber measured by 13C NMR. 3. Use of reaction probability model. *Macromolecules* **1977,** *10* (3), 536-544.

29. Cheng, H., Carbon-13 NMR analysis of ethylene-propylene rubbers. *Macromolecules* **1984,** *17* (10), 1950-1955.

30. Muller, A. J.; Hernandez, Z. H.; Arnal, M. L.; Sanchez, J. J., Successive self-nucleation/annealing (SSA): A novel technique to study molecular segregation during crystallization. *Polymer Bulletin* **1997,** *39,* 465-472.

31. Muller, A. J.; Arnal, M. L., Thermal fractionation of polymers. *Progress in Polymer Science* **2005,** *30,* 559-603.

32. Kang, J.; Wang, B.; Peng, H.; Chen, J.; Cao, Y.; Li, H.; Yang, F.; Xiang, M., Investigation on the structure and crystallization behavior of controlled-rheology polypropylene with different stereo-defect distribution. *Polymer Bulletin* **2014,** *71* (3), 563-579.

33. Horváth, Z.; Menyhárd, A.; Doshev, P.; Gahleitner, M.; Varga, J.; Tranninger, C.; Pukánszky, B., Chain regularity of isotactic polypropylene determined by different thermal fractionation methods. *Journal of Thermal Analysis and Calorimetry* **2014,** *118* (1), 235-245.

34. Fillon, B.; Wittmann, J. C.; Lotz, B.; Thierry, A., Self-Nucleation and Recrystallization of Isotactic Polypropylene (Alpha-Phase) Investigated by Differential Scanning Calorimetry. *Journal of Polymer Science Part B-Polymer Physics* **1993,** *31* (10), 1383-1393.

35. Nedkov, E.; Dobreva, T., Wide and small-angle X-ray scattering study of isotactic polypropylene gamma irradiated in bulk. *European Polymer Journal* **2004,** *40* (11), 2573-2582.

36. Feng, Y.; Hay, J., The characterisation of random propylene–ethylene copolymer. *Polymer* **1998,** *39* (25), 6589-6596.

37. Lieser, G.; Wegner, G.; Smith, J. A.; Wagener, K. B., Morphology and packing behavior of model ethylene/propylene copolymers with precise methyl branch placement. *Colloid and Polymer Science* **2004,** *282* (8), 773-781.

38. Mileva, D.; Androsch, R.; Funari, S. S.; Wunderlich, B., X-ray study of crystallization of random copolymers of propylene and 1-butene via a mesophase. *Polymer* **2010,** *51* (22), 5212-5220.

39. Bartczak, Z.; Chiono, V.; Pracella, M., Blends of propylene-ethylene and propylene-1-butene random copolymers: I. Morphology and structure. *Polymer* **2004,** *45* (22), 7549-7561.

40. Krimm, S.; Liang, C.; Sutherland, G., Infrared spectra of high polymers. II. Polyethylene. *The Journal of Chemical Physics* **1956,** *25* (3), 549-562.

41. Randall, J. C., Methylene sequence distributions and number average sequence lengths in ethylene-propylene copolymers. *Macromolecules* **1978,** *11* (1), 33-36.

42. Randall, H., Polymer sequence determination (the 13C method). Academic Press: New York: 1977.

43. Randall, J. C., A review of high resolution liquid 13carbon nuclear magnetic resonance characterizations of ethylene-based polymers. *Journal of Macromolecular Science—Reviews in Macromolecular Chemistry and Physics* **1989,** *29* (2-3), 201-317.

44. Wunderlich, B., *Macromolecular Physics, Volume 1. Crystal Structure, Morphology, Defects.* Academic Press, Inc.: New York, 1973; p 549.

45. Lorenzo, A. T.; Arnal, M. L.; Albuerne, J.; Müller, A. J., DSC isothermal polymer crystallization kinetics measurements and the use of the Avrami equation to fit the

data: Guidelines to avoid common problems. *Polymer Testing* **2007,** *26* (2), 222-231.

46. Geng, Y.; Wang, G.; Cong, Y.; Bai, L.; Li, L.; Yang, C., Shear-induced nucleation and growth of long helices in supercooled isotactic polypropylene. *Macromolecules* **2009,** *42* (13), 4751-4757.

47. Luongo, J., Infrared study of polypropylene. *Journal of Applied Polymer Science* **1960,** *3* (9), 302-309.

48. Ruiz-Orta, C.; Fernandez-Blazquez, J.; Pereira, E.; Alamo, R., Time-resolved FTIR spectroscopic study of the evolution of helical structure during isothermal crystallization of propylene 1-hexene copolymers. Identification of regularity bands associated with the trigonal polymorph. *Polymer* **2011,** *52* (13), 2856-2868.

49. An, H.; Li, X.; Geng, Y.; Wang, Y.; Wang, X.; Li, L.; Li, Z.; Yang, C., Shear-induced conformational ordering, relaxation, and crystallization of isotactic polypropylene. *The Journal of Physical Chemistry B* **2008,** *112* (39), 12256-12262.

50. Reddy, K. R.; Tashiro, K.; Sakurai, T.; Yamaguchi, N.; Sasaki, S.; Masunaga, H.; Takata, M., Isothermal crystallization behavior of isotactic polypropylene H/D blends as viewed from time-resolved FTIR and synchrotron SAXS/WAXD measurements. *Macromolecules* **2009,** *42* (12), 4191-4199.

CHAPTER 3
ALTERATION OF THERMOPLASTIC POLYURETHANE PROPERTIES BY TUNING CHAIN-EXTENDER ARCHITECTURE

3.1 Introduction

This chapter focuses on the utilization of TPUs for HMAs application. Polyurethanes are highly polar thus possessing self-adhesive properties which enables bonding to a broad range of substrates[1]. This self-adhering property of polyurethanes become even more attractive in the HMAs industry since components such as tackifiers, waxes, and other components which are typically added to promote adhesion in non-polar polymer systems need not be incorporated in a TPU system. From an engineering perspective, the reduction in the number of components thus reduces the tendency for interfacial failures to occur between the adhesive and substrate to be bonded since the presence of weak boundary layer, which is a consequence of having multiple non-homogenous components in the formulation will be eliminated by using just the TPU material. TPUs have great prospects for use as HMAs, to, however, optimize these prospects, some limiting factors have to be eliminated. One of such factors is the long time taken for morphological development in traditional TPU systems; this influences the speed of cohesive strength formation. Thus with traditional TPUs, rapid formation of cohesive property can be an issue. In this section, we have elected to obtain rapid morphology formation by changing the chain extender architecture.

Polyurethanes are synthesized from the reaction of a polyol, a diisocyanate and chain extender. The polyol serves as the soft segment matrix, which provides elasticity to the resultant polymer structure while the reaction between the diisocyanates, of which the

MDI and TDI are the most commercially used, and chain extenders constitute the hard segment (HS), which is responsible for the strength and rigidity of the TPU material[2]. Chain extenders are vitally relevant since they are not only used to increase the molecular weight of the polymer but also to control morphological properties such as the degree of phase separation amongst other properties[3]. The chain extenders could comprise of diol, amine, and even carboxylic acid functional group, all having the potential to control the morphology. In the midst of the abundant chain extender functionalities available for controlling morphology, it is therefore intriguing that only chain extenders based on 1,4-BDO have gained prevalence in polyurethane studies. The prevalence of the use of the 1,4-BDO chain extender may be due to the excellent phase separation obtained from this chain extender type This chain extender has been shown to adopt a low energy fully extended chain conformation and also possesses the adequate structural and geometric requirement for the formation of optimal hydrogen bonding interactions between its HS, therefore, leading to the creation of phase-separated domains.[4-6]

Thermoplastic polyurethanes based on the traditional 1,4-BDOs are heat processable. At high temperatures, its inherent hydrogen bond is broken down, and at low temperatures, reformation of the hydrogen bonds occurs making TPUs heat reversible. Even though this traditional PU is heat reversible, it should be pointed out that the reformation of its hydrogen bonds to attain equilibrium morphologies has slow dynamics; formation of equilibrium domain structures are heavily time-dependent in some cases taking about hours or more for the samples to attain equilibrium morphologies.[7-8]. This slow dynamics becomes a drawback for the use of traditional TPUs made from 1,4-BDO in HMA

application since fast setting speeds are one of the critical properties necessary for HMAs application. Few studies have been carried out on understanding the kinetics of domain formation in butanediol chain extenders [7-9]. In those studies, some factors such as the and greatly influenced by the HS flexibility/mobility as well as the system viscosity were suggested as possible causes for the slow kinetics of some of those studies with the mobility of the HS having a predominant effect[10].

In our study, we hypothesize that the symmetric structure of the traditional chain extenders facilitates the mobility of the HS and is responsible for the slow kinetics observed in its phase behavior. In this study, we want to not only take advantage of the interesting adhesive properties that polyurethanes possess but also be able to increase the speed at which the morphological properties set to make the polyurethanes suitable for HMA application. We elect to alter morphological properties by changing the symmetry of chain extenders used in the synthesis process. In other words, rather than incorporate the conventional symmetric 1,4-BDO chain extender which is mobile and leads to large time-dependent morphology formation, we choose to use an asymmetric chain extender based on 1,2-PDO and a host of other chain-extenders of the asymmetric type to control setting speed. The reasoning behind the choice of an asymmetric chain extender is to alter the degree of mobility in the TPU structure thereby reducing the time it takes for properties to set. The presence of the pendant group (methyl or phenyl) in the asymmetric chain extender structure will be used to alter the segmental mobility of the HS structure. Additionally, the chain packing and by extension the amount of self-association in the HS

structure will also decrease since the pendant groups will impose steric restrictions to prevent the effective formation of hydrogen bonds[11].

In this chapter; we present the study conducted on understanding the kinetics of domain structure formation by controlling the chain architecture of the chain-extender in the TPU system. A comparison between the conventional chain extended TPUs, and the new chain extender class will be carried out. More specifically, a comparison between the asymmetric 1,2 propanediol and other chain extenders of this category is compared with the more traditional and symmetric 1,4-butanediol chain extender and other chain extenders of this kind. Materials devoid of crystallizable soft segments are chosen to jettison complexity in the analysis that would otherwise arise from the crystallization of the soft-segment. Thus, an amorphous polyester polyol is chosen for the synthesis. By tuning the stoichiometric ratio of our polyurethanes, we have been able to synthesize polyurethanes that have relatively low molecular weight making them have the appropriate viscosity required for adhesive application enabling them to be sprayed, coated, and painted on various substrates. The focus will be to understand the morphology and mechanical properties obtained when these two different categories of chain extenders are utilized. The characterization of mobility will be done using LFNMR which is a technique sensitive to segmental mobility determination. The time dependent morphology development will be studied using FTIR spectroscopy, DSC, and mechanical testing.

3.2 Experimental

3.2.1 Synthesis

We have employed the prepolymer method for the synthesis of TPUs. A polyester polyol obtained from Henkel Corporation was used in the synthesis of the TPU. The polyol and a hindered phenol-based antioxidant used to prevent degradation were added to a flask and heated to 80 ºC under nitrogen and vacuum for approximately an hour to remove any moisture present in the polyol. Vacuum was removed, nitrogen reapplied, and MDI added to the mixture after which the resultant mixture was stirred at 300 rpm for 30 mins. NCO content was measured via titration until experimental value obtained was close to the theoretical value calculated. The chain extension step was subsequently carried out at 120 ºC using different chain extenders. Chain extenders employed were predominantly the 1,4-butanediol and the 1,2-propanediol chain extenders. Other chain extenders including the 1,12 dodecanediol DDO, 1,6 hexanediol HDO and 1,3-butanediol BDO) were also synthesized for some experiments.

3.2.2 Characterization methods

3.2.2.1 Gel Permeation Chromatography

Molecular weight and Đ measurements of the polymers were evaluated using a GPC 50 integrated gel permeation chromatography (GPC) system that was calibrated against polystyrene standards in tetrahydrofuran at a flow rate of 1.0 mL/min using a refractive index detector. Figure 3.1 shows the GPC traces obtained from both samples, and it can

be clearly seen from the values as shown in Table 3.1, that the values of the molecular weights are equivalent. This is done so as to ensure that any changes observed in the properties, especially the mechanical properties will have a morphological origin rather than emanating from molecular weight differences.

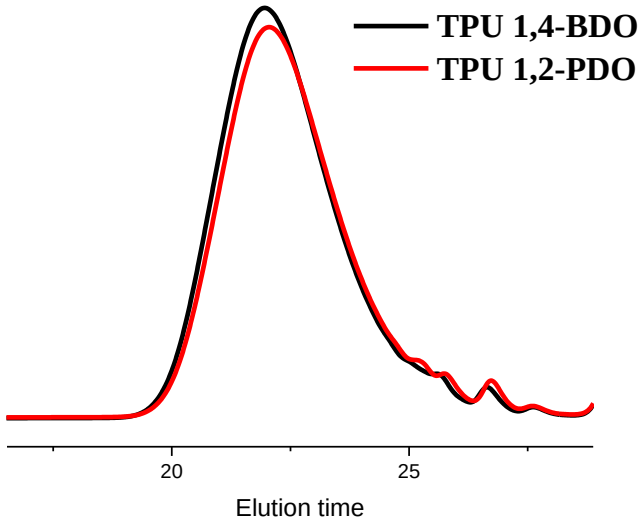

Figure 3.1 GPC traces of TPU 1,2-PDO and TPU 1,4-BDO

3.2.2.2 Nuclear Magnetic Resonance (NMR) Spectroscopy

A 400 MHz Bruker instrument was employed in determining the compositions of the chain extended materials. The samples were dissolved in deuterated DMSO. The ^{1}H signals were referred to tetramethylsilane (TMS) as the internal standard.

Figure 3.2 shows the 1H-NMR spectrum of the TPU 1,4-BDO. The blue arrows point to the characteristic peaks for the various components in the urethane structure: a polyol,

chain extender and urethane structures respectively. The molar ratio of the reaction was determined from which HS content was estimated. The HS was defined as:

$$HS = \frac{mMDI + mBDO}{mMDI + mBDO + mPolyol}$$

Table 3.1 shows the number average molecular weight, molecular weight distribution and HS content of the TPU12pdo and the TPU14bdo system. The number average molecular weight of the polyol used in the formulation was determined from the OH number given in the product MSDS a value of 830g/mol is obtained for the molecular weight of the polyol .

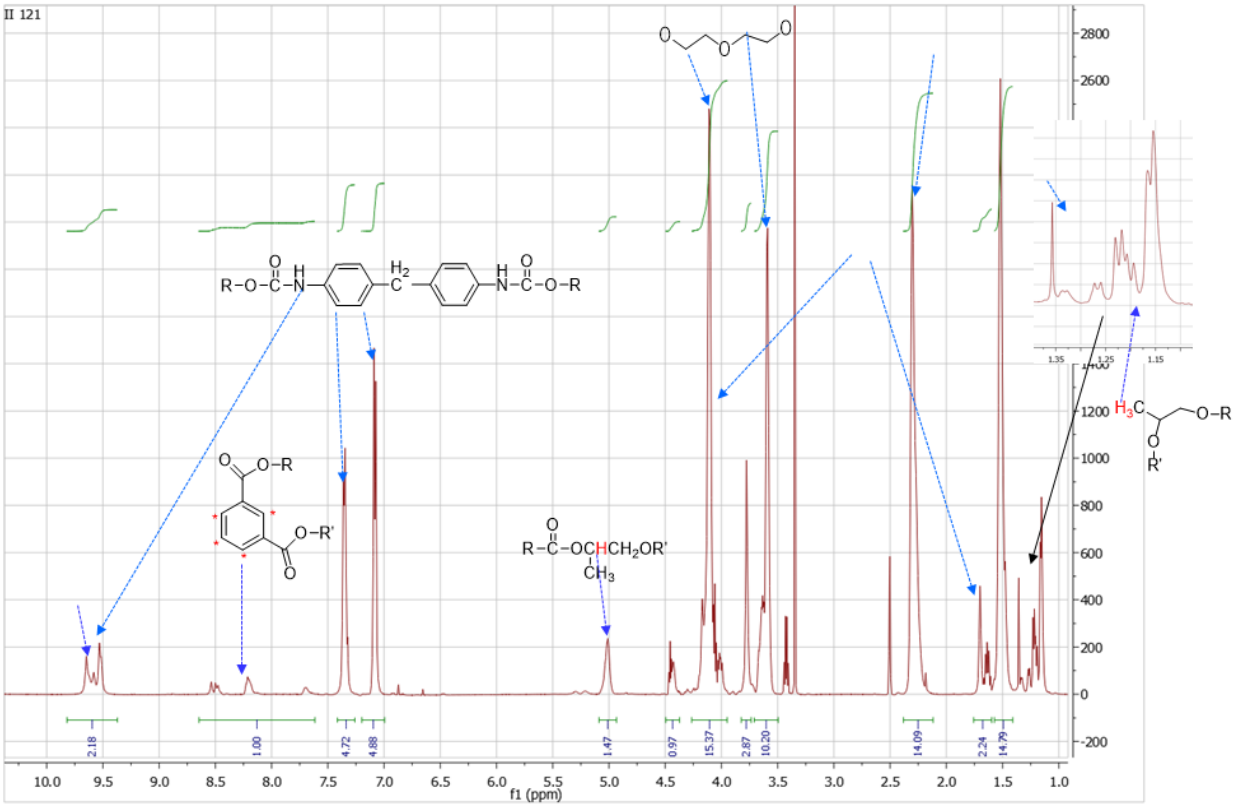

Figure 3.2 NMR trace showing the chemical structure of various units making up TPU 1,4-BDO

Table 3.1 Molecular weight and HS content of TPUs

Sample	Mn (g/mol)	PDI	HS%
TPU 1,2-PDO	10600	1.53	41.8
TPU 1,4-BDO	11000	1.54	42.5

Thermal properties:

A TA instrument Q100 DSC equipped with a nitrogen purged refrigerated cooling system was employed in determining the thermal transitions present in the polymer structures. The heating rates were 20 °C/min for all DSC measurements. Temperature calibration was carried out using Indium (T_m = 156.6 °C; equilibrium heat of fusion = 28.6 J/g).

3.2.2.3 Fourier transform infrared spectroscopy

All infrared data were obtained by either using attenuated total reflectance (ATR-IR) technique or in the transmission mode employing the use of KBr pellets. A PerkinElmer 100 FT-IR spectrometer was used in both configurations of the experiment. For all infrared data, 32 scans of 4 cm^{-1} resolution were co-added. A home-built heating cell was used for high-temperature studies when needed. The sample temperature was monitored using a T-type thermocouple embedded in the sample.

3.2.2.4 Mechanical Testing

Tensile testing was performed using an Instron universal testing machine. Dog bone specimens having a thickness of approximately 300 microns were employed. Testing was

performed at a crosshead speed of 250 mm/min with a 5 kN load cell. For each sample, three individual specimens were tested in separate analyses.

3.2.2.5 Low-field NMR (LFNMR) measurements

Proton NMR longitudinal and transverse magnetization relaxation decays T_1 and T_2 measurements were carried out using a Bruker Minispec NMR – mq20 spectrometer operating at a proton resonance frequency of 20 MHz. The 90° and 180° pulse times were 2.74μs and 5.22μs respectively with a dead time of ~10 μs. The spectrometer was equipped with a VT3000 variable temperature unit for temperature controlled studies. The achieved temperature stability is ±0.1 °C. All longitudinal magnetization relaxation experiments were performed at magnet temperature. An inversion recovery pulse sequence relaxation(180-τ-90) was used for the determination of the T_1.The purpose of the measurement was to determine the longitudinal relaxation time of the components of the TPUs to choose the optimum to recycle delay (~$5T_1$) for the T_2 experiments. FID experiments were performed to establish the soft domain T_2 relaxation behavior

3.3 Results and discussion

3.3.1 Influence of chain extender architecture on mobility of TPU

The two chain extender types examined are the symmetric chain extender based on 1,4-BDO and the asymmetric chain-extender based on 1,2-PDO. It is our hypothesis that the mobile nature of the symmetric chain-extender type is responsible for the long time dependency for the attainment of equilibrium morphology in the TPUs. We, therefore, sought to compare the mobility/flexibility of the two chain extended systems. The

molecular mobility or flexibility of a polymer is typically characterized using light scattering, wherein values for the persistence length, end-to-end distance or the radius of gyration are indicative of the degree of rigidity or mobility of that system[12-13]. In our case, light scattering experiments were unsuccessful possibly due to the low molecular weight of the system ~10,000 g/mol or the impurities inherent in the system even after filtration which. Another way in which molecular mobility was evaluated is using low field NMR technique.ethods[14-16]. This technique can be used to obtain information about the segmental dynamics by making correlations of mobility to the measured T_1 spin-lattice or the T_2 spin-spin relaxation behavior.

In our laboratory, the LFNMR technique has been successfully utilized in the characterization of highly dense crosslinked phenol systems [17-18]. These systems possess infinite molecular weights between their crosslinks and very rigid. As a result of the rigidity in these phenolic systems, the usual T_2 measurements done for most polymer systems characterized using LFNMR were not used since the T_2 in the relaxation time scale ($> 10^{-6}$ sec) of these crosslinked systems reaches a constant value and does not exhibit the sensitivity needed to characterize crosslinked structures therefore T_1 measurements were done. Polyurethanes are comparatively non-rigid and are of low molecular weights (~10,000 g/mol), so T_2 relaxation experiments can be used in measuring the segmental dynamics associated with different chain extender structures. By using T_2 measurements, the relaxation behavior of crystallizable materials, phase separated structures, and lightly crosslinked materials have been successfully determined [16, 19]. All these form the basis for the utilization of LFNMR for the determination of molecular mobility in our samples.

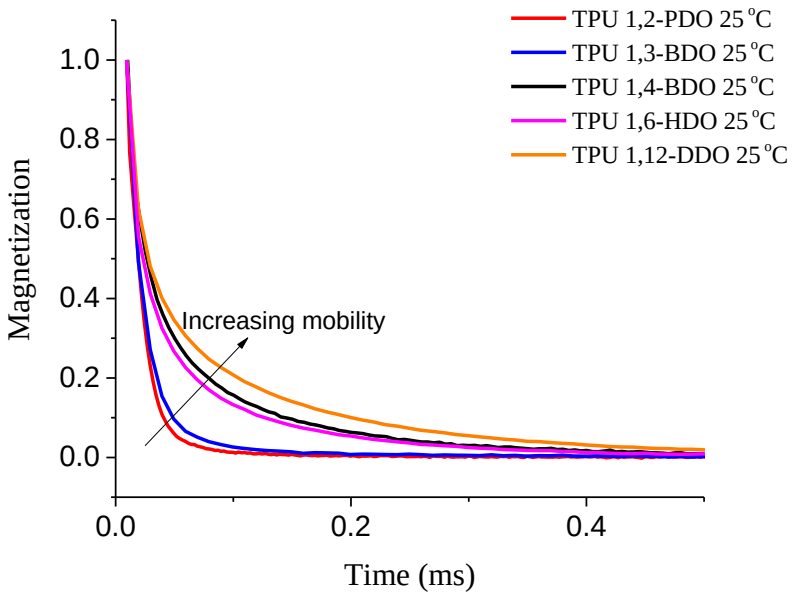

Figure 3.3 FID curves of different chain extended TPUs obtained from LFNMR

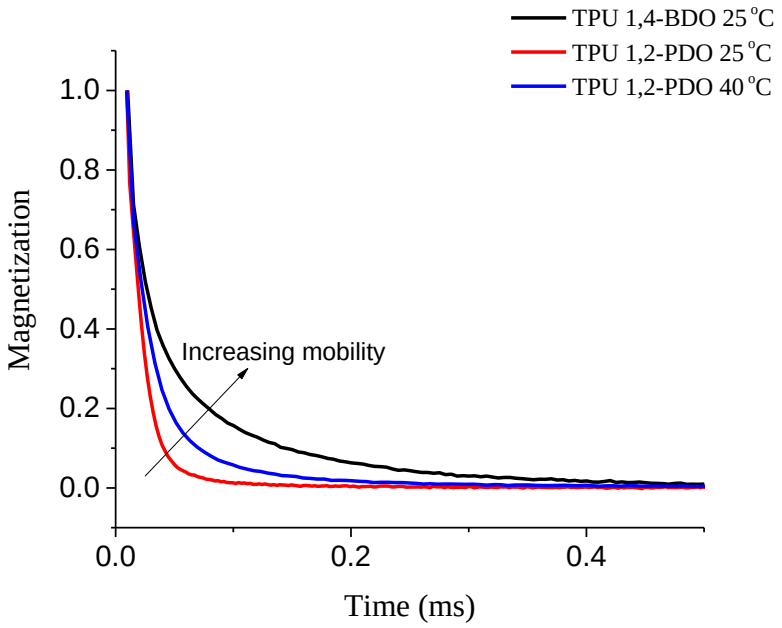

Figure 3.4 FID of TPU 1,4-BDO and TPU 1,2-PDO at different temperatures

The Figures 3.3 and 3.4 show the FID curves of TPUs synthesized from the two classes of chain extenders: symmetric and asymmetric chain extenders. In Figure 3.3, the FID

curves are for different categories of chain extender type with 1,4-BDO, 1,6-HDO and 1,12 DDO falling under the symmetric category while 1,3-BDO and 1,2-PDO fall under the asymmetric chain extender category. Figure 3.4 shows a comparison between the TPU 1,4-BDO and TPU 1,2-PDO at various temperatures. The decay curves reveal two regimes, the fast decay regime corresponding to the HS and the slow decay regime corresponding to the decay of the soft segment[15]. The FID curves were fit to the exponential decay equation to derive the value of T_2 relaxation time which is indicative of the influence of chain extenders on the flexibility of the TPUs.

Equation 3.1 $$M = M_o exp^{-\frac{t}{T_2}}$$

Table 3.2 shows the results of T_2 relaxation times obtained from the fitting exercise. from the table, a a clear distinction between symmetric vs. asymmetric chain extenders are established. For example in the TPU made from 1,2-PDO, the T_2 value is 14 μs as compared to the value of 53 μs obtained from the 1,4-BDO chain extender type. The value of the T_2 relaxation represents the time taken for the protons in the material to lose coherence after a rf pulse is applied [20]. The length of time taken for the spins to return to their equilibrium position is an indicator of the molecular mobility inherent in the polymer sample. Thus a longer T_2 value indicates greater mobility and more time to be taken to return to equilibrium. Thus when the T_2 values of the 1,2 PDO and 1,4-BDO are compared, the longer T_2 value of the symmetric chain extender type is an indicator for greater mobility for the symmetric 1,4-BDO chain extender in comparison to the 1,2-PDO chain extender having lower mobility possibly due to the presence of asymmetric methyl pendant group in its structure. Other chain extenders such as the (1,6-hexanediol and 1,12 dodecanediol) for the symmetric case and 1,3-butanediol for the asymmetric

chain extender class were also measured as shown in Figure 3.3 and Tables 3.2. The same conclusions were reached: symmetric chain extenders possesses larger T_2 values and thus greater mobilities than the asymmetric chain extender type with shorter T_2 values and more inflexible structures.

Table 3.2 T_2 relaxation value for the various chain extended TPUs

Sample	T_2 relaxation (μs)
TPU 1,2-PDO 25 ºC	14
TPU 1,3-BDO 25 ºC	18
TPU 1,2-PDO 40 ºC	26
TPU 1,4-BDO 25 ºC	53
TPU 1,6-HDO 25 ºC	57
TPU 1,12-DDO 25 ºC	86

3.3.2 Effect of chain-extender architecture on morphology and properties

3.3.2.1 Thermal Properties

The consequence of having different degrees of flexibilities of chain extender (symmetric and asymmetric) on the thermal properties of the synthesized TPUs can be verified using DSC. The DSC thermogram of the samples is shown in Figure 3.5 below. The black curve indicates the thermogram of the symmetric 1,4-BDO chain-extended TPU while the red curve is for the asymmetrically chain-extended system. In the TPU 1,4-BDO system, the presence of phase-separation is clearly detected. The evidence for phase separation in this system is characterized by the presence of two Tgs, corresponding to the soft segment rich (-5 ºC) and HS rich domains. The existence of melting transitions,

which has been previously observed in butanediol chain-extended polyurethanes is characteristic of the aggregation states present in the HS domain structure[21-22]. The increased value of the soft segment Tg from -51 ºC to -5 ºC indicates that phase separation is incomplete as some fraction of HS could be entrapped in the soft segment domain making its Tg of a much higher value[22]. The higher Tg corresponds to the HS rich domain. The values obtained fall short of the theoretical value 110 ºC obtained for pure HSs constituting of MDI and BDO [23], which is also indicative of incomplete separation in this TPU.

Nonetheless, the ability of this system to undergo phase separation is strongly related to the very mobile nature of the chain extender as we established in the previous section. The formation of phase separated structures as described earlier is a slow time-consuming process and thus becomes disadvantageous for HMA application where fast setting speed is needed. The incorporation of asymmetry to the backbone has been shown in the previous section to alter the degree of mobility and flexibility of the TPUs derived from this chain-extender class. The presence of the rigid methyl pendant group in the structure results in a polyurethane characterized by a single T_g at ~15 ºC rather than two T_gs and an endotherm as is seen for the BDO system thus creating more phase-mixed morphologies. The absence of melting transitions as is due to. the presence of pendant structures that hinders adequate chain packing and limits the amount and strength of interactions in this TPU system.

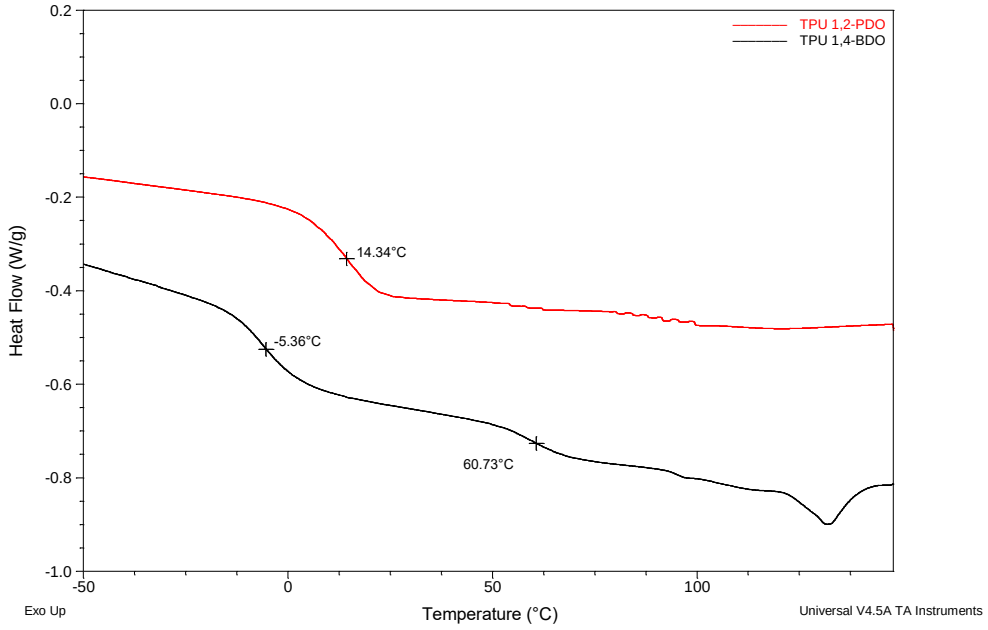

Figure 3.5 Thermal characterization of chain-extended TPUs

3.3.2.2 Determination of morphology of TPU materials

SAXS is an appropriate technique for determining the microstructural properties of materials. It can yield qualitative and quantitative morphological detail about the phase structure of materials provided there be electron density contrast contained in the system. The observation of scattering depends on the presence of electron density contrast between the phases involved (hard and soft phase for TPUs), therefore relatively more pronounced scattering is observed in samples with high electron density contrast and weak or no scattering is observed when there is no contrast in both phases. The interdomain spacing of the scattering profile can be calculated using the relation (d=2π /$q$max).Figure 3.6 shows the scattering profile of the TPU 1,4-BDO and the TPU 1,2-PDO. Evidently, the symmetric chain-extended system shows some degree of order in its

structure as shown by the presence of two scattering peaks. Analysis of the TPU 1,4-BDO peaks for the interdomain spacing gives two peaks with values of ~21nm and 10.5nm, following a lamellar type of morphology. In contrast, the TPU 1,2-PDO does not exhibit any scattering peaks which emphasizes the lack of electron density contrast in this system. Just like in the DSC where a single Tg and the absence of any endothermic peak attributable to the ordering of HS is observed, the scattering profile of the asymmetric chain extender shows no order. Its phase mixed morphology does not generate sufficient electron density contrast between the HS and SS due to the lower segmental mobility of its HS leading to a system in which the HS is trapped in the soft segment matrix thus creating homogeneous rather than discrete domains structures.

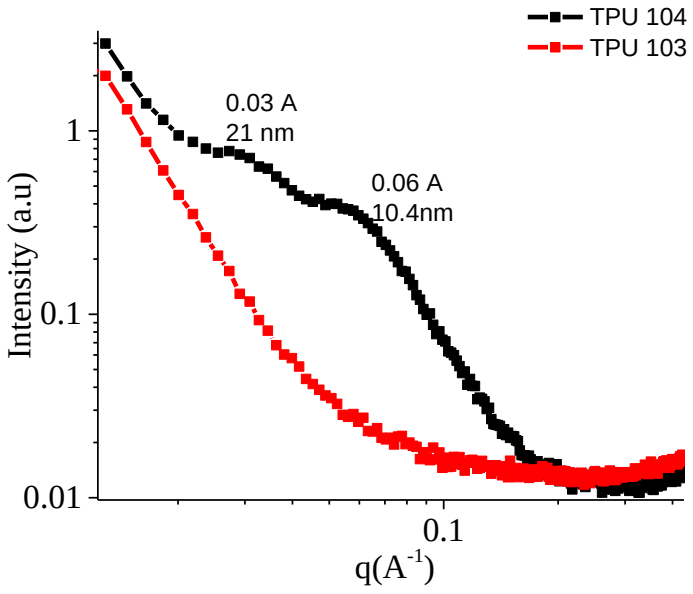

Figure 3.6 SAXS characterization of chain-extended TPUs

The morphological behavior of the TPUs can also be studied by employing vibrational spectroscopy. Vibrational spectroscopy, particularly infrared spectroscopy has been successfully employed in characterizing the hydrogen bonding characteristics in each domain[24-25]. With the aid of FTIR spectroscopy, the influence of changing the symmetry of the chain-extenders on the hydrogen bonding behavior was studied. Figure 3.7 shows the overlaid transmission FTIR spectra of the two chain-extended TPUs. The carbonyl region between 1650 and 1800 cm^{-1} is emphasized. With the TPU 1,4-BDO system, we observed distinct doublets at frequencies of 1703 cm^{-1} and 1732 cm^{-1}. These peaks have been observed in previous studies of 1,4-BDO based polyurethanes and are assignable to the hydrogen bonded and free carbonyl regions [24-25].

The carbonyl region for the TPU 1,2-PDO shows a predominant peak at 1732 $cm^{-1}$and an almost insignificant shoulder at around 1710 cm^{-1} is observed in the spectra, corresponding to the free carbonyl and partially hydrogen bonded carbonyl peaks. As discussed in the previous section, the presence of the asymmetric methyl groups evidently reduces the tendency for the formation of strong intermolecular hydrogen bonding interactions in the resultant TPU system. This is seen by the much higher frequency of the hydrogen bonded carbonyl group 1710 $cm^{-}$when compared to that formed in the1703 cm^{-1}peak of the TPU 1,4-BDO sample. The lack of mobility of the asymmetric HS should prove advantageous in HMA application. The mobility restrictions would become beneficial when the adhesives are applied because the lack of mobility in the HS structure would mean that the properties will not change as time progresses. The characterization of the time dependent properties can be evaluated using time dependent spectroscopy and DSC as will be shown in the next section.

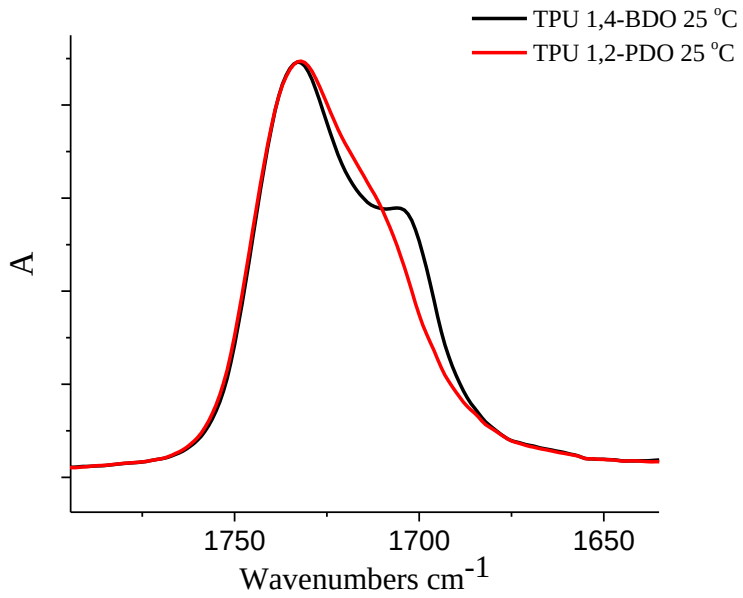

Figure 3.7 FTIR spectra of the as received sample

3.3.4 Characterization of annealing behavior

The essence of this study is to maximize the interesting properties that polyurethanes possess and to particularly use chain-extenders to control the morphology of polyurethanes making them suitable for hot melt adhesive applications. One of the advantages of HMAs is their fast setting speed which makes them attractive for rapid packaging process in industry and the requirement for their properties/morphology to set as soon as the adhesive is applied to the substrate. In this section, we will like to simulate use conditions and observe how the thermal and spectroscopic properties evolve with time. Time-dependent studies were performed using DSC and FTIR. Figure 3.8 shows the temperature profile for the annealing studies

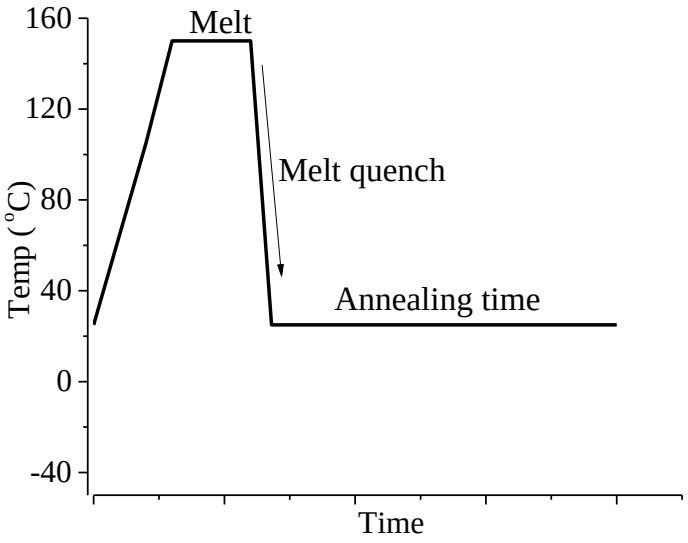

Figure 3.8 Temperature profile employed for annealing studies

The sample was heated dissociate equilibrium hydrogen bonds and create a homogenous molten phase. The melt were then quickly quenched using a cooling device to room temperatures (25 ºC), the evolution of morphology was monitored using DSC and FTIR. Figure 3.9 shows the DSC trace of the TPU 1,4-BDO sample. The times in which the DSC curves were obtained are labeled on the curves. The initial curve (0hr) shows the thermal profile immediately after quenching from the homogenous molten phase. At this timescale, the presence of a single T_g accompanied by the appearance of multiple melting transitions is observed, these multiple endothermic transitions are representative of different degrees of HS ordering (short and long scale ordering) present in the sample. The initial T_g of the 0hr sample which is ~2.6 ºC is higher than the T_g of the pure polyol -51 ºC, this, indicating the dissolution of some HS in the SS domain. As time progresses, the soft segment rich phase begins to get purer with time as seen by the further reduction

in the value of the T_g. The curves show that for the symmetric chain extender type the attainment of equilibrium T_gs is a slow process and has been documented in other studies of this chain extender type.

Figure 3.10 shows the time-dependent DSC trace of the TPU 1,2-PDO sample annealed at the use temperature. The curve shows just a single transition: that is the T_g transition and an absence of multiple endotherms this T_g value remains constant for the whole duration of the experiments. This demonstrates that the incorporation of asymmetric chain extender units can be used advantageously to create polyurethanes whose property do not change overtime, thus making the concept of alteration of symmetry a viable route for making TPUs which have utility as HMAs.

To test out the validity of this symmetry arguments, other chain extenders under the symmetric and asymmetric categories were also investigated. Figure 3.11 shows a summary of the results for all the chain extenders tried in the two different symmetry types. The curves represent two samples each from each chain-extender class, i.e., two symmetric chain extenders (1,4-butanediol and 1,6-hexanediol) as well as two asymmetric types (1,2-propanediol and 1,3-butanediol) systems. From the curve, it can be deduced that the symmetry of the chain-extenders plays an enormous role in determining the phase behavior and also the setting of the TPUs intended to be employed in the area of HMAs. The curve proves the validity of the symmetry argument and establishes that changing just the chain extender architecture can be used to alter the morphological behavior of TPUs.

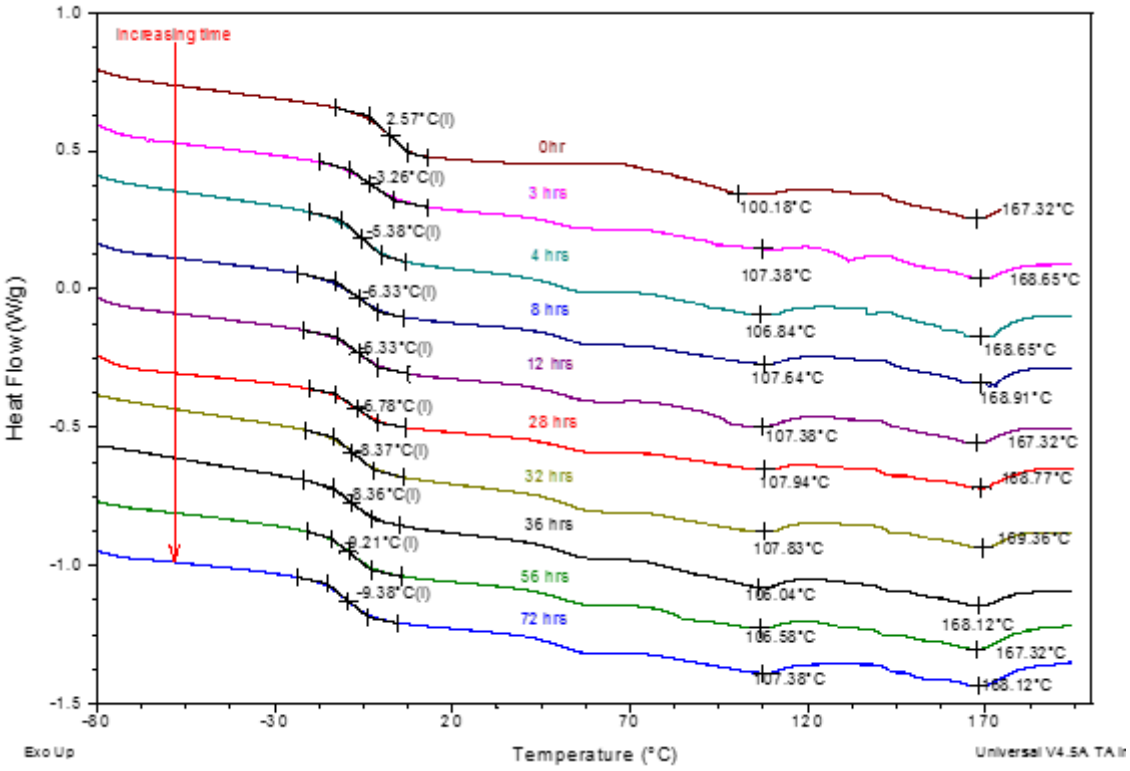

Figure 3.9 DSC profiles of time dependent annealing behavior at 25 ºC for TPU-1,4 BDO

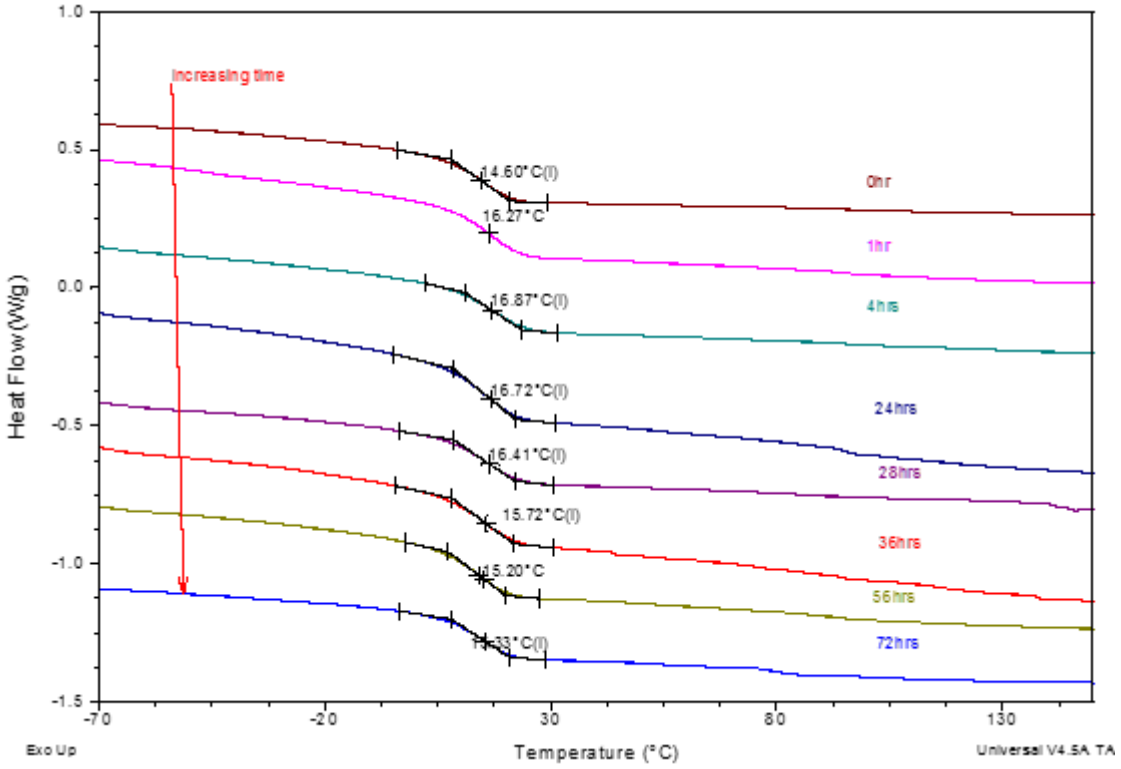

Figure 3.10 DSC profiles of time dependent annealing behavior at 25 ºC for TPU-1,2 PDO

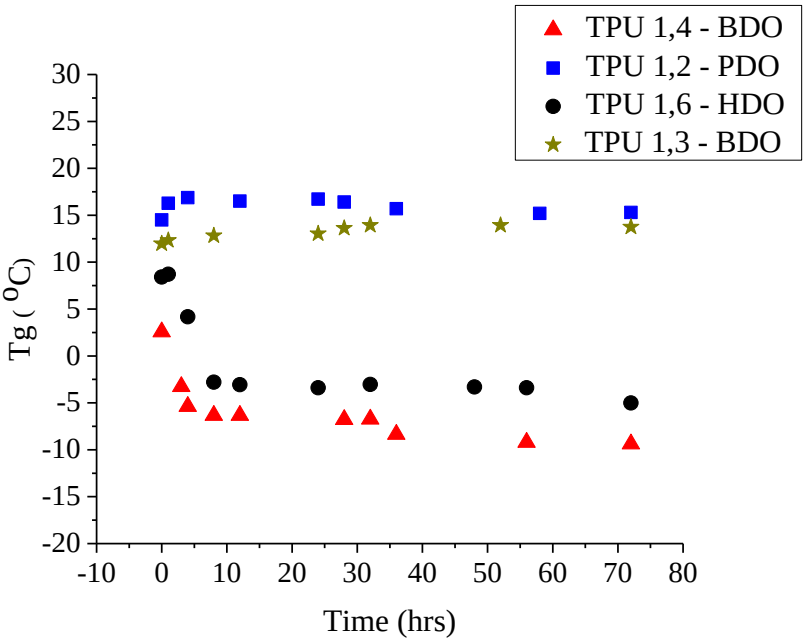

Figure 3.11 Summary of DSC profiles for different symmetries of chain extenders

Time dependent FTIR spectroscopy can also be used to corroborate the annealing DSC studies. The same schematic of thermal treatment shown in Figure 3.8 was applied to this sample. The results of the experiments are overlaid in Figure 3.12. The spectra emphasizes the carbonyl region between 1650 and 1800 cm^{-1} obtained at different times for the TPU 1,4-BDO sample. At early times after the sample is quenched from high temperatures, the 0 min spectra is dominated by the 1732 cm^{-1} peak and just a slight shoulder appearing at 1710 cm^{-1}, denoting that soon after quenching, a phase-mixed structure is formed that is to say some carbonyl groups are free from hydrogen bonding interactions on cooling from high temperature to RT. As time further progresses, HS-HS self-association proceeds in this sample and two predominant peaks are observed, which is attributed to free carbonyl peaks at high frequencies and Hydrogen bonded peak denoting phase separation. This development of phase separation leading to discrete domains is slow and takes couple of hours to saturate within the experimental time frame examined. The slow evolution of phase separation is what makes this chain extender type unattractive for HMAs.

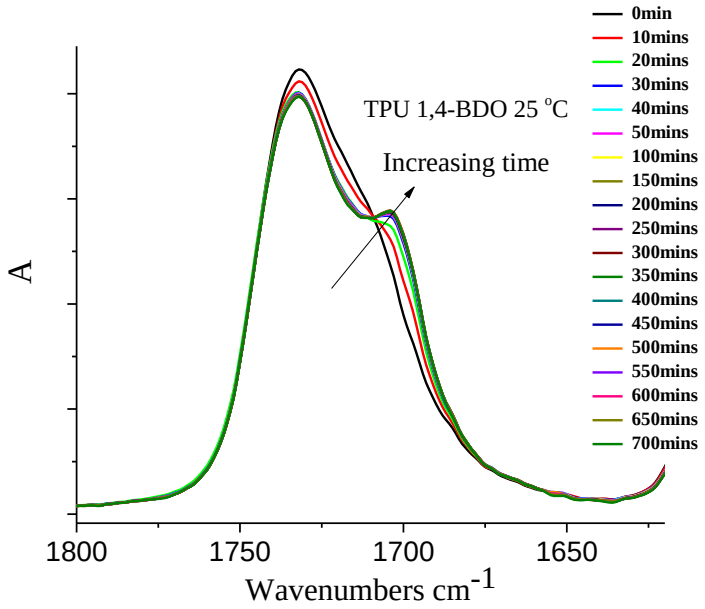

Figure 3.12 FTIR profile of time dependent annealing behavior at 25 ºC for TPU-1,4 BDO

Figure 3.13 reveals the time dependent FTIR of the TPU-1,2-PDO sample. Just like the 1,4-BDO system, on quenching from the initial elevated temperatures sample, the spectra taken at 0 mins shows a dominant 1732 cm^{-1} peak and a slight shoulder at 1710 cm^{-1}. As time evolves, there still remains no significant change in the peaks of the carbonyl region carbonyl region. Even though extremely strong hydrogen bonding is not observed in this system, the invariance in the properties point to rapid formation of its morphology, making this chain extender class attractive for HMA application. Nevertheless, the drawback of slow domain formation obtained using the traditional 1,4-BDO has been addressed by integrating asymmetric chain extenders (1,2-PDO) into the structure of the polymer system.

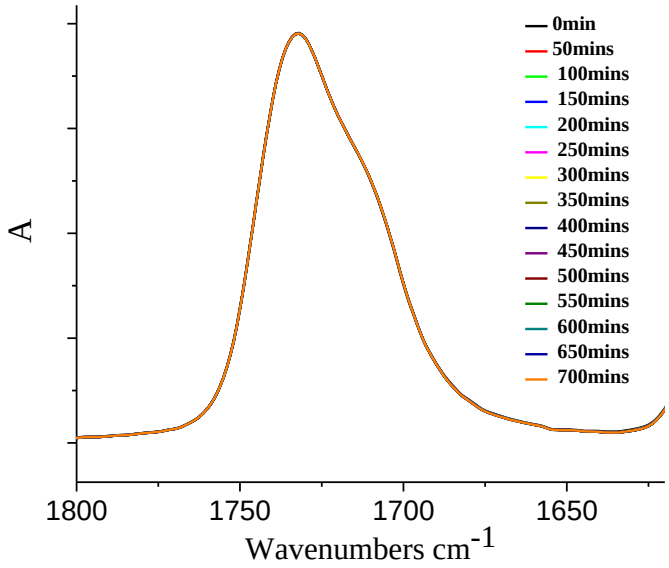

Figure 3.13 FTIR profiles of time dependent annealing behavior at 25 ºC for TPU-1,2 PDO

3.3.5 Mechanical response of chain extended TPUs

The mechanical performance of polymers are controlled by their morphological and thermal properties; the case is no difference in TPUs. In fact, the mechanical properties of conventional polyurethane materials have been ascribed to their ability to form discrete domains (hard and soft domains) in which the HS domain controls the modulus and tensile strength while the soft domains influences the elongational behavior[6, 26]. Various micro mechanical models have been used in literature to predict the modulus behaviors of polyurethanes[27-28]. The predictions are idealistic and fail to account for the complicated nature of the morphology of polyurethanes in real systems. The mechanical behaviors are complicated by stoichiometry, morphological inhomogeneity, hard and soft segment polydispersity amongst other factors[27]. Our studies will just make a comparison between

the physical properties of the differently chain extended systems. It has been established that our materials exhibit two different morphologies depending on chain extender type: phase mixed and phase separated structures, with the traditional 1,4-BDO exhibiting phase separation and the non-conventional 1,2-PDO systems showing phase-mixing. Figure 3.14 shows the use-temperature mechanical properties of the two chain-extended TPUs.

The mechanical response of both systems is remarkably different because of morphological differences. The values of the modulus and the percent elongation are shown in Table 3.3. The TPU 1,4-BDO based samples exhibit greater HS-HS interchain interaction and forms more ordered structures as confirmed by SAXS, FTIR and DSC measurements. Therefore, its modulus is greater (16MPa), than in the TPU 1,2-PDO system, which has a weaker hydrogen bonding structure, and lack of ordered phases that can bear load. It should be noted, however, that for these systems, with low molecular weights, that the emphasis is more on developing systems that possess fast setting speeds and invariance in their properties under use conditions. As has been shown in the annealing studies, the TPU 1,2-PDO systems perform favorably in this regard.

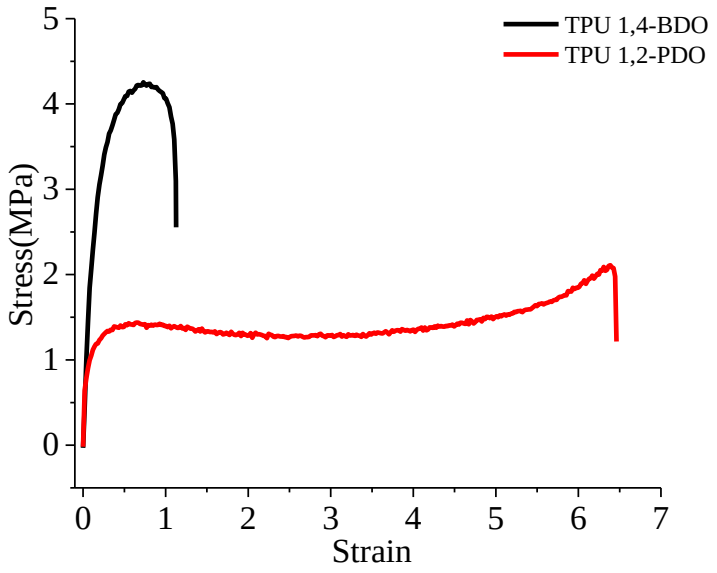

Figure 3.14 Mechanical properties comparison in both symmetries of chain extended TPUs

Table 3.3 Summary of mechanical properties of the TPUs

Sample	**Modulus (MPa)**	**Percent elongation**
TPU 1,2-PDO	4.3	640
TPU 1,4-BDO	16	128

3.4 Conclusion

Polyurethanes, were explored as possible candidates for HMA application due to the polarity inherent in its structure which makes it capable of binding to a variety of substrates. For these systems, chain configurational control was facilitated by changing the symmetry of the chain extenders used in synthesizing the TPUs. Traditional chain extenders based on 1,4-BDO systems though provided phase separation, however proved unsuitable because of the long times taken for their morphology to set which is

disadvantageous for HMAs. In order to circumvent this problem of slow kinetics in the morphology of conventional systems, we have elected to change the mobility associated with the chain extenders, a seldom studied subject. A comparatively inflexible asymmetric chain extender based on 1,2-PDO was used to alter the morphology of the TPUs. The presence of the pendant groups in this system reduces its mobility and makes the HS made from it lack the mobility to move away from the SS matrix. We have shown this to be vital in creating stable domains whose properties do not change over time. For our investigation, we employed LFNMR was used to distinguish between the segmental mobility of both chain extender classes. Morphological studies were done with the aid of FTIR, SAXS and DSC. In order to simulate in-use properties, time dependent measurements of morphology were made. The results showed that by altering the chain architecture of the chain extenders used in the synthesis of TPUs, adequate morphology required for a particular application can be obtained. In our case our annealing studies using the asymmetric chain extenders showed time-independence in morphology development, which can be correlated to the setting speed required in HMA application.

3.5 References

1. Tang, Q.; He, J.; Yang, R.; Ai, Q., Study of the synthesis and bonding properties of reactive hot-melt polyurethane adhesive. *Journal of Applied Polymer Science* **2013,** *128* (3), 2152-2161.
2. Yilgör, I.; Yilgör, E.; Wilkes, G. L., Critical parameters in designing segmented polyurethanes and their effect on morphology and properties: A comprehensive review. *Polymer* **2015,** *58,* A1-A36.
3. Szycher, M., *Szycher's handbook of polyurethanes*. CRC press: 2012.
4. Blackwell, J.; Nagarajan, M.; Hoitink, T., Structure of polyurethane elastomers. X-ray diffraction and conformational analysis of MDI-propandiol and MDI-ethylene glycol hard segments. *Polymer* **1981,** *22* (11), 1534-1539.
5. Bonart, R.; Müller, E., Phase separation in urethane elastomers as judged by low-angle X-ray scattering. II. Experimental results. *Journal of Macromolecular Science—Physics* **1974,** *10* (2), 345-357.
6. Prisacariu, C., *Polyurethane elastomers: from morphology to mechanical aspects*. Springer Science & Business Media: 2011.
7. Wilkes, G. L.; Wildnauer, R., Kinetic behavior of the thermal and mechanical properties of segmented urethanes. *Journal of Applied Physics* **1975,** *46* (10), 4148-4152.
8. Wilkes, G. L.; Bagrodia, S.; Humphries, W.; Wildnauer, R., The time dependence of the thermal and mechanical properties of segmented urethanes following thermal treatment. *Journal of Polymer Science Part C: Polymer Letters* **1975,** *13* (6), 321-327.

9. Yoon, P. J.; Han, C. D., Effect of thermal history on the rheological behavior of thermoplastic polyurethanes. *Macromolecules* **2000,** *33* (6), 2171-2183.

10. Li, Y.; Gao, T.; Chu, B., Synchrotron SAXS studies of the phase-separation kinetics in a segmented polyurethane. *Macromolecules* **1992,** *25* (6), 1737-1742.

11. Das, S.; Cox, D. F.; Wilkes, G. L.; Klinedinst, D. B.; Yilgor, I.; Yilgor, E.; Beyer, F. L., Effect of Symmetry and H-bond Strength of Hard Segments on the Structure-Property Relationships of Segmented, Nonchain Extended Polyurethanes and Polyureas. *Journal of Macromolecular Science, Part B: Physics* **2007,** *46* (5), 853-875.

12. Arteca, G. A., Scaling behavior of some molecular shape descriptors of polymer chains and protein backbones. *Physical Review E* **1994,** *49* (3), 2417.

13. Zagar, E., Solution properties of polyurethanes studied by static light scattering, SEC-MALS, and viscometry. *Acta chimica slovenica* **2005,** *52* (3), 245.

14. Assink, R., The study of domain structure in polyurethanes by nuclear magnetic resonance. *Journal of Polymer Science Part B: Polymer Physics* **1977,** *15* (1), 59-69.

15. Voda, A. E.; Haberstroh, U. D.-I. E. *Low Field NMR for Analysis of Rubbery Polymers*; Fakultät für Mathematik, Informatik und Naturwissenschaften: 2006.

16. Nierzwicki, W., Microphase separation in urethane elastomers as seen through NMR measurements. *Journal of applied polymer science* **1984,** *29* (4), 1203-1213.

17. Patel, J. P.; Zhao, C. X.; Deshmukh, S.; Zou, G. X.; Wamuo, O.; Hsu, S. L.; Schoch, A. B.; Carleen, S. A.; Matsumoto, D., An analysis of the role of reactive plasticizers in the crosslinking reactions of a rigid resin. *Polymer* **2016,** *107*, 12-18.

18. Patel, J. P.; Deshmukh, S.; Zhao, C.; Wamuo, O.; Hsu, S. L.; Schoch, A. B.; Carleen, S. A.; Matsumoto, D., An analysis of the role of nonreactive plasticizers in the crosslinking reactions of a rigid resin. *Journal of Polymer Science Part B: Polymer Physics* **2017,** *55* (2), 206-213.

19. Hertlein, C.; Saalwächter, K.; Strobl, G., Low-field NMR studies of polymer crystallization kinetics: Changes in the melt dynamics. *Polymer* **2006,** *47* (20), 7216-7221.

20. Jacobsen, N. E., *NMR spectroscopy explained: simplified theory, applications and examples for organic chemistry and structural biology*. John Wiley & Sons: 2007.

21. Saiani, A.; Rochas, C.; Eeckhaut, G.; Daunch, W.; Leenslag, J.-W.; Higgins, J., Origin of multiple melting endotherms in a high hard block content polyurethane. 2. Structural investigation. *Macromolecules* **2004,** *37* (4), 1411-1421.

22. Saiani, A.; Daunch, W.; Verbeke, H.; Leenslag, J.-W.; Higgins, J., Origin of multiple melting endotherms in a high hard block content polyurethane. 1. Thermodynamic investigation. *Macromolecules* **2001,** *34* (26), 9059-9068.

23. MacKnight, W.; Yang, M.; Kajiyama, T., Amer. 34. Chem. Soc. *Polymer Prepr* **1968,** *9*, 860.

24. Lee, H. S.; Hsu, S. L., An analysis of phase separation kinetics of model polyurethanes. *Macromolecules* **1989,** *22* (3), 1100-1105.

25. Lee, H. S.; Wang, Y. K.; Hsu, S. L., Spectroscopic analysis of phase separation behavior of model polyurethanes. *Macromolecules* **1987,** *20* (9), 2089-2095.

26. Abouzahr, S.; Wilkes, G. L., Structure property studies of polyester-and polyether-based MDI–BD segmented polyurethanes: Effect of one-vs. two-stage

polymerization conditions. *Journal of applied polymer science* **1984,** *29* (9), 2695-2711.

27. Ginzburg, V. V.; Bicerano, J.; Christenson, C. P.; Schrock, A. K.; Patashinski, A. Z., Theoretical modeling of the relationship between Young's modulus and formulation variables for segmented polyurethanes. *Journal of Polymer Science Part B: Polymer Physics* **2007,** *45* (16), 2123-2135.

28. Yanagihara, Y.; Osaka, N.; Iimori, S.; Murayama, S.; Saito, H., Relationship between modulus and structure of annealed thermoplastic polyurethane. *Materials Today Communications* **2015,** *2*, e9-e15.

CHAPTER 4
INFLUENCE OF INCORPORATION OF SEMI-CRYSTALLINE COMPONENT TO VARIOUSLY CHAIN EXTENDED TPUs

4.1 Introduction

In chapter 3, structural analysis of TPUs were carried out using an amorphous polyol system. The presence of amorphous structure, however,, leads to long open times and low moduli in the samples [1-2]. Control of TPU properties can be attained by changing the chemical constituents of the HS or SS. Studies on PU foams and elastomers have shown the improvement of thermal and mechanical properties by using a composite hard segment as compared to a single component[3]. It is also possible to control process parameters by the incorporation of a composite SS structure [1, 4-5]. Here in chapter 4, we will like to observe the changes that occur in both the morphology and mechanical properties of these TPUs when we introduce some degree of crystallinity to the backbone structure of the TPU.

. The different architectures of the chain extenders motivate our quest to determine the two symmetries of chain extenders influence the crystallization of the semi-crystalline components.

I have elected to use polyhexamethylene adipate (PHMA), a biodegradable aliphatic polyol. This polyol has been previously used in our laboratory for the study of moisture curable polyurethanes[6-7]. In the previous studies from our group, PHMA was incorporated to improve the mechanical properties of the originally amorphous system. Based on those studies, we have incorporated PHMA units to introduce some degree of

crystallinity into the originally amorphous polyol units, to control process parameters. On incorporating PHMA units, several morphological events will be observed, thus making the study a complex one In the symmetric chain extended TPU in which phase-separated morphologies have been shown to occur, the introduction of the SC unit will lead to the creation of a third phase consisting of the crystallizable PHMA units. In the asymmetric chain extender that shows phase-mixed structures, two phases will be formed when this semi crystalline PHMA units are incorporated into the copolymer structure. Due to these complexities, the main focus of this chapter will be solely directed to understanding the specific role the symmetry of the chain extender plays in influencing the crystallization and properties of the PHMA-modified TPUs. The symmetric and asymmetric chain extenders from chapter 3 will be modified by incorporating PHMA units to their structure.

Studies on the crystallization behavior of strongly interacting chains had been carried out before in our laboratory[8]. Those systems were devoid of polyols or chain extenders but were model systems formed by the polyaddition reaction of long aliphatic chains having terminal isocyanate groups with long aliphatic diols to form carbamate functional groups. It will be interesting to follow the crystallization behavior in “real” systems that have polyol and chain extender in their structure.

4.2 Experimental

4.2.1 Materials

About ~20 % of PHMA polyol was incorporated into the amorphous polyester polyol structure, and the TPUs contain different chain extenders were synthesized using the same methods explained in the previous chapter. The chemical structure of the semicrystalline PHMA is shown below:

Polyhexamethylene adipate (PHMA)

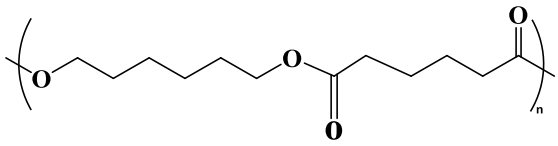

4.2.2 Characterization methods

4.2.2.1 Gel Permeation Chromatography

Molecular weight and Đ measurements of the polymers were evaluated using a GPC 50 integrated gel permeation chromatography (GPC) system that was calibrated against polystyrene standards in tetrahydrofuran at a flow rate of 1.0 mL/min using a refractive index detector. Figure 4.1 shows the GPC traces obtained from both samples, and it can be seen from the values as indicated in table 4.1, that the molecular weights are equivalent. The equivalence in molecular weight is essential for making sure that difference in properties is a consequence of morphological rather molecular weight difference

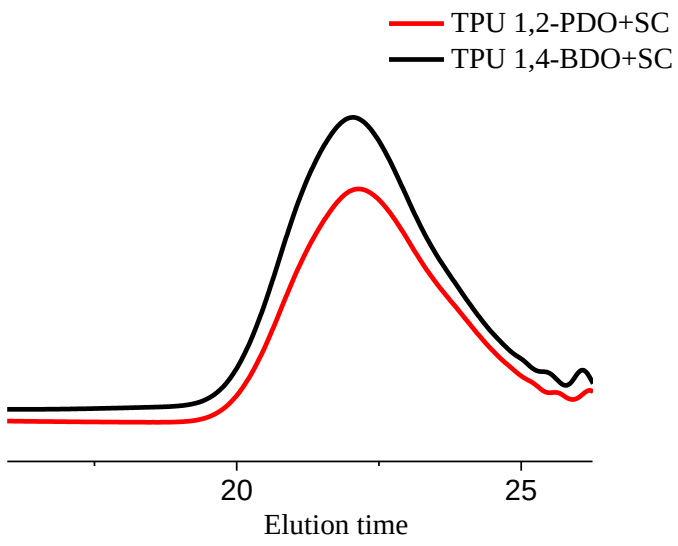

Figure 4.1 GPC traces of the PHMA-modified TPUs

4.2.2.2 Nuclear Magnetic Resonance (NMR) Spectroscopy

A 400 MHz Bruker instrument was employed in determining the compositions of the chain extended materials. The samples were dissolved in deuterated DMSO. The ^{1}H signals were referred to tetramethylsilane (TMS) as the internal standard.

Figure 4.2 shows the 1H-NMR spectrum of the TPU 1,4-BDO. The blue arrows point to the characteristic peaks for the various components in the urethane structure: a polyol, chain extender and urethane structures respectively. The molar ratio of the reaction was determined from which the HS content was estimated. The HS was defined as:

$$HS = \frac{mMDI + mBDO}{mMDI + mBDO + mPolyol}$$

Table 4.1 shows the number average molecular weight, molecular weight distribution and HS content of the TPU1,2-PDO and the TPU 1,4-BDO system. The number average molecular weight of the polyol used in the formulation was determined from the OH

number given in the product MSDS a value of 830g/mol is obtained for the molecular weight of the polyol.

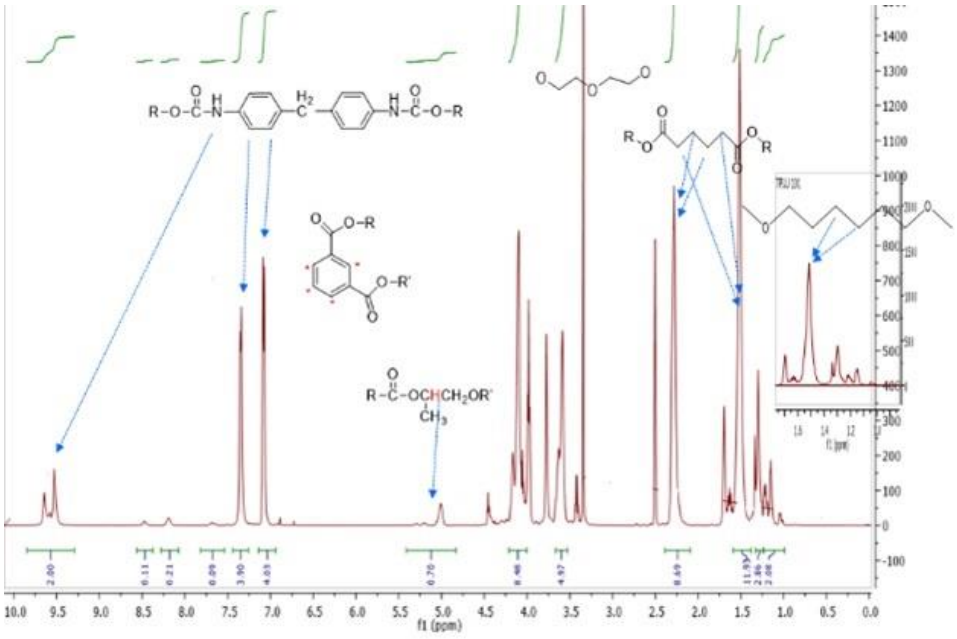

Figure 4.2 NMR trace showing the chemical structure of various units making up TPU 1,4-BDO+SC sample

Table 4.1 Molecular constitution of TPUs

Sample	Mn (g/mol)	PDI	HS%	%SC
TPU 1,2-PDO+SC	13400	1.67	37.70	18.4
TPU 1,4-BDO+SC	14700	1.63	38.50	18.9

4.2.2.3 Thermal analysis

A TA instrument Q100 DSC equipped with a nitrogen purged refrigerated cooling system was employed in determining the various glass transition temperature of samples studied.

The heating rates were 20 °C/min for all DSC measurements. Temperature calibration was carried out using Indium (T_m = 156.6 °C; equilibrium heat of fusion = 28.6 J/g).

4.2.2.4 Fourier transform infrared spectroscopy

All infrared data were obtained by either using attenuated total reflectance (ATR-IR) technique or in the transmission mode employing the use of KBr pellets. A PerkinElmer 100 FT-IR spectrometer was used in both types of experiments. For all infrared data, 16 scans of 4 cm^{-1} resolution were co-added. A home-built heating cell was used for high-temperature studies. The sample temperature was monitored using a thermocouple embedded in the sample.

4.2.2.5 Low-field NMR (LFNMR) measurements

Proton NMR longitudinal and transverse magnetization relaxation decays T_1, and T_2 measurements were carried out using a Bruker Minispec NMR – mq20 spectrometer operating at a proton resonance frequency of 20 MHz. The 90° and 180° pulse times were 2.74 µs and 5.22 µs respectively with a dead time of ~10 µs. The spectrometer was equipped with a VT3000 variable temperature unit for temperature controlled studies. The achieved temperature stability is ±0.1 °C. All longitudinal magnetization relaxation experiments were performed at magnet temperature. An inversion recovery pulse sequence180-τ-90) was used for the determination of the T_1 .The purpose of the measurement was to determine the longitudinal relaxation time of the components of the TPUs in order to choose the optimum recycle delay (~5T_1) for the T_2 experiments. FID experiments were performed to establish the soft domain T_2 relaxation behavior

4.2.2.6 Mechanical Testing

Tensile testing was performed using an Instron universal testing machine. Dog bone specimens having a thickness of approximately 300 microns were employed. Testing was conducted at a crosshead speed of 250 mm/min with a 5 kN load cell. For each sample, three individual specimens were tested in separate analyses.

4.3 Results and discussion

4.3.1 Influence of the incorporation of semicrystalline components on thermal properties

The thermal properties of the modified TPUs were characterized using DSC. The DSC curves are shown in Figure 4.3. The plot shows superimposed curves for the TPU 1,2-PDO+SC and the TPU 1,4-BDO-SC samples. In the TPU 1,2-PDO+SC sample, the presence of a single T_g is detected. The T_g which is observed at ~ 10 ºC is higher than the glass transition temperature of the pure SS (Tg= -51 ºC) matrix from which it was synthesized from. As was seen in the previous chapter, the increase in the T_g was attributed to the inherent rigidity of the chain extender structure which restricts its mobility and makes its HS to be trapped in the SS domain thereby preventing the formation of phase separation. The endotherm observed in the TPU 1,2-PDO+SC is attributed to the melting transition of the PHMA units which was incorporated into the structure of the TPU. When this sample is compared to the pure PHMA, a depression in the melting enthalpy and temperature is observed which indicates that the presence of chain extender hinders the complete crystallization in the TPU 1,2-PDO+SC.

In the TPU 1,4-BDO+SC, a single T_g at -11 ºC, large endothermic transition corresponding to the melting of the SC component and small melting endotherms corresponding to different degrees of order in the HS is observed. Just as is seen in the TPU 1,2-PDO+SC sample, the semicrystalline component's melting temperature and degree of crystallinity are also lower than that of pure PHMA segment, indicating that with this chain extender also influences the crystallization behavior of the resulting TPU. The significant reduction to the enthalpy of crystallization of both TPUs emanates from the confinement of the crystallizable SS by the HS, thus obstructing the formation of well-ordered crystallites [4, 9]

The Table 4.2 depicts the thermal properties extracted from the DSC curves for the pure PHMA samples as well as for the TPU samples in which the two symmetries of chain extenders have been incorporated into their structure. The slightly more depressed endotherm for the TPU 1,4-BDO+SC systems is due to the more ordered HS structures which the symmetric possesses which hinders the realization of optimal crystallization of the PHMA unit in the sample, and thus yielding smaller enthalpies of crystallization of the PHMA units. This has been observed in urea based foams where crystallization of the SS was shown to be inhibited by the presence of infusible ordered urea HS [9]. In the TPU 1,2-PDO+SC sample, the thermal events are much simplified: the presence of a single T_g from the phase mixed morphology resulting in the absence of ordering in the HS structure and the crystallization of the SS. In this simpler system, the degree of crystallization is higher.

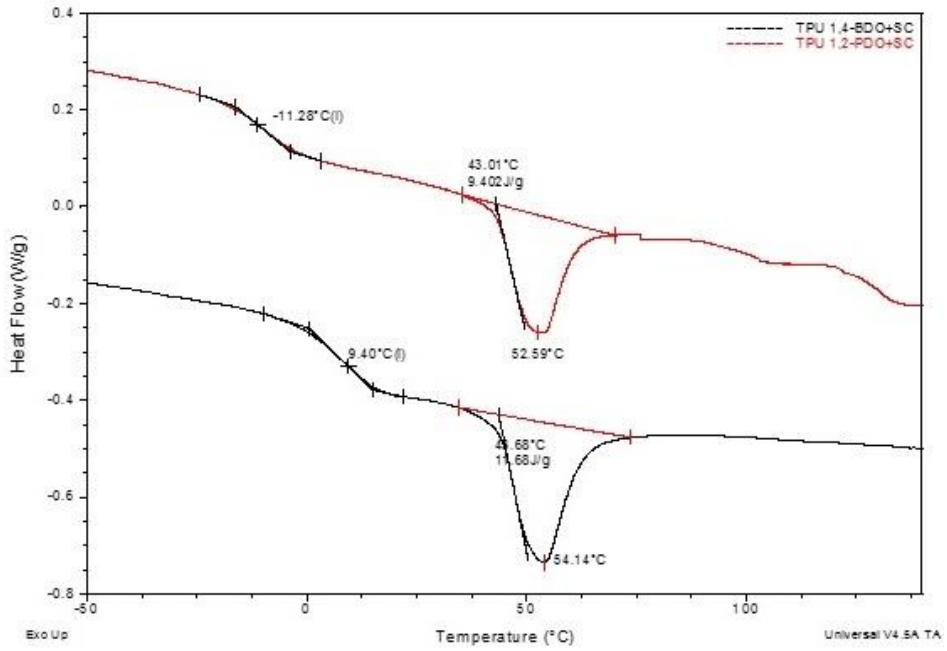

Figure 4.3 Overlay of the thermal properties of the PHMA-modified TPUs

Table 4.2 Thermal properties showing SS melting and degree of crystallinity

Sample	**Tm ºC (SS)**	**ΔH (J/g) DSC**	**ΔH normalized (~20%) (J/g)**
TPU 1,2-PDO+SC	54	11.7	62
TPU 1,4-BDO+SC	53	9.4	50
Pure PHMA	56	87	87

Using FTIR spectroscopy, we can observe the effect of incorporating SC components into the structure of the variously chain extended TPUs. Figure 4.4 shows spectra for the asymmetric and symmetric chain-extender systems before and after the incorporation of SC components. The region 1800-1000 cm^{-1} is emphasized in both samples. The integrated absorbance of the carbonyl region of the sample to which SC components have been incorporated is significantly increased compared to the samples from the previous chapter. The addition of semi-crystalline PHMA peaks, possessing ester groups

introduces more carbonyl character to the sample and explains the increase in the carbonyl concentration as seen from the Figure 4.4. The splitting observed in the carbonyl region of the TPU 1,4-BDO+SC arises from the ordered structure of that chain extender type and this is absent in the TPU 1,2-PDO+SC sample.

The phase behavior of the HS aggregation seen in chapter 3 in the amorphous systems from the previous chapter is also preserved on the incorporation of SC units, i.e., the symmetric chain extender type shows phase-separation evidenced by the splitting of the carbonyl region and the asymmetric chain extender does not as seen by the singular carbonyl region. The emergence of new peaks can also be monitored using FTIR spectroscopy. Peaks attributable to the PHMA units are shown to occur as seen in the literature. Some of the peaks overlap with the amorphous samples but show a higher integrated absorbance. The peak at 972 cm^{-1} attributable to the υ (C-C) stretching did not overlap with any previous band and will be used in the subsequent section for analysis. Table 4.3 represents the assignment of the peaks observed in the spectra [10-11].

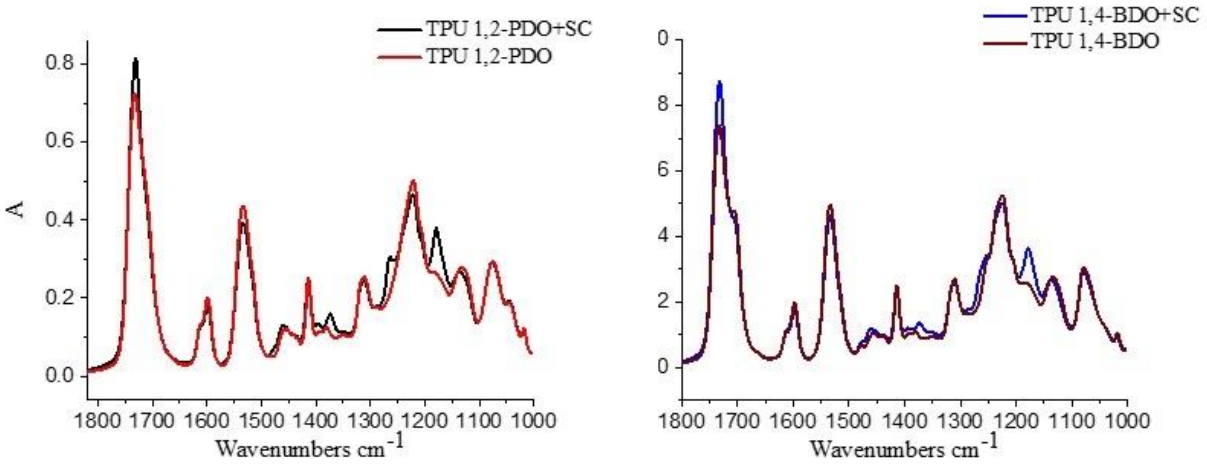

Figure 4.4 Room temperature FTIR spectra showing the effect of incorporation of PHMA units

Table 4.3 Assignment of IR bands of PHMA crystalline phase [10, 11]

Frequency cm^{-1}	**Assignment**
972	υ (C-C)
1176	υ (OC-O)
1264	υ_{as}(C-O-C)
1371, 1398	γ_w (CH_2)
1416, 1464	δ(CH_2)

Where γ_w=wagging, υ =stretching, υ_{as}=asymmetric stretching andδ =bending

4.3.2 Effect of annealing on the morphology of PHMA modified TPU

In-situ FTIR spectroscopic studies were carried out on the samples evaluate the kinetics associated with the crystallization process. We imposed a known and equivalent thermal profile on both samples in order to normalize morphological response. The temperature profile is shown in Figure 4.5. First, the sample was heated to a temperature (150 ºC) high enough to create a homogeneous phase or melting; sample was subsequently isothermally held at that temperature for five minutes, quenched to the annealing temperature of interests and held at that temperature for a period of time.

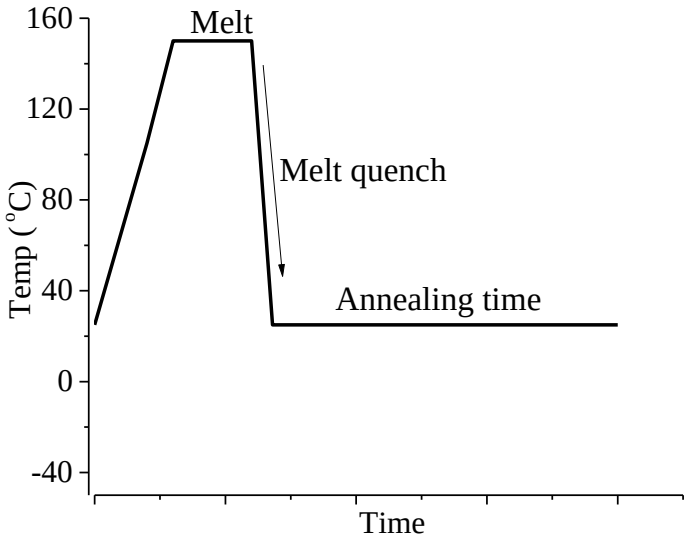

Figure 4.5 Temperature profile employed for annealing studies

4.3.2.1 Time-dependent FTIR studies

To understand the morphology formed in the modified TPUs as well as the kinetics associated with the attainment of the morphology, time and temperature dependent FTIR studies were carried out. Using temporal FTIR studies, the rate associated with the crystallization of the PHMA unit in the various chain extended systems can be obtained. From an applications perspective, since HMAs are applied from a high temperature to the substrate which is typically at room temperature (25 ºC), we can investigate morphological evolution by simulating application conditions. Figures 4.6–4.9 show the temperature and time-dependent annealing behavior of the semicrystalline-modified TPU samples. Figures 4.6a and 4.6b show the room temperature, time dependent response of the carbonyl regions 1800-1650 $cm^{-1}$and the crystalline peaks of the PHMA for the TPU 1,2-PDO + SC 25 ºC sample of HMAs. The structural evolution of the carbonyl peak does not differ from the structures observed in the previous chapter, as it also shows

phase-miscible behavior. On the other hand, the time evolution of the crystallization bands at 1265, 1178 and 970 cm^{-1} is observed. The room temperature behavior of the TPU 1,4-BDO + SC 25 ºC sample is shown in Figure 4.7a and 4.7b. The carbonyl region of this sample as shown in Figure 4.7a reveals the evolution of phase separation due to the stronger intermolecular interactions which are present in the symmetric butanediol chain extender unit but absent in the PDO sample. Additionally, the regions in 1265, 1178 and 970 cm^{-1} frequencies reveal the evolution of the crystalline PHMA bands. The changes observed in the 1225 and 1080 $cm^{-1}$are due to the HS interactions in the system [12-13]. Quantitative evaluation of the relative rate of crystallization is studied in the following section.

We tested the temperature dependency by carrying out temporal FTIR studies at other temperatures besides 25 ºC. Temperatures at 15 ºC and 35 ºC were imposed for these studies. The figures 4.8 and 4.9 are representative plots for the two symmetries of chain extenders carried out at 15 ºC. The influence of the experimental temperature and by extension the effect of mobility in controlling the crystallization behavior is observed clearly in Figure 4.8, which contains the symmetric chain extender. The test temperature of 15 ºC is just 5 ºC higher than the T_g of the system (10 ºC). At this temperature, the sample does not have the adequate segmental mobility required for the crystallization to occur and the curves do not show changes in their crystallization peaks. For the TPU 1,4-BDO + SC 15 ºC, a restriction in crystallization is not encountered as the T_g of the sample is much lower (-10 ºC) making the sample have the adequate mobility for crystallization to occur. The influence of molecular mobility in controlling the crystallization process will be studied in a subsequent section.

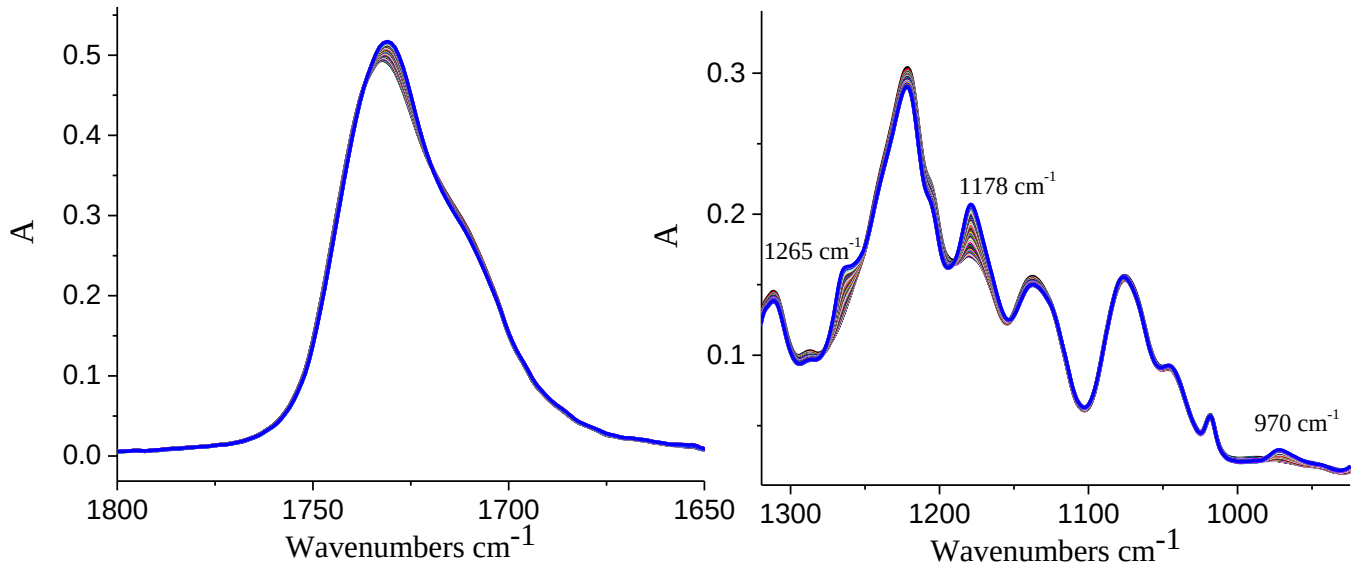

Figure 4.6 Time-dependent evolution of FTIR spectra for the TPU 1,2-PDO + SC 25 ºC sample

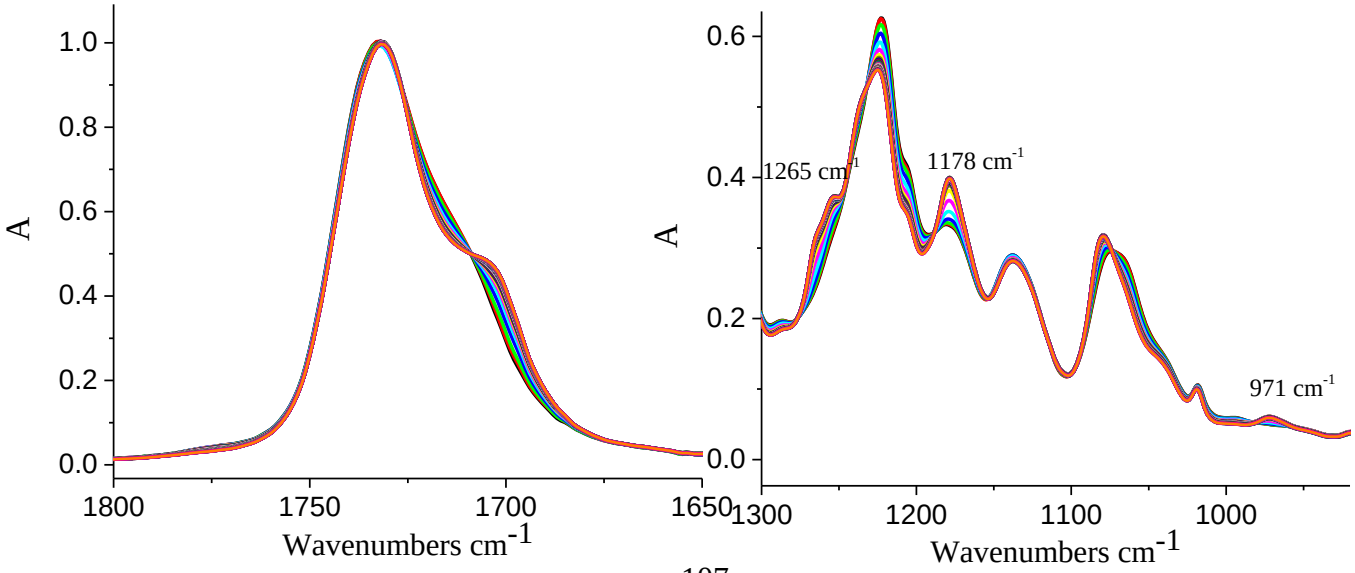

Figure 4.7 Time-dependent evolution of FTIR spectra for the TPU 1,4-PDO + SC 25 ºC sample

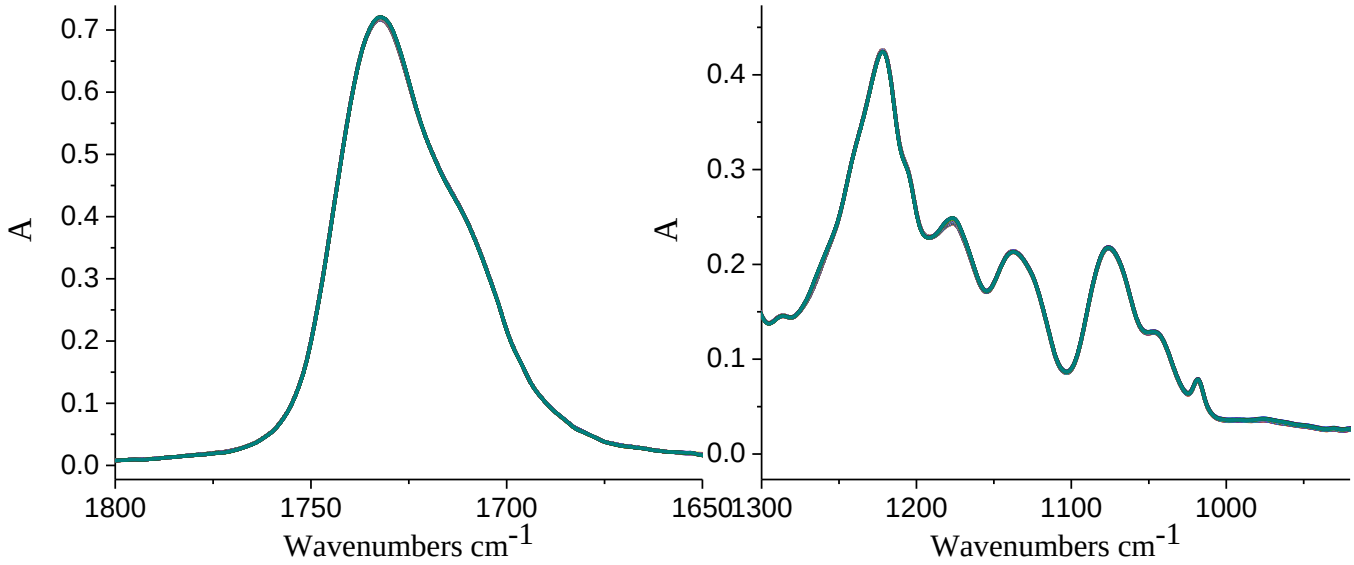

Figure 4.8 Time-dependent evolution of FTIR spectra for the TPU 1,2-PDO + SC 15 ºC sample

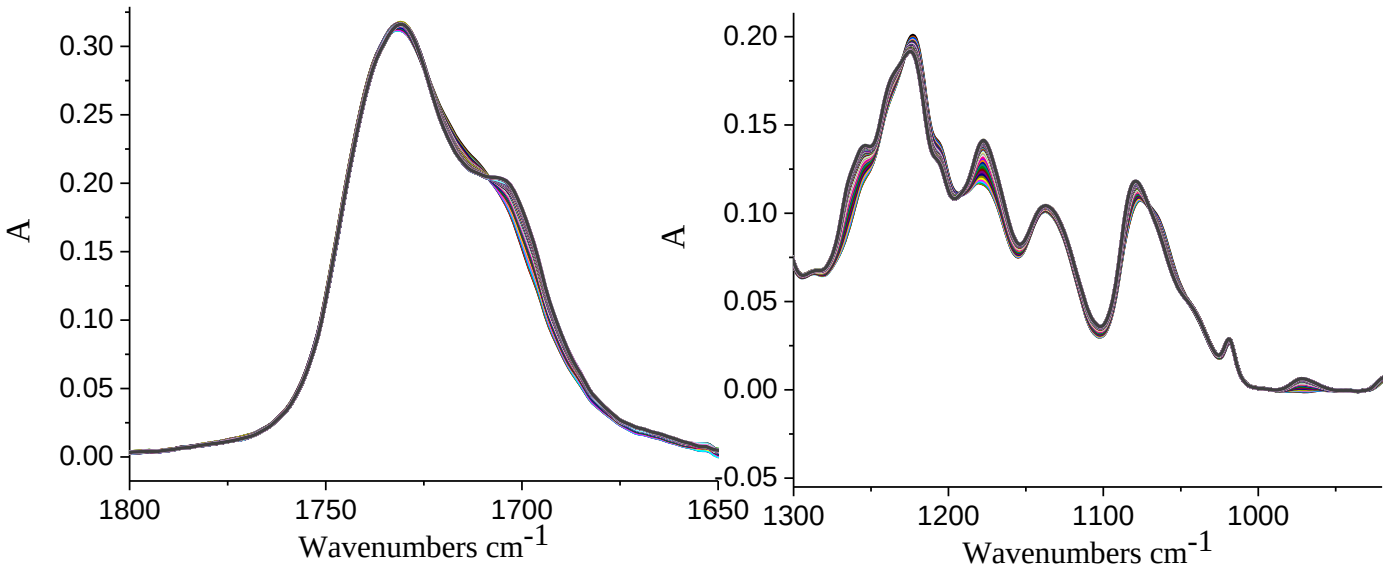

Figure 4.9 Time-dependent evolution of FTIR spectra for the TPU 1,2-PDO + SC 15 ºC sample

4.3.2.2 Quantification of rates associated with crystallization

To obtain a reasonable analysis of the morphological transitions present in the sample using IR analysis, appropriate band assignment is required. A prior investigation of the crystallization of PHA-PSA has been reported [10-11]. This report provides proper assignment of the bands of interest in the PHMA incorporated TPU samples. Most of the characteristic bands listed in Table 4.3 show a variation of their integrated absorbance with time, indicative of conformational changes due to ordering/crystallization occurring in the polymer sample. Most of the bands except the 972 cm^{-1}, however, overlap with some characteristic peaks of the polyurethane segment or the amorphous polyester polyol. Thus the IR spectra for the 972 cm^{-1} peak was analyzed quantitatively to investigate the kinetics associated with the crystallization of PHMA at various temperatures for the two symmetry types.

Figure 4.10 shows the integrated intensities plotted as a function of time during the crystallization process. The plot takes on a sigmoidal shape like most isothermal crystallization processes. The inference that can be made from the plots is that the TPU 1,4-BDO+SC system has faster crystallization speed than the TPU 1,2-PDO+SC for all temperatures studied. The TPU 1,4-BDO+SC possesses a lower T_g and thus greater segmental mobility its lower T_g gives it a broader range of temperatures for performing crystallization experiments (T_g= -10 ºC, T_m=53 ºC) when compared to the TPU 1,2-PDO+SC in which the range is narrower (T_g= 10 ºC, T_m=54 ºC)

For a quantitative description of the transformation process, the curves were fitted to the Avrami equation as shown below.

Equation 4.1 $$X = 1 - \exp(-Kt^n)$$

The equation can be re-written thus:

Equation 4.2 $$\log(-\ln(1 - X) = logK + nlogt$$

Where the degree of transformation, X is defined as $X = \frac{I_t - I_0}{I_\infty - I_0}$ where I_0, $I\infty$ and I_t represents the initial, final and integrated intensity at a time, t.

A sample Avrami plot is shown in Figure 4.11. A linear regression fit was applied to the curve and values of the slope and intercept were obtained from the fitting exercise. The crystallization half-life was obtained using the equation below. The crystallization half-time $t_{1/2}$, defined as the time at which the extent of crystallization is completed 50% is obtained below. The shorter the half-time is, the faster the crystallization rate.

Equation 4.3 $$t_{1/2} = \left(\frac{\ln 2}{K}\right)^{1/n}$$

Table 4.4 shows the $t_{1/2}$values for the two systems studied at different isothermal temperatures. Consistent with the qualitative conclusion from the crystallization isotherms obtained from Figures 4.10, the $t_{1/2}$ values which define the rate of crystallization follows the same trends. As the isothermal annealing temperature increases, the $t_{1/2}$ decreases and the rate of crystallization increases. Moreover, this is seen in both symmetries of chain extenders. The evolution of crystallization is heavily dependent on the crystallization temperature. At low temperatures, the supercooling becomes large. Additionally, the viscosity of the system is large making the transport of material to the growth front more restricted. As the temperature is increased, the system

should have the required mobility that favors the rapid formation of crystals. The mobility differences for the two different systems as a function of time can be probed using LFNMR and is reported in the following section.

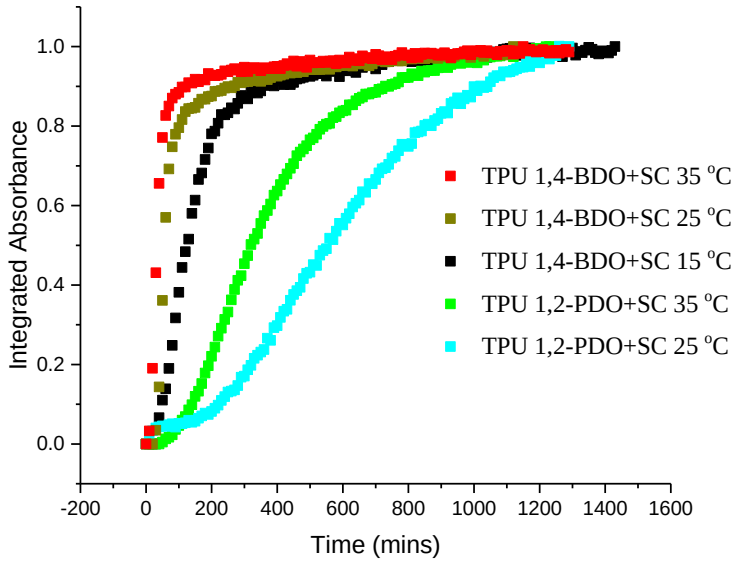

Figure 4.10 Overlay of the crystallization isotherms obtained at various temperatures for the different symmetries of chain extenders

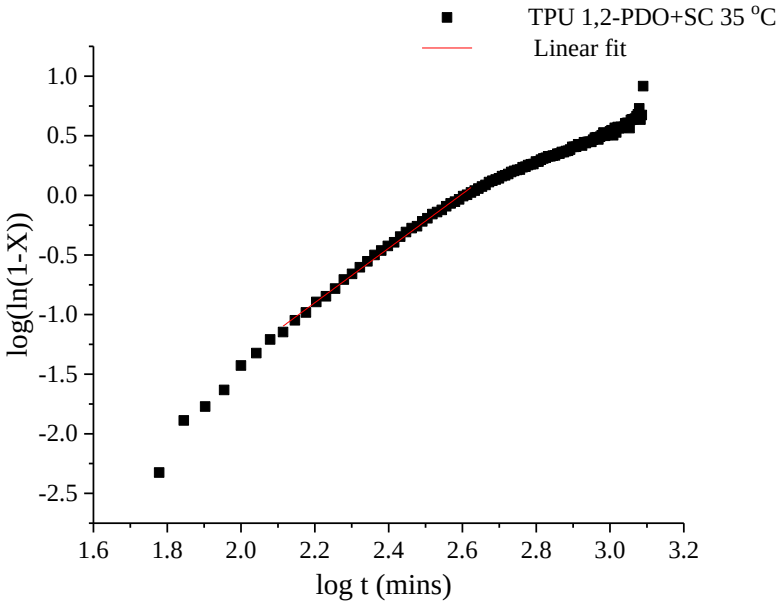

Figure 4.11 Representative Avrami plot for the determination of t1/2

Table 4.4 $t_{1/2}$ values for estimation of rate of crystallization

Sample	**$t_{1/2}$(mins)**
TPU 1,2-PDO + SC 25 ºC	550
TPU 1,2-PDO + SC 35 ºC	297
TPU 1,4-BDO + SC 15 ºC	124
TPU 1,4-BDO + SC 25 ºC	58
TPU 1,4-BDO + SC 35 ºC	34

4.3.3 Evaluation of molecular mobility of the TPU material

LFNMR, particularly the 1 H NMR is a technique that is sensitive to polymer chain dynamics on the microscopic scale and the segmental mobility inherent in a polymer sample. [14-15]. It is a complementary technique for the determination of segmental mobility to calorimetric, DMA technique amongst other bulk property characterization techniques. The NMR signals are usually obtained in the time domain and can distinguish different relaxation processes occurring in the sample. In this study, we have employed LFNMR to evaluate the role the symmetry of chain-extenders play in controlling the polymer chain dynamics and particularly in describing the limits accessible for the crystallization of the crystallizable SS.

Figure 4.12 shows the FID curves of the 2 classes of SC-modified chain extended TPUs isothermally annealed at various temperatures (15 ºC, 25 ºC, 35 ºC respectively). As is expected, as we increase the temperature, irrespective of the symmetry of the chain-

extended TPU, the molecular mobility of the polymer increases, this is shown in Table 4.5 after fitting the FID curve to the exponential decay equation.

Equation 4.4 $$M = M_o exp^{-\frac{t}{T_2}}$$

We can compare the T_2 values of the TPU 1,2-PDO + SC 35 ºC and TPU 1,4-BDO + SC 35 ºC as an example. The values of the asymmetric chain extender 48 µs is much smaller than that of the symmetric system with 275 µs indicative of the greater mobility that is present in the TPU 1,4-BDO. Just by changing chain extender structure, the significant variations in the molecular mobility occurs which affects the crystallization kinetics as is seen above. Rather than measuring the molecular mobility at just a specific temperature, we can also account for the differences in the SS T_g exhibited by both symmetries and compare FID curves at a normalized annealing temperature, T_a=T- T_g. As an example for the TPU 1,2-PDO+SC having T_g of ~10 ºC, the T_2 values obtained at a T_a value 25 ºC higher than T_g will be (T_g+25 ºC =35 ºC) compared with the TPU 1,4-BDO+SC sample with Tg=~-10 ºC (T_a = T_g+25 ºC =15 ºC). When the T_2 values are compared even after normalizing the annealing temperatures to their respective T_g, it is seen that the asymmetric TPU 1,2-PDO+SC (48 µs) still has the lower molecular mobility than the TPU 1,4-BDO (63 µs) sample due to its rigid pendant methyl group.

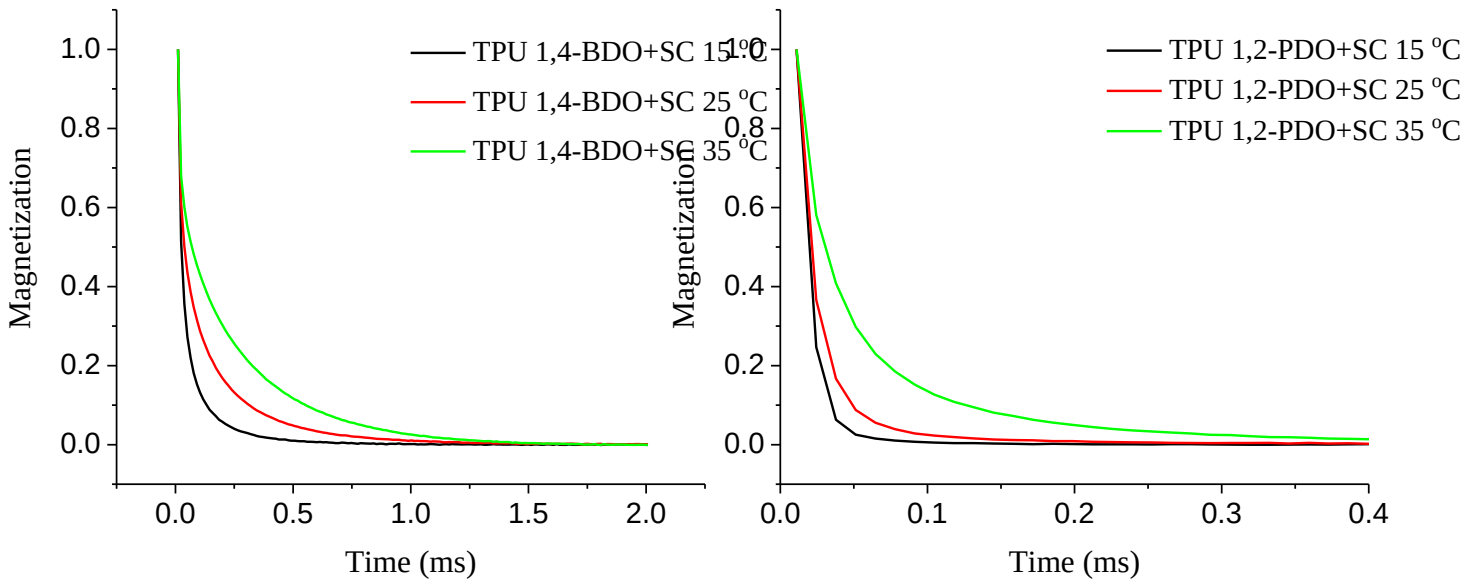

Figure 4.12 FID of TPU 1,4-BDO+SC and TPU 1,2-PDO+SC obtained at different temperatures

Table 4.5 T_2 relaxation value for the various chain extended TPUs obtained at different times

Sample	T_2 relaxation (μs)
TPU 1,2-PDO + SC 15 ºC	10
TPU 1,2-PDO + SC 25 ºC	19
TPU 1,2-PDO + SC 35 ºC	48
TPU 1,4-BDO + SC 15 ºC	63
TPU 1,4-BDO + SC 25 ºC	151
TPU 1,4-BDO + SC 35 ºC	275

4.3.4 Influence of incorporation of crystallinity of mechanical properties

Semicrystalline components have been incorporated to the samples from the previous chapter to not only control the open time but to increase the modulus of the TPUs studied

previously. It is well known that the introduction of crystallinity into an amorphous polymer can further enhance its modulus with the crystallites acting as rigid fillers to the amorphous matrix[1]. In the previous chapter, the morphological properties of the asymmetric chain extender system were shown to be ideal for HMA application since in those systems; the morphology development was shown to be rapid. In those studies, however, the modulus of the TPU 1,2-PDO was about 4MPa which is slightly lower than the modulus of the symmetric chain extender class. This study focuses on determining the change in mechanical properties that occur when ~ 20 % PHMA is introduced to the system. Figure 4.13, shows an overlay of the equilibrium modulus obtained after the samples were annealed for 3 days at room temperature. The samples before and after the incorporation of PHMA units are shown. From the Figure 4.13 and Table 4.5, it can be observed that the introduction of PHMA components significantly increased the value of the modulus. In the TPU 1,2-PDO+SC sample, the modulus is very significantly increased by about 500% from its initial state while in the sample TPU 1,4-BDO+SC a 75% increment was observed. Even though the symmetrical chain extender has the higher modulus values, the much larger percentage increase experienced in the TPU 1,2-PDO+SC sample may be related to the higher degree of crystallinity of the crystallizable SS observed in that sample as is shown in Table 4.5.

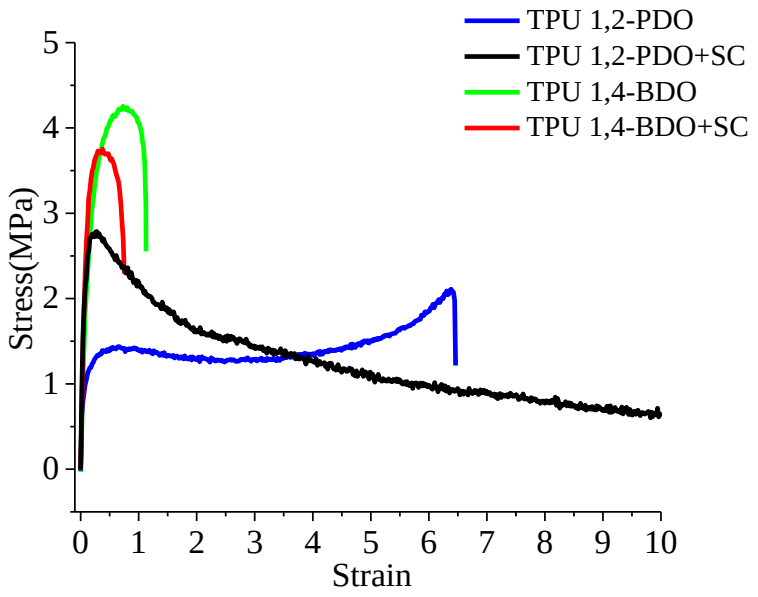

Figure 4.13 Mechanical behavior before and after the incorporation of PHMA units

Table 4.6 Table showing enhancement of modulus by introduction of PHMA units

Sample	Tensile Strength (MPa)	Modulus (MPa)	Percent elongation
TPU 100	2.8	25.6	1100
TPU 101	3.7	28	71
TPU 103	1.4	4.3	640
TPU 104	4.2	16	128

4.4 Conclusion

This study was carried out to determine the influence of the symmetry of chain extender on the crystallization behavior of TPUs to which some degree of crystallizable PHMA had been incorporated into. Using in situ FTIR spectroscopy, the effect of symmetry of the chain extender on the dynamics of crystallization was found to be profound. It was

observed that the higher segmental mobility of the symmetric chain extenders led to a comparatively faster crystallization speed for all temperatures examined than with the asymmetric chain extender showing relatively slower speeds for all temperatures studied. The higher Tg (~ 10 °C) of the asymmetric system narrows the range accessible for crystallization whereas the symmetric chain extender, with a lower Tg (~ -10 °C) has a broader range accessible for crystallization to proceed. Thermal properties, particularly the enthalpy of crystallization, at equilibrium morphologies revealed a greater degree of crystallinities for the asymmetric system. This was attributed to the less morphology present in the TPU 1,2-PDO+SC, i.e., the absence of phase separation which would have otherwise inhibited the crystallization process as is observed in the TPU 1,4-BDO+SC sample, where the ordered nature of its HS leads to the presence of phase separated domains which inhibit the crystallization of the PHMA SS. Even though the TPU 1,4-BDO+SC shows faster crystallization kinetics than the TPU 1,2-PDO+SC, it still occurs at a slower rate than is required for HMA. The slow rate of the morphology development relates to slow setting speeds, and slow setting speeds are disadvantageous for HMA application. Although enhancement to the modulus is observed as was expected, new polyols that have very rapid crystallization has to be studied in the future to make attractive HMAs.

4.5 References

1. Landel, R. F.; Nielsen, L. E., *Mechanical properties of polymers and composites*. Crc Press: 1993.
2. Meyer Jr, M. F.; McConnell, R. L., Amorphous and crystalline polyolefin based hot-melt adhesive. Google Patents: 1978.
3. Sonnenschein, M. F.; Rondan, N.; Wendt, B. L.; Cox, J. M., Synthesis of transparent thermoplastic polyurethane elastomers. *Journal of Polymer Science Part A: Polymer Chemistry* **2004,** *42* (2), 271-278.
4. Korley, L. T. J.; Pate, B. D.; Thomas, E. L.; Hammond, P. T., Effect of the degree of soft and hard segment ordering on the morphology and mechanical behavior of semicrystalline segmented polyurethanes. *Polymer* **2006,** *47* (9), 3073-3082.
5. Hood, M. A.; Wang, B.; Sands, J. M.; La Scala, J. J.; Beyer, F. L.; Li, C. Y., Morphology control of segmented polyurethanes by crystallization of hard and soft segments. *Polymer* **2010,** *51* (10), 2191-2198.
6. Jeong, Y. G.; Hashida, T.; Hsu, S. L.; Paul, C. W., Factors influencing curing Behavior in phase-separated structures. *Macromolecules* **2005,** *38* (7), 2889-2896.
7. Hashida, T.; Jeong, Y. G.; Hua, Y.; Hsu, S. L.; Paul, C. W., Spectroscopic study on morphology evolution in polymer blends. *Macromolecules* **2005,** *38* (7), 2876-2882.
8. Heintz, A. M.; McKiernan, R. L.; Gido, S. P.; Penelle, J.; Hsu, S. L.; Sasaki, S.; Takahara, A.; Kajiyama, T., Crystallization behavior of strongly interacting chains. *Macromolecules* **2002,** *35* (8), 3117-3125.

9. Sonnenschein, M. F.; Lysenko, Z.; Brune, D. A.; Wendt, B. L.; Schrock, A. K., Enhancing polyurethane properties via soft segment crystallization. *Polymer* **2005,** *46* (23), 10158-10166.

10. Liang, Z.; Pan, P.; Zhu, B.; Dong, T.; Hua, L.; Inoue, Y., Crystalline phase of isomorphic poly (hexamethylene sebacate-co-hexamethylene adipate) copolyester: Effects of comonomer composition and crystallization temperature. *Macromolecules* **2010,** *43* (6), 2925-2932.

11. Liang, Z.; Pan, P.; Zhu, B.; Inoue, Y., Isomorphic crystallization of poly (hexamethylene adipate-co-butylene adipate): Regulating crystal modification of polymorphic polyester from internal crystalline lattice. *Macromolecules* **2010,** *43* (15), 6429-6437.

12. Srichatrapimuk, V. W.; Cooper, S. L., Infrared thermal analysis of polyurethane block polymers. *Journal of Macromolecular Science, Part B: Physics* **1978,** *15* (2), 267-311.

13. Lee, H. S.; Hsu, S. L., An analysis of phase separation kinetics of model polyurethanes. *Macromolecules* **1989,** *22* (3), 1100-1105.

14. Nierzwicki, W., Microphase separation in urethane elastomers as seen through NMR measurements. *Journal of applied polymer science* **1984,** *29* (4), 1203-1213.

15. Hertlein, C.; Saalwächter, K.; Strobl, G., Low-field NMR studies of polymer crystallization kinetics: Changes in the melt dynamics. *Polymer* **2006,** *47* (20), 7216-7221.

CHAPTER 5
CONCLUSIONS AND FUTURE WORK

5.1 Conclusions

This thesis demonstrates the influence of chain configuration in influencing HMA properties such as the set speed, mechanical behavior, and green strength. The morphological behavior of the polymers studied was shown to influence HMA process parameters. In the case of the polypropylene based copolymers, two different types of chain configurations were examined, one random or following Bernoullian distribution, and the other exhibiting a bimodal distribution in crystallizable propylene sequences. Average sequence length and the distribution of propylene sequences of random PP-PE copolymers was experimentally determined by using ^{13}C-NMR. The actual distribution of crystallizable propylene sequences was obtained using a thermal fractionation technique (SSA). The effect of sequence distribution of the propylene chains on the crystallization behavior of PP-PE copolymers was significant. The individual crystallization behavior and the morphology formed have been investigated by using DSC and infrared spectroscopy. Longer sequence length led to an increase in T_c of PP-PE copolymer. The isothermal crystallization study demonstrated that the crystallization rate of PP-PE copolymer was increased with an increase in the sequence length of PP. From this comparison, it was concluded that the length of crystallizable sequences determines the crystallization temperature and the degree of crystallinity. It is possible that the longer ethylene sequence length between propylene segments enhances the mobility of copolymer chains, thus favoring the crystallization kinetics of copolymers containing a bimodal distribution of PP sequences. This study provides additional guidance in designing copolymers to act as special adhesives for use at elevated temperatures.

Polyurethanes were explored as possible candidates for HMA application due to the polarity inherent in its structure which makes it capable of binding to a variety of substrates. For these systems, chain configurational control was facilitated by changing the symmetry of the chain extenders used in synthesizing the TPUs. Traditional chain extenders based on 1,4-BDO systems though provided phase separation, however, proved unsuitable because of the long times are taken for their morphology to set which is disadvantageous for HMAs. To circumvent this problem of slow kinetics in the morphology of conventional systems, we have elected to change the mobility associated with the chain extenders, a seldom studied subject. A comparatively inflexible asymmetric chain extender based on 1,2-PDO was used to alter the morphology of the TPUs. The presence of the pendant groups in this system reduces its mobility and makes the HS made from it lack the mobility to move away from the SS matrix. We have shown this to be vital in creating stable domains whose properties do not change over time. For our investigation, we employed LFNMR was used to distinguish between the segmental mobility of both chain extender classes. Morphological studies were done with the aid of FTIR, SAXS, and DSC to simulate in-use properties, time dependent measurements of morphology were made. The results showed that by altering the chain architecture of the chain extenders used in the synthesis of TPUs, adequate morphology required for a particular application could be obtained. In our case, our annealing studies using the asymmetric chain extenders showed time-independence in morphology development, which can be correlated to the setting speed required in HMA application.

Even though the morphology of the TPUs obtained from the amorphous polyester polyols based on the 1,2-PDO systems was ideal for HMA application, the absence of

crystallizable segments in its structure leads to the long open times and also low moduli. Semi crystalline PHMA segments were incorporated into the various chain extended TPU structure to control process parameters. The study in chapter 4 focused on developing an understanding of the influence of the symmetry of chain extender on the crystallization behavior of PHMA-modified TPUs. Using in situ FTIR spectroscopy, the effect of symmetry of the chain extender on the dynamics of crystallization was found to be profound. It was observed that the higher segmental mobility of the symmetric chain extenders led to a comparatively faster crystallization speed for all temperatures examined than with the asymmetric chain extender showing relatively slower speeds for all temperatures studied. The higher Tg (~ 10 °C) of the asymmetric system narrows the range accessible for crystallization whereas the symmetric chain extender, with a lower Tg (~ -10 °C) has a broader range accessible for crystallization to proceed. Thermal properties, particularly the enthalpy of crystallization, at equilibrium morphologies revealed a greater degree of crystallinities for the asymmetric system. This was attributed to the less complicated morphology present in the TPU 1,2-PDO+SC i.e. the absence of phase separation which would have otherwise inhibited the degree of crystallinity even further as is observed in the TPU 1,4-BDO+SC sample, where the ordered nature of its HS leads to the presence of phase separated domains which inhibit the crystallization of the PHMA. Even though the TPU 1,4-BDO+SC shows faster crystallization kinetics than the TPU 1,2-PDO+SC, it still occurs at slower rates than is required for HMA. The slow rate of the morphology development relates to slow setting speeds, and slow setting speeds are disadvantageous for HMA application. Although enhancement to the modulus

is observed as was expected, new polyols that have very rapid crystallization has to be studied in the future to make attractive HMAs.

5.2 Future work

5.2.1 Origin of the bimodal melting peaks in PP copolymer structure

In chapter 2, bimodality in the melting endotherms was observed in the copolymers 1 and 2. Bimodality in the endothermic transition of polypropylene based polymers is commonly observed [1-2]. Various factors such as the presence of frustrated structures, the existence of different polymorphic transitions, the occurrence of crystal habitat containing varying degrees of perfection and due to the presence of a recrystallization or reorganization of some crystallized fractions during the heating experiments have been attributed to the reason for the occurrence of bimodality[1-2]. In our samples, we carried out tests to confirm if the origin of bimodality was based on the melting recrystallization and remelting (mrr) phenomenon by conducting heating/cooling experiments at different cooling rates. The Figure 5.1, shows the results obtained for the two classes of copolymers. In these kinds of thermal experiments, the emergence of a single peak at slow cooling rates typically points to the mrr phenomenon as the origin of bimodality. In our system as shown in Figure 5.1, at slow cooling rates, the bimodality became even further pronounced with slower cooling rates. This indicates that the mrr phenomenon is not the origin of the bimodality in the melting peak. A study of other possible reasons for the emergence of the doublet in melting endotherm will be necessary to give a more detailed understanding of chain configurational differences.

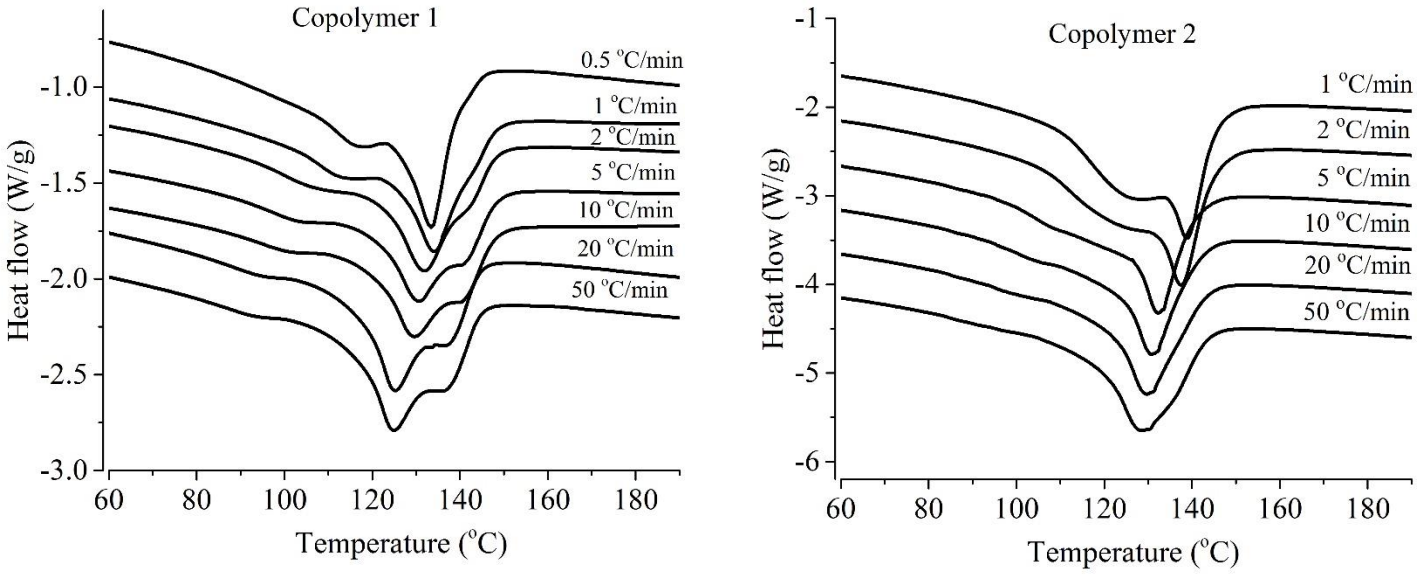

Figure 5.1 The melting transition of copolymers non-isothermally crystallized at different rates

5.2.2 Calibration curve for fractionation experiments

Thermal fractionation techniques based on SSA was used in studying the effect of chain configurational differences on the crystallization behavior of the crystallization kinetics. It will be interesting to see if the conclusions derived from SSA matches with the Temperature rising Elution fractionation technique TREF. The TREF technique is routinely used in industry and academia for the determination of the crystallizable sequence distribution, in the technique, molecular segregation of the short chain branches occur, and only the long sequences are revealed[3]. The downside of the TREF technique is related to the very long times required for the experimental procedure and a significant amount of solvents needed for the experiments. The SSA techniques are relatively easier, less expensive and require shorter time. It will be interesting to carry out both

experiments on the PP copolymer samples and observe if a linear correlation is observed to prove the validity and usefulness of the SSA technique.

5.2.3 Effect of architecture of chain extender on non-isocyanate polyurethanes

An advantage of HMAs over solvent based adhesives is the fact that HMAs are robust and thus are more environmentally friendly than their solvent counterparts. Polyurethanes are synthesized via an isocyanate route. Isocyanates are toxic and can cause health and environmental hazards. Health risks that emanate from exposure can include asthma and skin irritation. In order to obtain a entirely environmentally friendly HMAs based on urethane functionalities, the non-isocyanate polyurethane (NIPU) routes for the formation of TPUs can be studied. The chemistries for the formation of NIPUs involves the reaction of a cyclo-carbonate and an amine functionality. A one step reaction involving the cyclo-carbonate group, an amine based polyol and an amine based chain extender can be reacted[3-4]. The influence of the symmetry of the chain extender on the morphology of the polymer can be studied. For example rather than a 1,4-butanediamine, a 1,2-propanediamine can be reacted to reveal the morphologies. Figure 5.2 shown below reveals the synthetic path for the reaction between a cyclo carbonate, an amine based polyol and various symmetries of amine chain extenders. The major benefit of this system over the use of isocyanates will be the elimination of toxicity that comes with the handling of isocyanates. The same symmetry of chain extenders employed in the isocyanate route will also be used here for chain-configurational control.

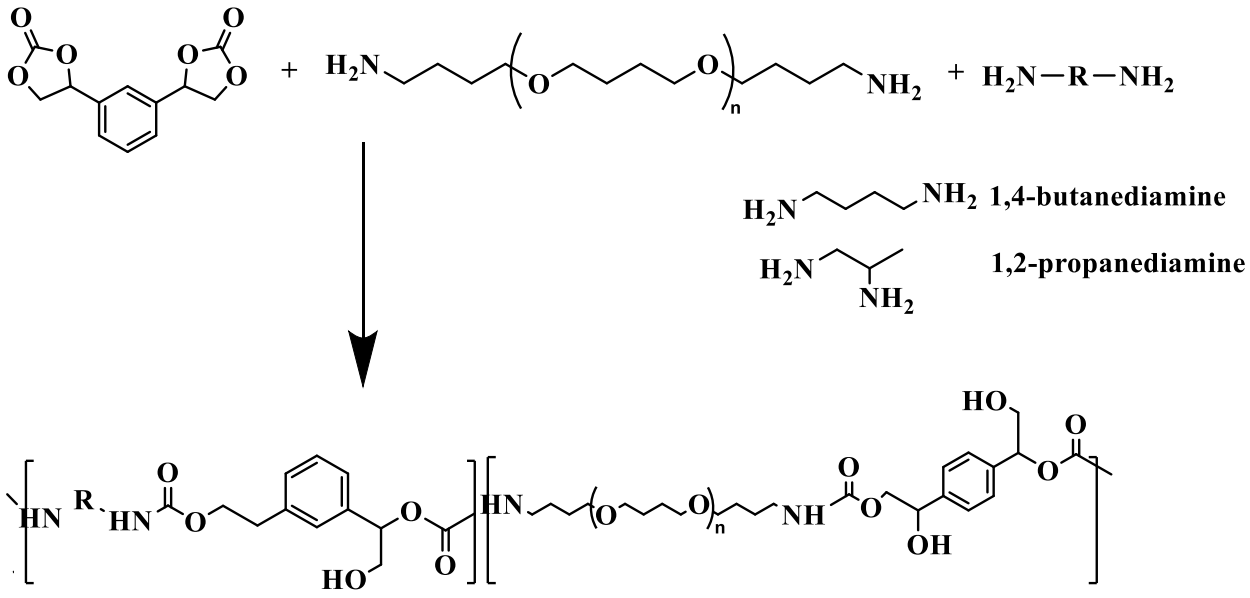

Figure 5.2 Schematic for synthesis of NIPU with different symmetry of chain-extenders

5.2.4 Segmental Dynamics studies using LFNMR

Literature is replete with studies on the morphological behavior of polyurethanes. However, detailed studies on the segmental dynamics occurring in polyurethanes have not been carried out before. Unlike in very rigid systems such as phenolics, in which crosslink density is enormously high with restricted and segmental mobility, polyurethanes such as the ones used in our studies have greater chain mobility. Therefore, interesting studies on chain mobility below and above the Tg can be explored. LFNMR is an excellent technique for these types of measurements. For these kinds of studies, rather than measure the T_2 relaxation at just one temperature, a temperature sweep can be carried out on the polymers at high and low temperatures by using the variable temperature controller connected to the LFNMR instrument and the T_1 values will yield more information about the segmental dynamics of the TPU. Differences between the

two symmetries of chain extenders will give information about how the chain extenders influence the relaxation times below and above Tg.

The curve of T1 versus temperature obtained from LFNMR is analogous to the tan delta versus temperature curves that are derived from DMA and dielectric experiments[5]. Just as a maximum is obtained in those techniques, a minimum in the T1 experiments is observed, and this has been correlated with a variety of Tg or sub Tg motions occurring in the polymer system. Quantitative analysis of T1 vs. temperature curves for small molecules is usually done by fitting the experimental data using the Bloembergen, Purcell, and Pound (BPP) analysis[6]. In polymers, however, the nuclear spins are highly coupled and a distribution of correlation times will be needed to account for the relaxation behavior adequately. A distribution function such as the Fuoss-Kirkwood function[7], which has been used in dielectric spectroscopy studies can be introduced into to BPP equation to give equation such as the one below, which can be applied to analyze the curves of the different chain extended TPUs

Equation 5.1

$$\frac{1}{T_1} = A\left(\frac{\beta}{\omega}\right)\left[\frac{\left(\omega\tau_0 \exp\left(\frac{E}{RT}\right)\right)^{\beta}}{1+\left(\omega\tau_0 \exp\left(\frac{E}{RT}\right)\right)^{2\beta}} + 2\frac{\left(2\omega\tau_0 \exp\left(\frac{E}{RT}\right)\right)^{\beta}}{1+\left(2\omega\tau_0 \exp\left(\frac{E}{RT}\right)\right)^{2\beta}}\right]$$

5.2.5 Incorporation of faster crystallizing polyols

In chapter 4, the inclusion of semi-crystalline polyol system to the different symmetries of chain extender was explored. It was necessary to incorporate semi-crystalline components to the already amorphous system in order to control process parameters like setting speed, open time and the ultimate mechanical properties. The incorporation of PHMA based polyols revealed slow kinetics for both symmetries of chain extenders. The

slow crystallization behavior we believe can be circumvented by either increasing the composition of the PHMA units from ~20 % to higher compositions until optimal properties are derived. We can also replace the PHMA polyols with other higher aliphatic polyols such as polyhexamethylene sebacate PHMS among others which can crystallize at a more rapid rate than the PHMA. Process temperature can also be tuned in this newer systems to achieve optimal crystallization speeds.

5.3 References

1. Kardos, J.; Christiansen, A.; Baer, E., Structure of pressure-crystallized polypropylene. *Journal of Polymer Science Part B: Polymer Physics* **1966,** *4* (5), 777-788.
2. Samuels, R. J., Quantitative structural characterization of the melting behavior of isotactic polypropylene. *Journal of Polymer Science Part B: Polymer Physics* **1975,** *13* (7), 1417-1446.
3. Anantawaraskul, S.; Soares, J. B.; Wood-Adams, P. M., Fractionation of Semicrystalline Polymers by Crystallization Analysis Fractionationand Temperature Rising Elution Fractionation. In *Polymer Analysis Polymer Theory*, Springer: 2005; pp 1-54.
4. Beniah, G.; Heath, W. H.; Jeon, J.; Torkelson, J. M., Tuning the properties of segmented polyhydroxyurethanes via chain extender structure. *Journal of Applied Polymer Science* **2017**.
5. Connor, T.; Blears, D.; Allen, G., Proton spin-lattice relaxation in polypropylene oxides. *Transactions of the Faraday Society* **1965,** *61*, 1097-1109.
6. Bloembergen, N.; Purcell, E. M.; Pound, R. V., Relaxation effects in nuclear magnetic resonance absorption. *Physical review* **1948,** *73* (7), 679.
7. Kirkwood, J. G.; Fuoss, R. M., Anomalous dispersion and dielectric loss in polar polymers. *The Journal of Chemical Physics* **1941,** *9* (4), 329-340.

BIBLOGRAPHY

Abouzahr, S.; Wilkes, G. L., Structure property studies of polyester-and polyether-based MDI–BD segmented polyurethanes: Effect of one-vs. two-stage polymerization conditions. Journal of applied polymer science 1984, 29 (9), 2695-2711.

Alamo, R. G.; Viers, B. D.; Mandelkern, L., A re-examination of the relation between the melting temperature and the crystallization temperature: linear polyethylene. Macromolecules 1995, 28 (9), 3205-3213.

An, H.; Li, X.; Geng, Y.; Wang, Y.; Wang, X.; Li, L.; Li, Z.; Yang, C., Shear-induced conformational ordering, relaxation, and crystallization of isotactic polypropylene. The Journal of Physical Chemistry B 2008, 112 (39), 12256-12262.

Anantawaraskul, S.; Soares, J. B.; Wood-Adams, P. M., Fractionation of Semicrystalline Polymers by Crystallization Analysis Fractionationand Temperature Rising Elution Fractionation. In Polymer Analysis Polymer Theory, Springer: 2005; pp 1-54.

Arteca, G. A., Scaling behavior of some molecular shape descriptors of polymer chains and protein backbones. Physical Review E 1994, 49 (3), 2417.

Assink, R., The study of domain structure in polyurethanes by nuclear magnetic resonance. Journal of Polymer Science Part B: Polymer Physics 1977, 15 (1), 59-69.

Badrossamay, M. R.; Sun, G., A study of radical graft copolymerization on polypropylene during extrusion using two peroxide initiators. Polymer International 2010, 59 (2), 155-161.

Bae, J.; Chung, D.; An, J.; Shin, D., Effect of the structure of chain extenders on the dynamic mechanical behaviour of polyurethane. Journal of materials science 1999, 34 (11), 2523-2527.

Baker, W.; Fuller, C., Intermolecular Forces and Chain Configuration in Linear Polymers—The Effect of N-Methylation on the X-Ray Structures and Properties of Linear Polyamides. Journal of the American Chemical Society 1943, 65 (6), 1120-1130.

Bartczak, Z.; Chiono, V.; Pracella, M., Blends of propylene-ethylene and propylene-1-butene random copolymers: I. Morphology and structure. Polymer 2004, 45 (22), 7549-7561.

Bedia, E. L.; Astrini, N.; Sudarisman, A.; Sumera, F.; Kashiro, Y., Characterization of polypropylene and ethylene–propylene copolymer blends for industrial applications. Journal of applied polymer science 2000, 78 (6), 1200-1208.

Benedek, I., Developments in pressure-sensitive products. CRC Press: 2005.

Benedek, I., Pressure-sensitive adhesives and applications. CRC Press: 2004.

Benedek, I.; Feldstein, M. M., Technology of pressure-sensitive adhesives and products. CRC Press: 2008.

Beniah, G.; Heath, W. H.; Jeon, J.; Torkelson, J. M., Tuning the properties of segmented polyhydroxyurethanes via chain extender structure. Journal of Applied Polymer Science 2017.

Blackwell, J.; Nagarajan, M.; Hoitink, T., Structure of polyurethane elastomers. X-ray diffraction and conformational analysis of MDI-propandiol and MDI-ethylene glycol hard segments. Polymer 1981, 22 (11), 1534-1539.

Bloembergen, N.; Purcell, E. M.; Pound, R. V., Relaxation effects in nuclear magnetic resonance absorption. Physical review 1948, 73 (7), 679.

Bonart, R.; Müller, E., Phase separation in urethane elastomers as judged by low-angle X-ray scattering. II. Experimental results. Journal of Macromolecular Science—Physics 1974, 10 (2), 345-357.

Born, L.; Hespe, H.; Crone, J.; Wolf, K., The physical crosslinking of polyurethane elastomers studied by X-ray investigation of model urethanes. Colloid & Polymer Science 1982, 260 (9), 819-828.

Braude, F., Adhesives. 1943.

Carman, C.; Harrington, R.; Wilkes, C., Monomer sequence distribution in ethylene-propylene rubber measured by 13C NMR. 3. Use of reaction probability model. Macromolecules 1977, 10 (3), 536-544.

Cheng, H., Carbon-13 NMR analysis of ethylene-propylene rubbers. Macromolecules 1984, 17 (10), 1950-1955.

Coates, G. W.; Waymouth, R. M., Oscillating stereocontrol: a strategy for the synthesis of thermoplastic elastomeric polypropylene. Science 1995, 267 (5195), 217.

Coleman, M. M.; Painter, P. C.; Graf, J. F., Specific interactions and the miscibility of polymer blends. CRC Press: 1995.

Connor, T.; Blears, D.; Allen, G., Proton spin-lattice relaxation in polypropylene oxides. Transactions of the Faraday Society 1965, 61, 1097-1109.

Crist, B.; Howard, P., Crystallization and melting of model ethylene-butene copolymers. Macromolecules 1999, 32 (9), 3057-3067.

Das, S.; Cox, D. F.; Wilkes, G. L.; Klinedinst, D. B.; Yilgor, I.; Yilgor, E.; Beyer, F. L., Effect of Symmetry and H-bond Strength of Hard Segments on the Structure-Property Relationships of Segmented, Nonchain Extended Polyurethanes and Polyureas. Journal of Macromolecular Science, Part B: Physics 2007, 46 (5), 853-875.

De Rosa, C.; Auriemma, F., Crystals and crystallinity in polymers: diffraction analysis of ordered and disordered crystals. John Wiley & Sons: 2013.

Delmonte, J., Technology of adhesives. 1947.

Diogo, A. C., Polymers in Building and Construction. In Materials for Construction and Civil Engineering, Springer: 2015; pp 447-499.

Engels, H. W.; Pirkl, H. G.; Albers, R.; Albach, R. W.; Krause, J.; Hoffmann, A.; Casselmann, H.; Dormish, J., Polyurethanes: versatile materials and sustainable problem solvers for today's challenges. Angewandte Chemie International Edition 2013, 52 (36), 9422-9441.

Feng, Y.; Hay, J., The characterisation of random propylene–ethylene copolymer. Polymer 1998, 39 (25), 6589-6596.

Fillon, B.; Wittmann, J. C.; Lotz, B.; Thierry, A., Self-Nucleation and Recrystallization of Isotactic Polypropylene (Alpha-Phase) Investigated by Differential Scanning Calorimetry. Journal of Polymer Science Part B-Polymer Physics 1993, 31 (10), 1383-1393.

Flory, P. J., Theory of crystallization in copolymers. Transactions of the Faraday Society 1955, 51, 848-857.

Gahleitner, M.; Jääskeläinen, P.; Ratajski, E.; Paulik, C.; Reussner, J.; Wolfschwenger, J.; Neißl, W., Propylene–ethylene random copolymers: Comonomer effects on crystallinity and application properties. Journal of Applied Polymer Science 2005, 95 (5), 1073-1081.

Geng, Y.; Wang, G.; Cong, Y.; Bai, L.; Li, L.; Yang, C., Shear-induced nucleation and growth of long helices in supercooled isotactic polypropylene. Macromolecules 2009, 42 (13), 4751-4757.

Gibbs, J. W., The scientific papers of J. Willard Gibbs. Longmans, Green and Company: 1906; Vol. 1.

Ginzburg, V. V.; Bicerano, J.; Christenson, C. P.; Schrock, A. K.; Patashinski, A. Z., Theoretical modeling of the relationship between Young's modulus and formulation variables for segmented polyurethanes. Journal of Polymer Science Part B: Polymer Physics 2007, 45 (16), 2123-2135.

Harrell Jr, L., Segmented polyurethans. Properties as a funcation of segment size and distribution. Macromolecules 1969, 2 (6), 607-612.

Hashida, T.; Jeong, Y. G.; Hua, Y.; Hsu, S. L.; Paul, C. W., Spectroscopic study on morphology evolution in polymer blends. Macromolecules 2005, 38 (7), 2876-2882.

Heintz, A. M.; McKiernan, R. L.; Gido, S. P.; Penelle, J.; Hsu, S. L.; Sasaki, S.; Takahara, A.; Kajiyama, T., Crystallization behavior of strongly interacting chains. Macromolecules 2002, 35 (8), 3117-3125.

Hertlein, C.; Saalwächter, K.; Strobl, G., Low-field NMR studies of polymer crystallization kinetics: Changes in the melt dynamics. Polymer 2006, 47 (20), 7216-7221.

Hood, M. A.; Wang, B.; Sands, J. M.; La Scala, J. J.; Beyer, F. L.; Li, C. Y., Morphology control of segmented polyurethanes by crystallization of hard and soft segments. Polymer 2010, 51 (10), 2191-2198.

Horst, R. H.; Winter, H. H., Stable Critical Gels of a Crystallizing Copolymer of Ethene and 1-Butene. Macromolecules 2000, 33 (1), 130-136.

Horváth, Z.; Menyhárd, A.; Doshev, P.; Gahleitner, M.; Varga, J.; Tranninger, C.; Pukánszky, B., Chain regularity of isotactic polypropylene determined by different thermal fractionation methods. Journal of Thermal Analysis and Calorimetry 2014, 118 (1), 235-245.

Hosier, I.; Alamo, R.; Esteso, P.; Isasi, J.; Mandelkern, L., Formation of the α and γ polymorphs in random metallocene-propylene copolymers. Effect of concentration and type of comonomer. Macromolecules 2003, 36 (15), 5623-5636.

Hosoda, S.; Nozue, Y.; Kawashima, Y.; Suita, K.; Seno, S.; Nagamatsu, T.; Wagener, K. B.; Inci, B.; Zuluaga, F.; Rojas, G., Effect of the Sequence Length Distribution on the Lamellar Crystal Thickness and Thickness Distribution of Polyethylene: Perfectly Equisequential ADMET Polyethylene vs Ethylene/α-Olefin Copolymer. Macromolecules 2010, 44 (2), 313-319.

Houwink, R.; Bruyne, N. A. d.; Salomon, G., Adhesion and adhesives. 1965.

Jacobsen, N. E., NMR spectroscopy explained: simplified theory, applications and examples for organic chemistry and structural biology. John Wiley & Sons: 2007.

Janevski, A.; Bogoeva-Gaceva, G.; Grozdanov, A., Crystallization and melting behavior of iPP studied by DSC. Journal of applied polymer science 1998, 67, 395-404.

Jeon, K.; Palza, H.; Quijada, R.; Alamo, R. G., Effect of comonomer type on the crystallization kinetics and crystalline structure of random isotactic propylene 1-alkene copolymers. Polymer 2009, 50 (3), 832-844.

Jeong, Y. G.; Hashida, T.; Hsu, S. L.; Paul, C. W., Factors influencing curing Behavior in phase-separated structures. Macromolecules 2005, 38 (7), 2889-2896.

Kalish, J. P.; Ramalingam, S.; Bao, H. M.; Hall, D.; Wamuo, O.; Hsu, S. L.; Paul, C. W.; Eodice, A.; Low, Y. G., An analysis of the role of wax in hot melt adhesives. International Journal of Adhesion and Adhesives 2015, 60, 63-68.

Kalish, J. P.; Ramalingam, S.; Wamuo, O.; Vyavahare, O.; Wu, Y.; Hsu, S. L.; Paul, C. W.; Eodice, A., Role of n-alkane-based additives in hot melt adhesives. International Journal of Adhesion and Adhesives 2014, 55, 82-88.

Kang, J.; Wang, B.; Peng, H.; Chen, J.; Cao, Y.; Li, H.; Yang, F.; Xiang, M., Investigation on the structure and crystallization behavior of controlled-rheology polypropylene with different stereo-defect distribution. Polymer Bulletin 2014, 71 (3), 563-579.

Kardos, J.; Christiansen, A.; Baer, E., Structure of pressure-crystallized polypropylene. Journal of Polymer Science Part B: Polymer Physics 1966, 4 (5), 777-788.

Kirkwood, J. G.; Fuoss, R. M., Anomalous dispersion and dielectric loss in polar polymers. The Journal of Chemical Physics 1941, 9 (4), 329-340.

Koberstein, J. T.; Stein, R. S., Small-angle X-ray scattering studies of microdomain structure in segmented polyurethane elastomers. Journal of Polymer Science Part B: Polymer Physics 1983, 21 (8), 1439-1472.

Koenig, J. L., Chemical microstructure of polymer chains. Wiley: 1980.

Korley, L. T. J.; Pate, B. D.; Thomas, E. L.; Hammond, P. T., Effect of the degree of soft and hard segment ordering on the morphology and mechanical behavior of semicrystalline segmented polyurethanes. Polymer 2006, 47 (9), 3073-3082.

Krimm, S.; Liang, C.; Sutherland, G., Infrared spectra of high polymers. II. Polyethylene. The Journal of Chemical Physics 1956, 25 (3), 549-562.

Krol, P., Synthesis methods, chemical structures and phase structures of linear polyurethanes. Properties and applications of linear polyurethanes in polyurethane elastomers, copolymers and ionomers. Progress in materials science 2007, 52 (6), 915-1015.

Landel, R. F.; Nielsen, L. E., Mechanical properties of polymers and composites. Crc Press: 1993.

Lauritzen, J. I.; Hoffman, J. D., Theory of formation of polymer crystals with folded chains in dilute solution. J. Res. Natl. Bur. Stand. A 1960, 64 (1), 73102.

Lee, H. S.; Hsu, S. L., An analysis of phase separation kinetics of model polyurethanes. Macromolecules 1989, 22 (3), 1100-1105.

Lee, H. S.; Wang, Y. K.; Hsu, S. L., Spectroscopic analysis of phase separation behavior of model polyurethanes. Macromolecules 1987, 20 (9), 2089-2095.

Li, S. H.; Woo, E. M., Effects of chain configuration on UCST behavior in blends of poly (L-lactic acid) with tactic poly (methyl methacrylate) s. Journal of Polymer Science Part B: Polymer Physics 2008, 46 (21), 2355-2369.

Li, W.; Bouzidi, L.; Narine, S. S., Current research and development status and prospect of hot-melt adhesives: A review. Industrial & Engineering Chemistry Research 2008, 47 (20), 7524-7532.

Li, Y.; Gao, T.; Chu, B., Synchrotron SAXS studies of the phase-separation kinetics in a segmented polyurethane. Macromolecules 1992, 25 (6), 1737-1742.

Li, Y.; Ren, Z.; Zhao, M.; Yang, H.; Chu, B., Multiphase structure of segmented polyurethanes: effects of hard-segment flexibility. Macromolecules 1993, 26 (4), 612-622.

Liang, Z.; Pan, P.; Zhu, B.; Dong, T.; Hua, L.; Inoue, Y., Crystalline phase of isomorphic poly (hexamethylene sebacate-co-hexamethylene adipate) copolyester: Effects of comonomer composition and crystallization temperature. Macromolecules 2010, 43 (6), 2925-2932.

Liang, Z.; Pan, P.; Zhu, B.; Inoue, Y., Isomorphic crystallization of poly (hexamethylene adipate-co-butylene adipate): Regulating crystal modification of polymorphic polyester from internal crystalline lattice. Macromolecules 2010, 43 (15), 6429-6437.

Licari, J. J.; Swanson, D. W., Adhesives technology for electronic applications: materials, processing, reliability. William Andrew: 2011.

Lieser, G.; Wegner, G.; Smith, J. A.; Wagener, K. B., Morphology and packing behavior of model ethylene/propylene copolymers with precise methyl branch placement. Colloid and Polymer Science 2004, 282 (8), 773-781.

Lorenzo, A. T.; Arnal, M. L.; Albuerne, J.; Müller, A. J., DSC isothermal polymer crystallization kinetics measurements and the use of the Avrami equation to fit the data: Guidelines to avoid common problems. Polymer Testing 2007, 26 (2), 222-231.

Luongo, J., Infrared study of polypropylene. Journal of Applied Polymer Science 1960, 3 (9), 302-309.

MacKnight, W.; Yang, M.; Kajiyama, T., Amer. 34. Chem. Soc. Polymer Prepr 1968, 9, 860.

Maddah, H. A., Polypropylene as a promising plastic: A review. American Journal of Polymer Science 2016, 6 (1), 1-11.

Mandelkern, L., Crystallization of polymers. McGraw-Hill New York: 1964; Vol. 38.

Meyer Jr, M. F.; McConnell, R. L., Amorphous and crystalline polyolefin based hot-melt adhesive. Google Patents: 1978.

Michell, R. M.; Muller, A. J.; Castelletto, V.; Hamley, I.; Deshayes, G.; Dubois, P., Effect of Sequence Distribution on the Morphology, Crystallization, Melting, and Biodegradation of Poly (ε-caprolactone-co-ε-caprolactam) Copolymers. Macromolecules 2009, 42 (17), 6671-6681.

Michell, R. M.; Müller, A. J.; Deshayes, G.; Dubois, P., Effect of sequence distribution on the isothermal crystallization kinetics and successive self-nucleation and annealing (SSA) behavior of poly (ε-caprolactone-co-ε-caprolactam) copolymers. European Polymer Journal 2010, 46 (6), 1334-1344.

Mileva, D.; Androsch, R.; Funari, S. S.; Wunderlich, B., X-ray study of crystallization of random copolymers of propylene and 1-butene via a mesophase. Polymer 2010, 51 (22), 5212-5220.

Muller, A. J.; Arnal, M. L., Thermal fractionation of polymers. Progress in Polymer Science 2005, 30, 559-603.

Muller, A. J.; Hernandez, Z. H.; Arnal, M. L.; Sanchez, J. J., Successive self-nucleation/annealing (SSA): A novel technique to study molecular segregation during crystallization. Polymer Bulletin 1997, 39, 465-472.

Müller, A. J.; Michell, R. M.; Pérez, R. A.; Lorenzo, A. T., Successive Self-nucleation and Annealing (SSA): Correct design of thermal protocol and applications. European Polymer Journal 2015, 65, 132-154.

Nedkov, E.; Dobreva, T., Wide and small-angle X-ray scattering study of isotactic polypropylene gamma irradiated in bulk. European Polymer Journal 2004, 40 (11), 2573-2582.

Ng, H.; Allegrezza, A.; Seymour, R.; Cooper, S. L., Effect of segment size and polydispersity on the properties of polyurethane block polymers. Polymer 1973, 14 (6), 255-261.

Nierzwicki, W., Microphase separation in urethane elastomers as seen through NMR measurements. Journal of applied polymer science 1984, 29 (4), 1203-1213.

Oertel, G.; Abele, L., Polyurethane handbook: chemistry, raw materials, processing, application, properties. Hanser Publishers. Distributed in USA by Scientific and Technical Books, Macmillan: 1985.

Pae, K., γ–α Solid–solid transition of isotactic polypropylene. Journal of Polymer Science Part B: Polymer Physics 1968, 6 (4), 657-663.

Painter, P. C.; Park, Y.; Coleman, M. M., Hydrogen bonding in polymer blends. 2. Theory. Macromolecules 1988, 21 (1), 66-72.

Parenteau, T.; Ausias, G.; Grohens, Y.; Pilvin, P., Structure, mechanical properties and modelling of polypropylene for different degrees of crystallinity. Polymer 2012, 53 (25), 5873-5884.

Park, Y.-J.; Kim, H.-J., Hot-melt adhesive properties of EVA/aromatic hydrocarbon resin blend. International journal of adhesion and adhesives 2003, 23 (5), 383-392.

Patel, J. P.; Deshmukh, S.; Zhao, C.; Wamuo, O.; Hsu, S. L.; Schoch, A. B.; Carleen, S. A.; Matsumoto, D., An analysis of the role of nonreactive plasticizers in the crosslinking reactions of a rigid resin. Journal of Polymer Science Part B: Polymer Physics 2017, 55 (2), 206-213.

Patel, J. P.; Zhao, C. X.; Deshmukh, S.; Zou, G. X.; Wamuo, O.; Hsu, S. L.; Schoch, A. B.; Carleen, S. A.; Matsumoto, D., An analysis of the role of reactive plasticizers in the crosslinking reactions of a rigid resin. Polymer 2016, 107, 12-18.

Paukkeri, R.; Lehtinen, A., Thermal behaviour of polypropylene fractions: 2. The multiple melting peaks. Polymer 1993, 34 (19), 4083-4088.

Paul, C., Hot-melt adhesives. MRS bulletin 2003, 28 (6), 440-444.

Petraccone, V.; De Rosa, C.; Guerra, G.; Tuzi, A., On the double peak shape of melting endotherms of isothermally crystallized isotactic polypropylene samples. Die Makromolekulare Chemie, Rapid Communications 1984, 5 (10), 631-634.

Pizzi, A.; Mittal, K. L., Handbook of adhesive technology, revised and expanded. CRC press: 2003.

Pocius, A. V.; Dillard, D. A., Adhesion science and engineering: surfaces, chemistry and applications. Elsevier: 2002.

Prisacariu, C., Polyurethane elastomers: from morphology to mechanical aspects. Springer Science & Business Media: 2011.

Rahaman, M.; Tsuji, H., Isothermal crystallization and spherulite growth behavior of stereo multiblock poly (lactic acid) s: effects of block length. Journal of Applied Polymer Science 2013, 129 (5), 2502-2517.

Randall, H., Polymer sequence determination (the 13C method). Academic Press: New York: 1977.

Randall, J. C., A review of high resolution liquid 13carbon nuclear magnetic resonance characterizations of ethylene-based polymers. Journal of Macromolecular Science—Reviews in Macromolecular Chemistry and Physics 1989, 29 (2-3), 201-317.

Randall, J. C., Methylene sequence distributions and number average sequence lengths in ethylene-propylene copolymers. Macromolecules 1978, 11 (1), 33-36.

Reddy, K. R.; Tashiro, K.; Sakurai, T.; Yamaguchi, N.; Sasaki, S.; Masunaga, H.; Takata, M., Isothermal crystallization behavior of isotactic polypropylene H/D blends as viewed from time-resolved FTIR and synchrotron SAXS/WAXD measurements. Macromolecules 2009, 42 (12), 4191-4199.

Reid, B. O.; Vadlamudi, M.; Mamun, A.; Janani, H.; Gao, H.; Hu, W.; Alamo, R. G., Strong memory effect of crystallization above the equilibrium melting point of random copolymers. Macromolecules 2013, 46 (16), 6485-6497.

Robert, D. H., Hot melt. Google Patents: 1940.

Ruiz-Orta, C.; Fernandez-Blazquez, J.; Pereira, E.; Alamo, R., Time-resolved FTIR spectroscopic study of the evolution of helical structure during isothermal crystallization of propylene 1-hexene copolymers. Identification of regularity bands associated with the trigonal polymorph. Polymer 2011, 52 (13), 2856-2868.

Saiani, A.; Daunch, W.; Verbeke, H.; Leenslag, J.-W.; Higgins, J., Origin of multiple melting endotherms in a high hard block content polyurethane. 1. Thermodynamic investigation. Macromolecules 2001, 34 (26), 9059-9068.

Saiani, A.; Rochas, C.; Eeckhaut, G.; Daunch, W.; Leenslag, J.-W.; Higgins, J., Origin of multiple melting endotherms in a high hard block content polyurethane. 2. Structural investigation. Macromolecules 2004, 37 (4), 1411-1421.

Samuels, R. J., Quantitative structural characterization of the melting behavior of isotactic polypropylene. Journal of Polymer Science Part B: Polymer Physics 1975, 13 (7), 1417-1446.

Sanchez, I.; Eby, R., Thermodynamics and crystallization of random copolymers. Macromolecules 1975, 8 (5), 638-641.

Sangroniz, L.; Cavallo, D.; Santamaria, A.; Müller, A. J.; Alamo, R. G., Thermorheologically Complex Self-Seeded Melts of Propylene–Ethylene Copolymers. Macromolecules 2017.

Sastri, V. R., Commodity Thermoplastics-6: Polyvinyl Chloride, Polyolefins, and Polystyrene. 2014.

Satriana, M., Hot melt adhesives: manufacture aad applications. In Chemical technological review, Noyes Data Corporation.; New Jersey: 1974.

Saunders, J. H.; Frisch, K. C., Polyurethanes: chemistry and technology. 1962.

Sonnenschein, M. F.; Lysenko, Z.; Brune, D. A.; Wendt, B. L.; Schrock, A. K., Enhancing polyurethane properties via soft segment crystallization. Polymer 2005, 46 (23), 10158-10166.

Sonnenschein, M. F.; Rondan, N.; Wendt, B. L.; Cox, J. M., Synthesis of transparent thermoplastic polyurethane elastomers. Journal of Polymer Science Part A: Polymer Chemistry 2004, 42 (2), 271-278.

Srichatrapimuk, V. W.; Cooper, S. L., Infrared thermal analysis of polyurethane block polymers. Journal of Macromolecular Science, Part B: Physics 1978, 15 (2), 267-311.

Szycher, M., Szycher's handbook of polyurethanes. CRC press: 2012.

Tang, Q.; He, J.; Yang, R.; Ai, Q., Study of the synthesis and bonding properties of reactive hot-melt polyurethane adhesive. Journal of Applied Polymer Science 2013, 128 (3), 2152-2161.

Thitithammawong, A.; Nakason, C.; Sahakaro, K.; Noordermeer, J., Effect of different types of peroxides on rheological, mechanical, and morphological properties of thermoplastic vulcanizates based on

Thomson, J. J., Applications of dynamics to physics and chemistry. Macmillan: 1888.

Voda, A. E.; Haberstroh, U. D.-I. E. Low Field NMR for Analysis of Rubbery Polymers; Fakultät für Mathematik, Informatik und Naturwissenschaften: 2006.

Wamuo, O.; Wu, Y.; Hsu, S. L.; Paul, C. W.; Eodice, A.; Huang, K.-Y.; Chen, M.-H.; Chang, Y.-H.; Lin, J.-L., Effects of chain configuration on the crystallization behavior of polypropylene based copolymers. Polymer 2017, 116, 342-349.

Wilkes, G. L.; Bagrodia, S.; Humphries, W.; Wildnauer, R., The time dependence of the thermal and mechanical properties of segmented urethanes following thermal treatment. Journal of Polymer Science Part C: Polymer Letters 1975, 13 (6), 321-327.

Wilkes, G. L.; Wildnauer, R., Kinetic behavior of the thermal and mechanical properties of segmented urethanes. Journal of Applied Physics 1975, 46 (10), 4148-4152.

Wunderlich, B., Macromolecular Physics, Volume 1. Crystal Structure, Morphology, Defects. Academic Press, Inc.: New York, 1973; p 549.

Wunderlich, B., Macromolecular physics. Elsevier: 2012; Vol. 2.

Xu, J.; Srinivas, S.; Marand, H.; Agarwal, P., Equilibrium Melting Temperature and Undercooling Dependence of the Spherulitic Growth Rate of Isotactic Polypropylene. Macromolecules 1998, 31 (23), 8230-8242.

Yanagihara, Y.; Osaka, N.; Iimori, S.; Murayama, S.; Saito, H., Relationship between modulus and structure of annealed thermoplastic polyurethane. Materials Today Communications 2015, 2, e9-e15.

Yilgör, I.; Yilgör, E.; Wilkes, G. L., Critical parameters in designing segmented polyurethanes and their effect on morphology and properties: A comprehensive review. Polymer 2015, 58, A1-A36.

Yoon, P. J.; Han, C. D., Effect of thermal history on the rheological behavior of thermoplastic polyurethanes. Macromolecules 2000, 33 (6), 2171-2183.

Zagar, E., Solution properties of polyurethanes studied by static light scattering, SEC-MALS, and viscometry. Acta chimica slovenica 2005, 52 (3), 245.

Zhang, M. C.; Guo, B.-H.; Xu, J., A Review on Polymer Crystallization Theories. Crystals 2016, 7 (1), 4.

Zimmermann, H.; Hoechst, A., Structural analysis of random propylene-ethylene copolymers. Journal of Macromolecular Science, Part B: Physics 1993, 32 (2), 141-161.